USDA Forest Service
Research Paper RM-194
October 1977

A System That Measures Blowing Snow

R. A. Schmidt

Rocky Mountain Forest and
Range Experiment Station
Forest Service
U. S. Department of Agriculture
Fort Collins, Colorado 80521

Abstract

A snow particle counter based on a prototype design that originated at the University of Washington, was developed and tested for research in the fundamentals of snow transport by wind. Further work created an electronic system that monitors visual range in blowing snow. The system has been applied to interstate highway traffic control.

All design and test data are included in this paper, together with shop drawings for fabrication of the sensor, and an operating and service manual for the visual range monitor.

USDA Forest Service
Research Paper RM-194

October 1977

A System That Measures Blowing Snow

R. A. Schmidt, Hydrologist

Rocky Mountain Forest and Range Experiment Station[1]

[1]Central headquarters is maintained at Fort Collins, in cooperation with Colorado State University.

Contents

A System That Measures Blowing Snow

R. A. Schmidt

Introduction

The concept of detecting particles of matter photoelectrically was first applied to measure blowing snow early in the 1960's. Instruments that produced electric signals proportional to light attenuation by blowing snow were tested in the Antarctic by Landon Smith and Woodberry (1965) and Wishart (1965), and in the Arctic by Sommerfeld and Bussinger (1965). It was the work of these latter authors, together with Rogers at the University of Washington, that sparked development of the electronic system described here.

The first blowing snow particle counter was designed in Seattle, Wash. and field tested at Alta, Utah in January 1966 (fig. 1). This work suggested the possibility of detecting individual snow particles by their shadows on photosensitive semiconductors (Hollung et al. 1966). In addition to a measure of the number of snow particles in the air stream, the instrument offered particle size and speed information. The exciting opportunity to test several long-standing hypotheses of blowing snow transport motivated further development of this instrument.

Dr. R. A. Sommerfeld redesigned the sensor housing to reduce interference with the windstream (Rogers and Sommerfeld 1968). Reasoning that windblown snow particles move along nearly horizontal trajectories, he oriented the sensor to minimize obstruction of both horizontal and vertical wind components (fig. 2). Field tests of this design, conducted at Chalk Mountain, Colorado in 1968, demonstrated several problems, including a poor signal to noise ratio, and the need for some method of field calibration.

Another summer of redesign produced the snow particle counter reported by Schmidt and Sommerfeld (1969). Further reduction in air stream interference (fig. 3) was again an objective, along with cleaner signals and easier field adjustment. A field experiment at Chalk Mountain in April 1969 recorded analog signals on magnetic tape from 12 sensors of this version. The snow particle counter seemed to be a fieldworthy research instrument, but much calibration followed before some idea of its true nature began to appear.

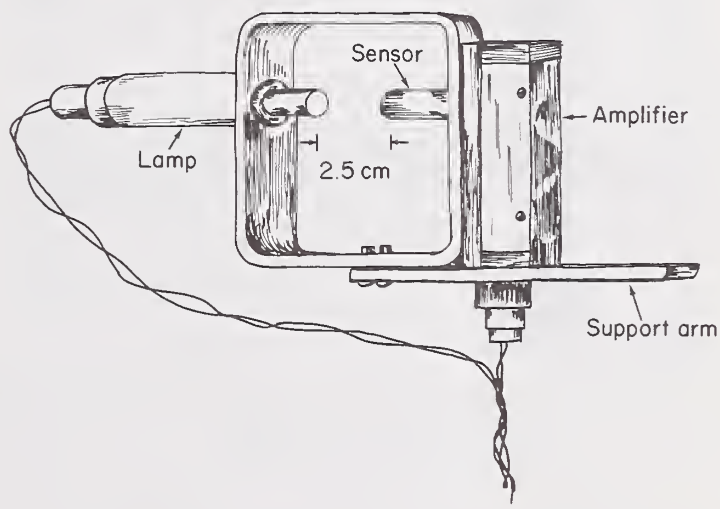

Figure 1.—Sketch of the prototype snow particle counter developed at the University of Washington (Hollung et al. 1966).

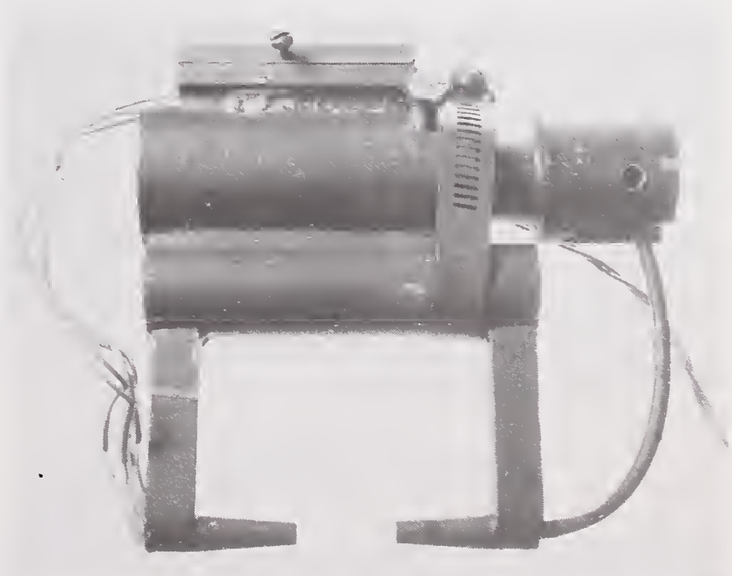

Figure 2.—Snow particle counter redesigned by Sommerfeld.

Figure 3.—Snow particle counter (SPC) of the design reported in this paper.

A research note by Schmidt and Holub (1971) reported efforts to explore this sensor's response in the laboratory. Reduced signal amplitude at lower temperatures could be explained almost entirely by the specified temperature drift of the phototransistors. A data processing procedure developed to estimate particle speed gave excellent results. Further, the average peak signal estimated from a storage oscilloscope display seemed to be a linear function of the sieve diameter of sand particles dropped past the particle counter. These results led to techniques for analyzing recordings from snow particle counters, presented in another research note (Schmidt 1971) along with some examples from the 1969 field experiment.

Summary of This Paper

The system described in this paper may be considered in three parts: the sensor, the electronics for monitoring the sensor, and a computer which estimates visual range from the voltages generated by the monitor. The next few paragraphs present a summary of the system to provide the framework for details on each of these parts.

Blowing snow particles move almost horizontally with strong winds, at least for heights greater than 10 cm above the surface. The sensor, a snow particle counter, produces voltage pulses when these small ice particles intercept its light beam. The pulse rate measures number of particles per unit time moving downwind through the area of the light beam. Particle diameter determines how much of the light beam is intercepted from the light detectors, so, the amplitude of these pulses should be related to particle size. The first part of this paper describes the sensor and experiments that determined relationships between sensor signals and snow particle size, frequency and speed.

Continuous records of intensity and duration of snow transport by wind required electronic circuits that convert the train of pulses from the sensor into more slowly varying voltages. These circuits, called the blowing snow monitor, produce direct current voltages that represent running averages of particle size and frequency over about a 5-second interval. The second part of this paper gives details of these circuits which provide strip chart records of the intensity of drifting.

Particle size, frequency and wind speed are the main parameters we need to estimate visibility in blowing snow, according to the theory of light attenuation by particles. A computer that combines the voltages from the monitor electronics as an electronic analog of this theoretical equation proved to give a useful measure of visual range in snowstorms and blizzards. Traffic control on a section of interstate highway where drifting snow caused dangerous conditions was improved by telemetering this data to the highway maintenance office. The third part of this paper presents the design equation and circuits that accomplish this computation.

From the sensor, through the electronics to a record of visual range, this paper presents the testing and development from 1971 through 1976. An operating and service manual for the visual range monitor comprises Appendix I, and shop drawings for construction of the sensor are Appendix II.

The Snow Particle Counter

Although certainly not ideal, this instrument has proved useful for measuring windblown snow. Following a description of the device, this section presents all the known computations, tests, and results that determine and limit the instrument's usefulness.

Sensor Description

The snow particle counter (fig. 4) is simply a light source that produces a light beam exposed to the windstream across a 25-mm path, and two light-sensitive semiconductors that detect the shadow of any obstacle as it crosses two separate portions of this light beam. Parallel optical windows limit the view of the light receivers. A small (T1-¼) incandescent lamp, connected to a 28-V direct-current power supply, provides the light. The slightly diverging light beam passes through a clear acetate window mounted flush in the end of the lamp housing, then across the active sampling area of the counter to fall on the sensor windows. These optical slits are produced by photographic reduction on high contrast, acetate base negative material, providing windows with very precise dimensions. Inside the sensor housing, a separator of brass shim stock limits the view of each phototransistor to its corresponding window. Both the lamp and sensor housing are painted flat black inside to reduce reflections.

Machined from seamless steel tubing, the instrument housing is formed by brazing with a silver alloy, while the components are held in a jig that maintains accurate alinement and spacing. Threaded plastic plugs seal the tubing ends, and provide access to install the small, shielded cables that connect the electronics. An enlarged portion at the end of the support arm holds an amplifier, which couples the sensor to remote recording equipment through a six-conductor connector in the end of the arm. Exterior enamel is baked onto the housing to prevent rust. Appendix II includes shop drawings required to build this instrument.

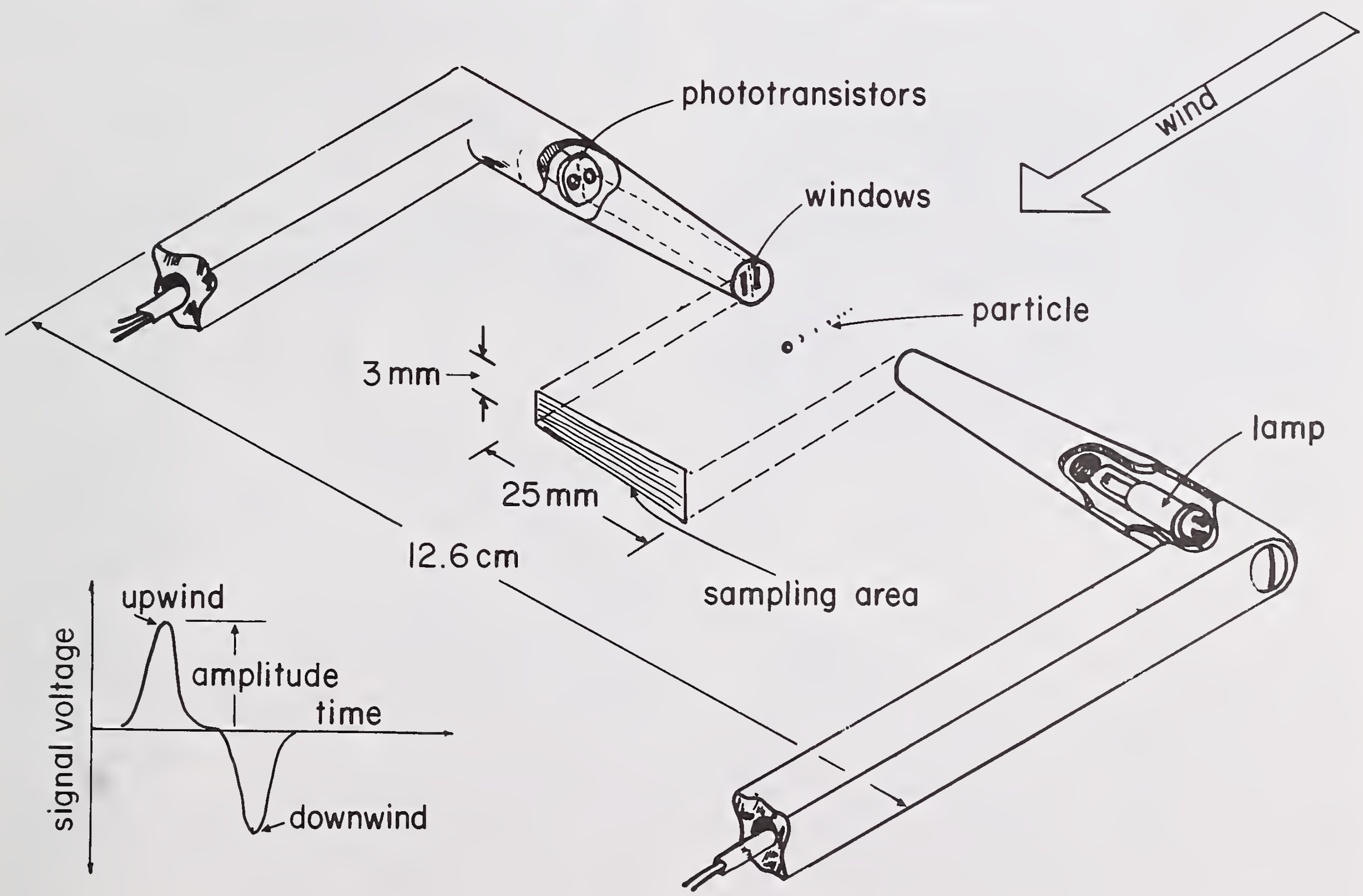

Figure 4.—Sensing elements of the SPC.

The amplifier connects the two phototransistors in such a way that a particle passing through the light beam produces a positive voltage pulse as it shadows the first window, and a negative pulse at the second window. Particle frequency is estimated from the number of positive (or negative) pulses per unit time. Together, the known distance between windows and the time interval between pulses provide an estimate of particle speed (at least the horizontal component). Since the pulse amplitude depends on shadow size (among other factors), it is a measure of particle size.

Signal Amplifier

In most applications, the sensor is located from 50 to several hundred feet away from the recording device, which means some amplification at the sensor is essential. The design reported here resulted from efforts to provide temperature compensation, better time response, and more rapid field adjustments than the single operational amplifier design reported by Schmidt and Sommerfeld (1969). These improvements were possible mainly because microcircuit technology advanced so rapidly during the development of this system.

Amplifiers A1 and A2 (fig. 5) provide low-impedance current-to-voltage converters for the phototransistors. This design feature permits more rapid signal rise and fall times without reducing amplitude (Graeme 1972). By adjusting the gain of A1, differences in phototransistor amplitude response are eliminated, making R1 the sensor BALANCE adjustment. Differential amplifier A3 inverts the signal from the second slit, while rejecting noise common to both phototransistors.

Temperature compensation is provided at A4, which also inverts the signal and provides final amplification by a factor of about 30. The decrease in output amplitude at lower temperatures (fig. 6) is due primarily to the phototransistors, which have a specified temperature coefficient of 0.67%/°C. Gain of the final amplifier is determined by the ratio of feedback resistance to

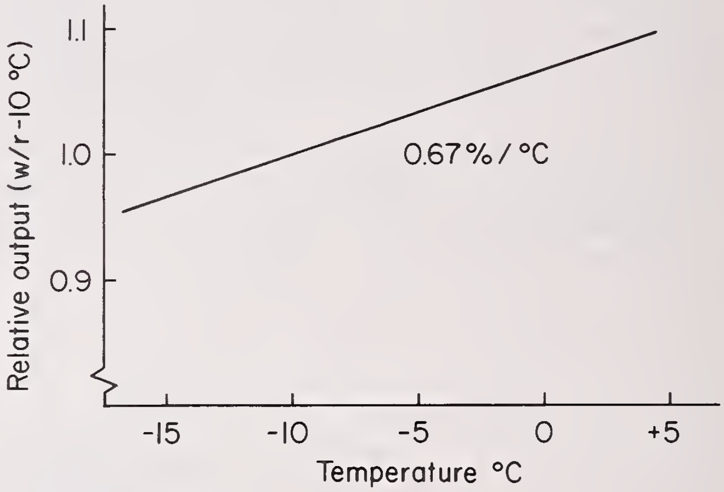

Figure 6.—Temperature effects on calibration signal output, before compensation (Schmidt and Holub 1971).

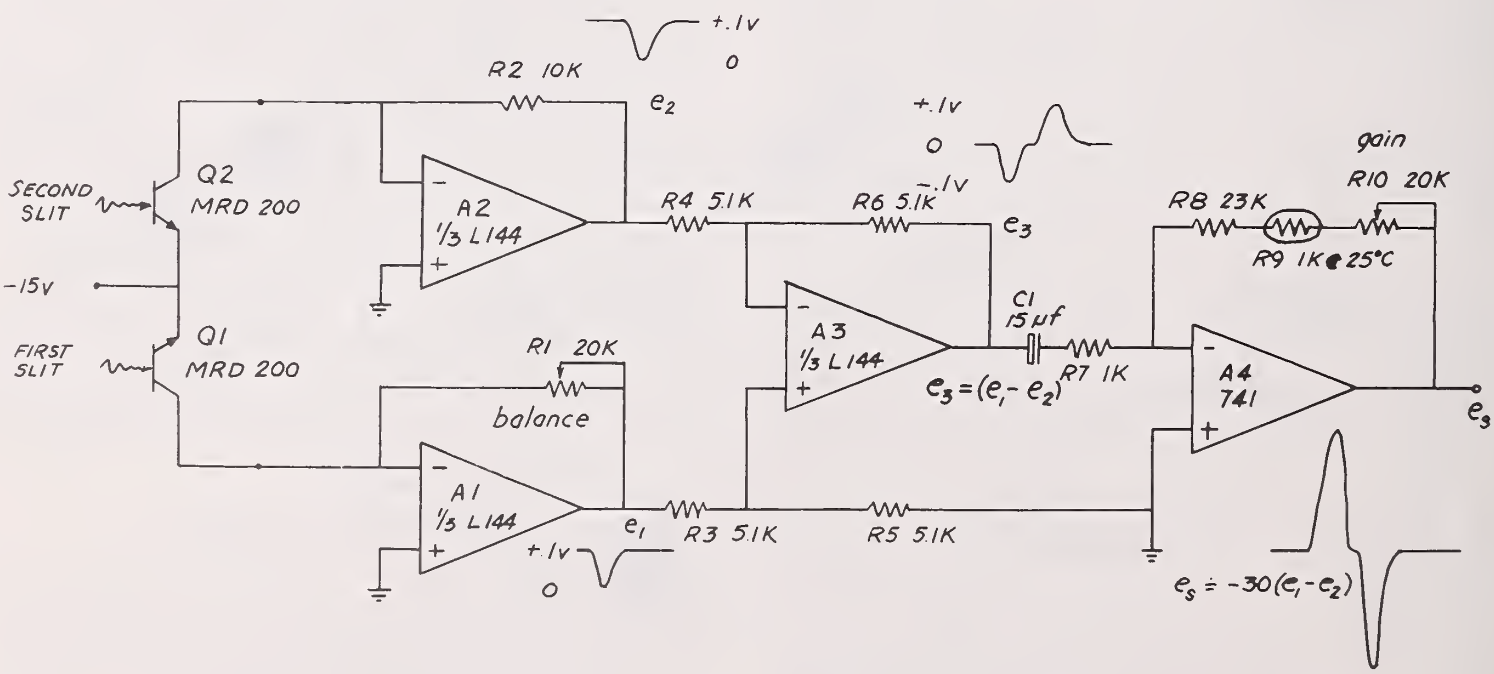

Figure 5.—Snow particle counter circuit diagram.

input resistance $A = (R_f/R_i)$. In figure 5, the total feedback resistance around A4 is the sum of the fixed resistance R8, the variable resistor R10 (sensor GAIN adjustment), and a thermistor R9, which is rated at 1,000 ohms for 25°C and increases resistance as temperature decreases.

Suppose we center calculations around -10°C, where an amplification factor of 30, operating on a signal amplitude with peak E_s of 0.1 V, gives the desired output of 3.0 V (table 1). The tabulated values of E_s are calculated from the temperature coefficient of 0.67%/°C. Values for R9 at each temperature are furnished by the manufacturer. Since $A = (R_f/R_i)$, and the input resistor $R_i = R7$ is 1,000 ohms, the gain at each temperature may be calculated from $A = (R8+R9+R10)/R7$. At -10°C, $(R8+R10)+4172 = 30K$, so that $(R8+R10) = 25.83K$ ohms. Calculated values of $E_o = AE_s$ show a maximum temperature effect of 3% in the range from 0°C to -25°C. Values at +25°C and the uncompensated output are included for comparison. Tests of the instrument with this amplifier design verified the predicted temperature compensation.

Table 1.—Sensor Temperature Compensation

Temp °C	R9 ohms	A	E_s	$E_o = AE_s$	$E_u = 30E_s$
		....	.... Volts	....	....
25	1000	26.8	.1201	3.22	3.60
0	2691	28.5	.1067	3.04	3.20
-5	3339	29.1	.1033	3.01	3.10
-10	4172	30.0	.1000	3.00	3.00
-15	5248	31.1	.0967	3.01	2.90
-20	6649	32.5	.0933	3.03	2.80
-25	8489	34.3	.0900	3.09	2.70

A 6-V miniature lamp was used in the sensor reported by Schmidt and Sommerfeld (1969). Current was 0.2 A, and the ground return for the lamp was in common with the signal ground, creating 60-cycle noise in the output. Further, when we began to use these sensors in monitoring systems, where they ran continuously, output decreased with time because the inside of the lamp blub blackened. Blackening was probably caused by disintegration of the lamp filament due to the relatively large current. Two changes were incorporated in the present sensor. First, to isolate the lamp circuit from the signal circuit, the -28-V phototransistor bias was reduced to -15 V, which is one supply voltage for the operational amplifiers. This permitted a lamp ground return by separate line. The second change replaced the 6-V lamp with a 28-V lamp of similar size. At this voltage the lamp draws much less current (40 mA), and blackening of the lamp is much slower. Routine lamp replacement at 1-month intervals reduces the problem to acceptable limits.

Adjustment of the amplifier requires balancing the signal and setting the gain. The procedure uses an oscilloscope to measure signal amplitudes and check noise level. A standard signal is generated by spinning a 0.5-mm diameter wire through the light beam, so that each slit is completely shadowed. First, the amplitude of the positive pulse is adjusted to match the negative pulse, using R1. Then R10 is set to give the desired output amplitude (usually ±3.0 volts). Figure 7 shows the calibrator in place, and figure 8a is the typical oscilloscope trace for a properly adjusted calibration signal. Figure 8b is a photograph of the normal signal noise trace. Most of this noise is generated by the phototransistors.

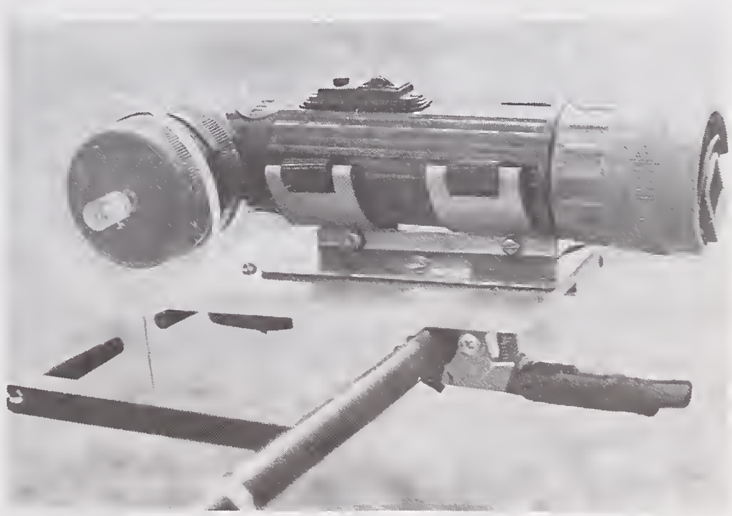

Figure 7.—Spinning wire calibrator attached to the SPC.

Sampling Volume Design

A snow particle anywhere within the volume defined in figure 9 is considered to be in the sampling volume of the particle counter. The design sampling area, perpendicular to the normal flux of blowing snow, is window height multiplied by light path length (3 mm x 25 mm), or 75 mm². The dimension along the wind or particle path is from the leading edge of the upwind window to the downwind edge of

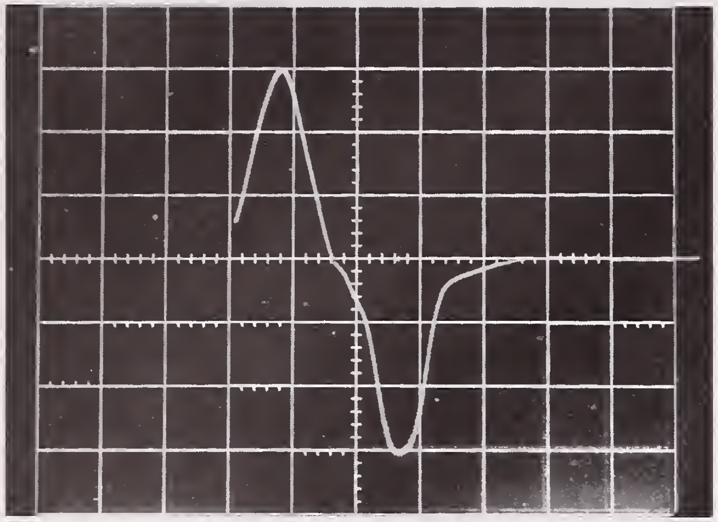

Figure 8a.—Oscilloscope trace of calibration signal (vertical sensitivity is 1 volt per division).

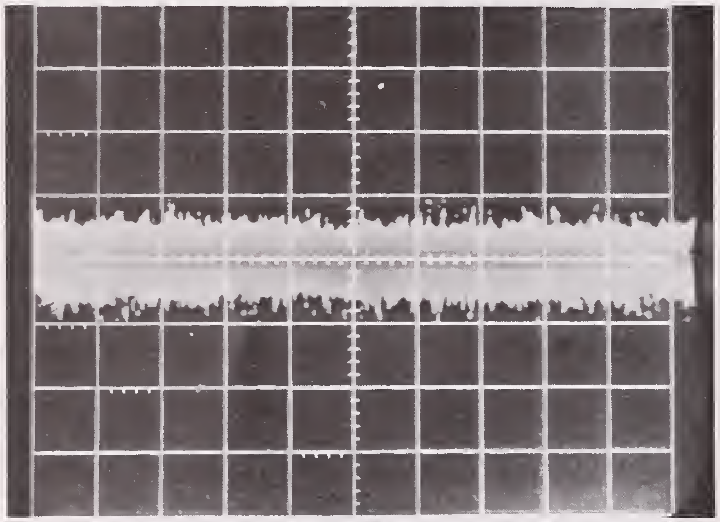

Figure 8b.—Typical SPC output noise level (vertical sensitivity is 10 mV per division).

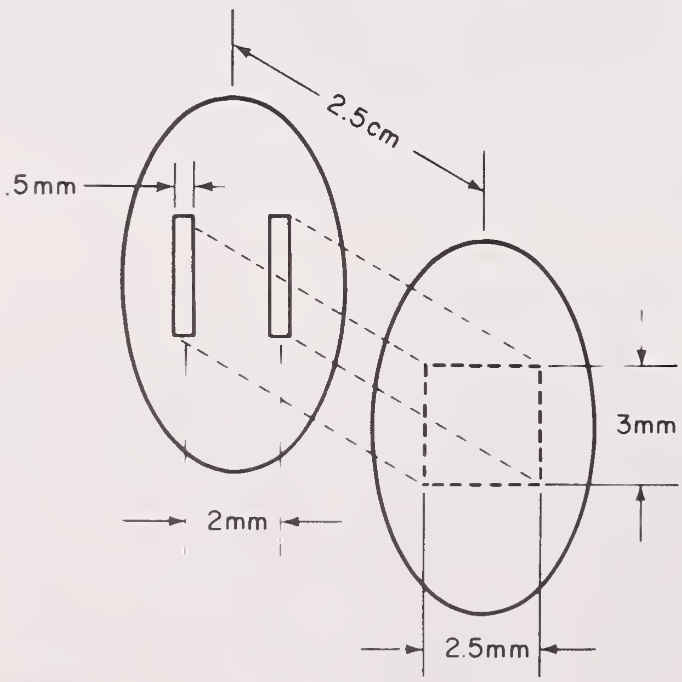

Figure 9.—SPC sampling volume.

the second window, so, the sampling volume is 2.5 mm x 75 mm², or 187.5 mm³. These dimensions are only slightly different from those chosen by Hollung et al. (1966), for the original design of the sensor.

To avoid having two particles in the sampling volume simultaneously, at least most of the time, the particle number concentration should not exceed 1 per 0.1875 cm³ or 5.33 particles per cubic centimeter. To estimate the corresponding mass concentration, let's assume blowing snow with uniform spherical ice particles of 200 μm diameter. These would have a mass of 3.85×10^{-6} g, assuming their density is 0.92 g/cm³. Therefore, the mass concentration would equal 3.05×10^{-5} g/cm³. Using Antarctic drift data from Budd et al. (1966), we could expect the snow particle counter to give reliable single particle measurements at 10 cm above the surface with windspeeds up to 15 m/s (measured at the 10-m height). Greater windspeeds and lower sensor heights increase the probability of two particles occupying the sensor volume at the same time. These calculations and actual field data both indicate that above 25 cm the particle counter should give reliable single particle data for all windspeeds.

Sensitivity Within the Sampling Area

It would be ideal if the electrical response (pulse amplitude) of this instrument was only a function of the particle's size. In reality, the peak signal produced by a particle can vary from some maximum value to almost nothing, depending on the location at which the particle crosses the light beam. Assuming the particle's shadow falls completely within a sensor window, the signal amplitude is usually maximum if the particle enters the beam near the sensor window. If the particle enters the beam near the lamp housing, and near the edge of the phototransistor's field of view (as limited by its window), then the pulse amplitude may not even be detectable in the signal's "noise."

There are two primary reasons for this less than ideal situation. First, the light beam is not well collimated (nor does it originate at a point source, since the lamp filament is at least a millimeter in length perpendicular to the beam), so, the shadow created by a particle near the lamp

is much less distinct than when the particle is near the transistor window. Second, as the angle between the phototransistor's optical axis and the shadow increases, electrical response decreases (Bliss 1971). The farther above or below the window center a particle crosses, the smaller the sensor response, and this effect is accentuated by the integral lens of the particular phototransistors used. Rather than try to predict the variation in sensitivity caused by the interaction of these factors, sensitivity was simply measured in the same manner as reported by Hollung et al. (1966).

A wire of measured diameter, placed (with its long axis parallel to the direction of particle motion) so it shadowed only one window, was moved from top to bottom of that window by a micrometer (fig. 10a). The wire position and sensor output were recorded by an x-y plotter, for transects near the sensor housing, in the center of the light path, and near the lamp housing. Several counters were tested, with wires ranging in diameter from 0.025 mm to 0.5 mm. When the response curves were normalized by the maximum signal at the center of the light path (fig. 10b), the relative response to wires of different sizes was about the same, and the differences between counters were usually small. (Occasionally, peculiar patterns were traced to an unusual filament configuration of the 28-V lamps.) A double peak, recorded near the lamp housing, is created by two "hot spots" where the

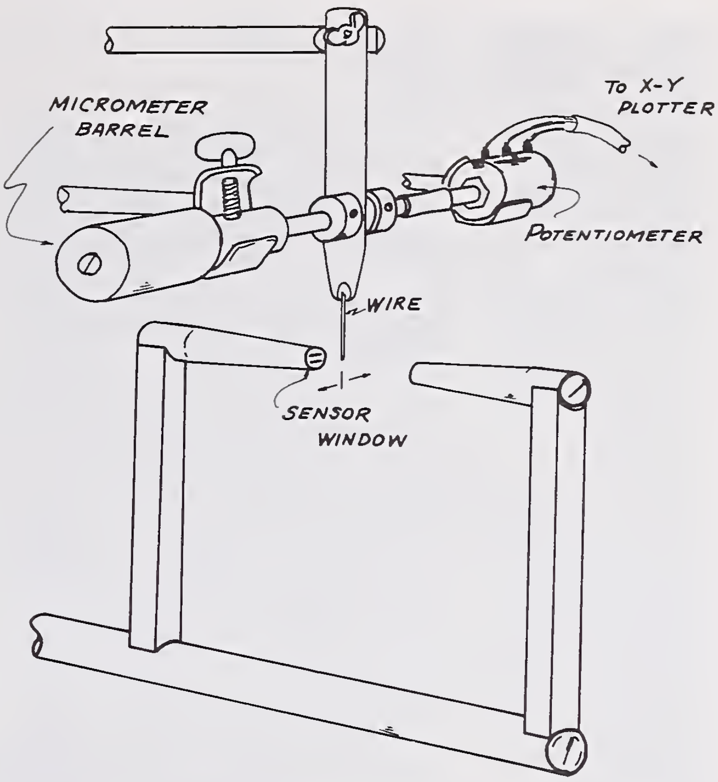

Figure 10a.—Sketch of sensitivity testing apparatus.

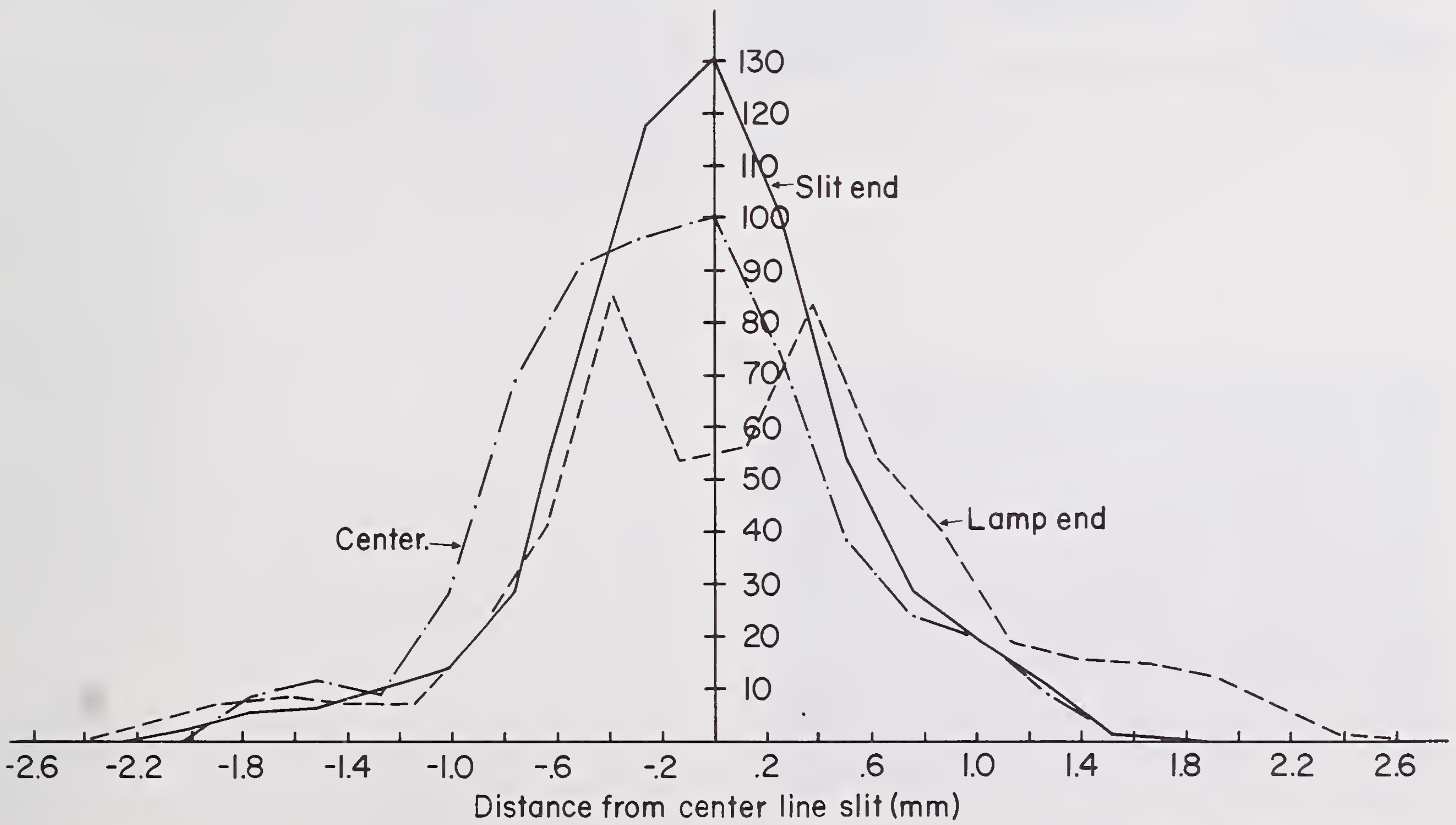

Figure 10b.—Relative response across one sensor window.

lamp filament is concentrated at its supports. When the wire is near the lamp, two shadows are cast on the sensor window.

A map of response levels across the sensor sampling area, constructed from these measurements (fig. 11a) produced estimates of the portion of total area with response of given levels. Because of divergence of the light beam and angular sensitivity of the photosensor, the actual sampling area is very close to 1 cm² rather than the 0.75 cm² design value. However, half of this total response area yields signals with amplitudes less than 20% of the maximum for that size shadow (fig. 11b). The figure also shows that response at the light path center is similar to the pattern for the total area. (It represents an average of sorts.)

Particle Size Estimates

For a blowing snow particle in a well-collimated light beam, the reduction in light received by a phototransistor should be directly proportional to the particle's cross-sectional area. This means that in the idealized case of spherical particles, if the relation between sensor output and light intensity is linear, signal amplitude should be in direct proportion to the square of particle diameter.

When initial laboratory experiments suggested a linear dependence between particle diameter and the average signal amplitude estimated from a storage oscilloscope, we rationalized that a nonlinear system response was masking the "diameter squared" relationship. It was

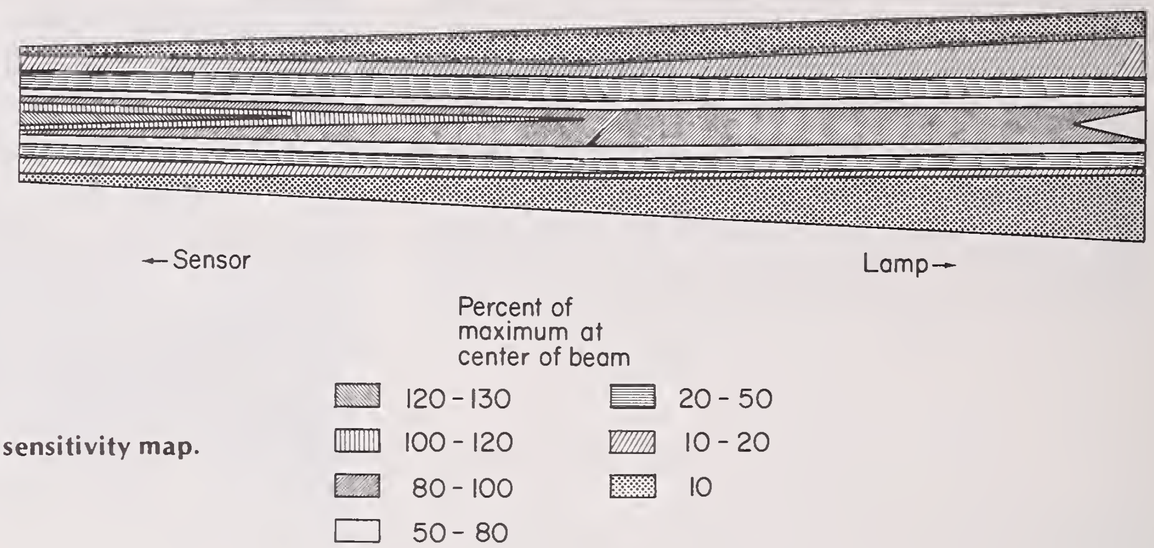

Figure 11a.— Sampling area sensitivity map.

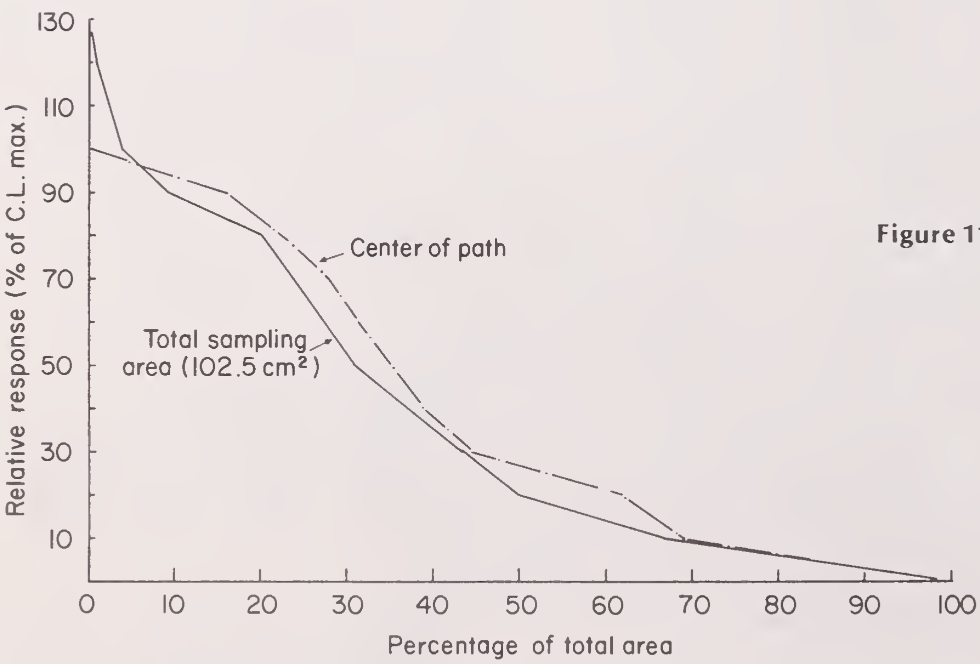

Figure 11b.— A summation plot of area sensitivity

some while after our first attempts to determine if signal amplitude could measure particle size that we made the detailed examination of sampling area sensitivity. Disconcerting estimates of mean snow particle diameter resulted when we used the linear relation reported in Schmidt and Holub (1971) to analyze field data tapes. Diameters in the size distribution shown by Schmidt (1971) were much smaller than those reported at similar height, for example, by Budd et al. (1966) (where formvar replicas of blowing snow particles were measured by microscope). More definitive experiments conducted with the aid of a multichannel analyzer (MCA) showed the linear calibration was a great oversimplification, to say the least.

Maximum Signal-Sieve Diameter Relationship.—To reduce the experimental problem, sieved sand was used again for most of the tests, eliminating the need to work in a cold room until we had the calibration fairly well established. Assuming the response at the center of the light beam would be representative, a glass funnel and tube (fig. 12) directed particles through this portion of the sample volume. A small artist's brush, twisted slowly over the funnel, dislodged particles held in the bristles at a rate that assured only one particle at a time was in the sensor volume. Particles appeared to fall straight through the tube with no noticeable tendency to spiral down the tube wall. The probability that a particle would pass across the windows at a given location was assumed equal for all locations across the beam.

Before a test run, the sensor output was checked for ± 3.0-V peaks from the calibrator wire. Then, a sand sample was dropped through the apparatus, and sensor output was recorded on analog magnetic tape. A multichannel analyzer accumulated in its digital memory a count of the number of positive signal peaks by 10-mV amplitude classes, displayed this record graphically on a cathode ray tube (fig. 13), and produced a punched paper tape for computer analysis.

From this procedure, the first relationship that became obvious was between the upper limits of the particle size classes and the maximum signal peaks. Stated formally, there proved to be a unique correspondence between a particle's sieve diameter (the smallest sieve

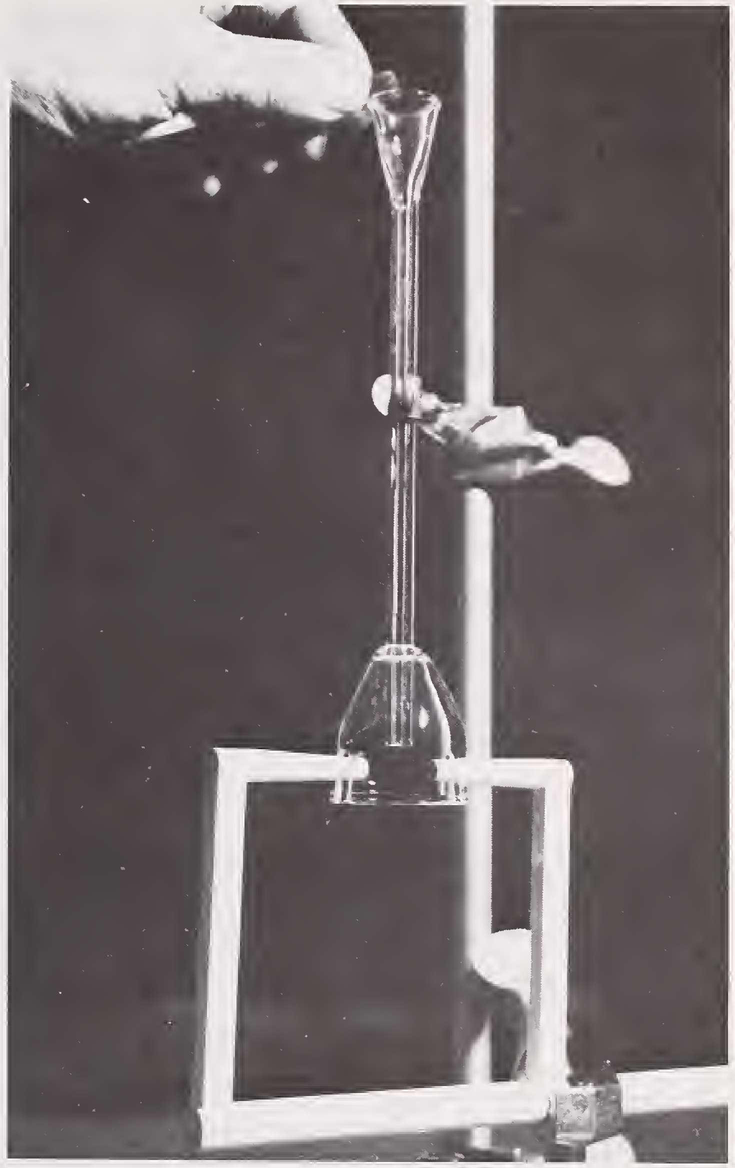

Figure 12.— Test apparatus for particle size response.

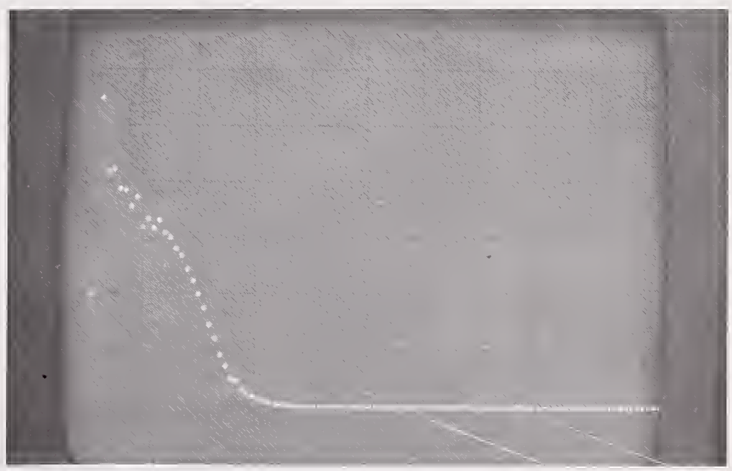

Figure 13.— Cathode ray tube display of signal amplitude distribution produced by the multichannel analyzer.

opening that will let it pass), and the maximum signal it will produce. To reduce scatter caused by small numbers of particles in classes near the tail of the signal amplitude distribution, the relationship was quantified in terms of the voltage at which less than 1% of the sample signals were larger. Signals from several hundred to several thousand particles were recorded in a sample run. Data for both sand and snow are included on figure 14. Thus, given a signal peak, the particle which generated that signal was not larger than the sieve diameter shown in figure 14.

Signal Distribution-Size Class Relationship.—Next, the distribution of signal amplitudes for each sieved sand fraction was studied more closely. If spherical particles, all of the same diameter, were dropped through the particle counter calibration apparatus, the resulting signal amplitude distribution should be very similar in shape to the response curve for a wire at the center of the light path (fig. 11b). A slightly different curve results from irregular sand grains with a range in diameters of 10 μm or more (fig. 15). Since the number of particles in such a sample is approximately equal to the area under its signal amplitude distribution, a technique which estimates this area could lead to an approximation of particle size distributions.

To see how a size distribution might be deduced from the corresponding distribution of signals, the procedure was reversed; that is, a signal distribution was generated from a known size distribution, formed by adding a predetermined number of particles from each size class, one class at a time. Beginning with the largest size class, particles were dropped through the

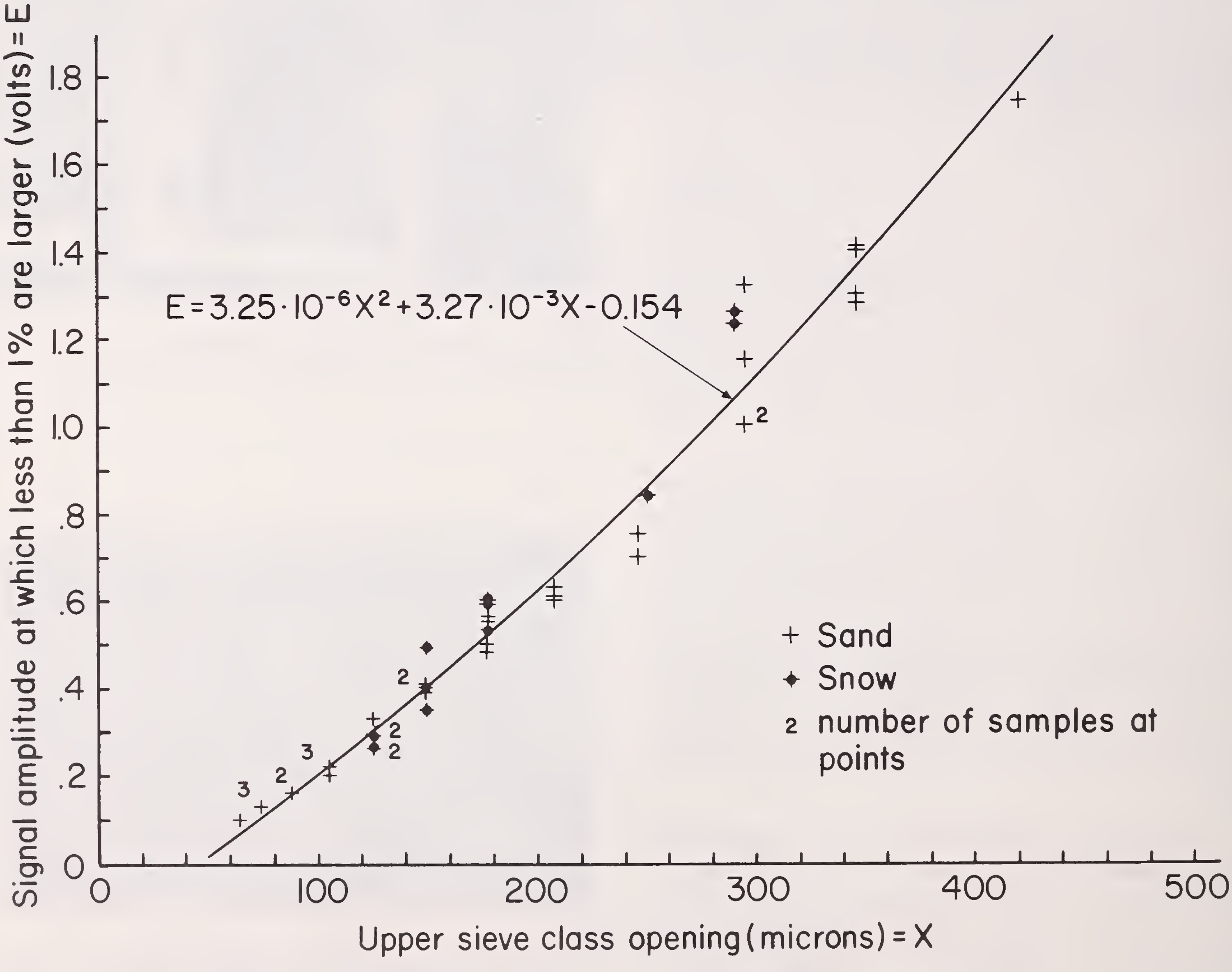

Figure 14.—Snow particle counter calibration data for maximum signals from sieved sand and snow particles.

particle counter until an electronic counter indicated the desired number of particles for that class. An x-y plotter recorded the resulting distribution of signal amplitudes which was stored in the MCA memory. Without erasing the memory, the procedure was repeated for the next smaller size class. After the smallest class of particles was dropped, the MCA held a signal distribution corresponding to the predetermined distribution of particle sizes.

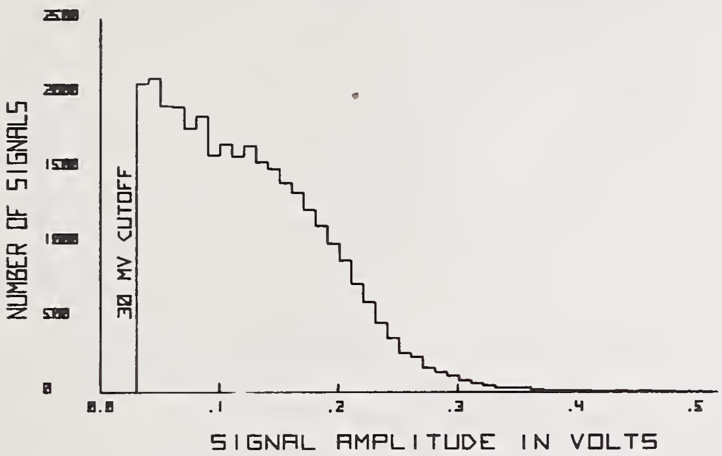

Figure 15.—A signal amplitude distribution for sieved sand in the 105 to 125 μm class. Each channel is a 10 mV signal class.

One such signal amplitude plot is shown in figure 16. Each size class contributes to the signal distribution only up to some maximum amplitude, as already noted. Plots resulting from this procedure led to the hypothesis that the number of particles in each size class could be estimated from the area of a trapezoid that approximated the area under the corresponding signal distribution (fig. 17). On each plot, a horizontal line was drawn so that it approximated the average number of signals per amplitude class over the main part of each distribution. Signal amplitudes corresponding to the intersection of the horizontal lines and signal distribution curve were plotted against the corresponding lower size class limit, and a curve was fitted to the data. This relationship was termed the "read" curve, since it indicates the signal amplitude at which the computer reads the distribution curve to estimate the number of signals generated by particles of that size class.

If L denotes the signal amplitude at which the distribution is read, and D is the difference between the number of signals per 10 mV at that point and at the next larger class limit, then as a

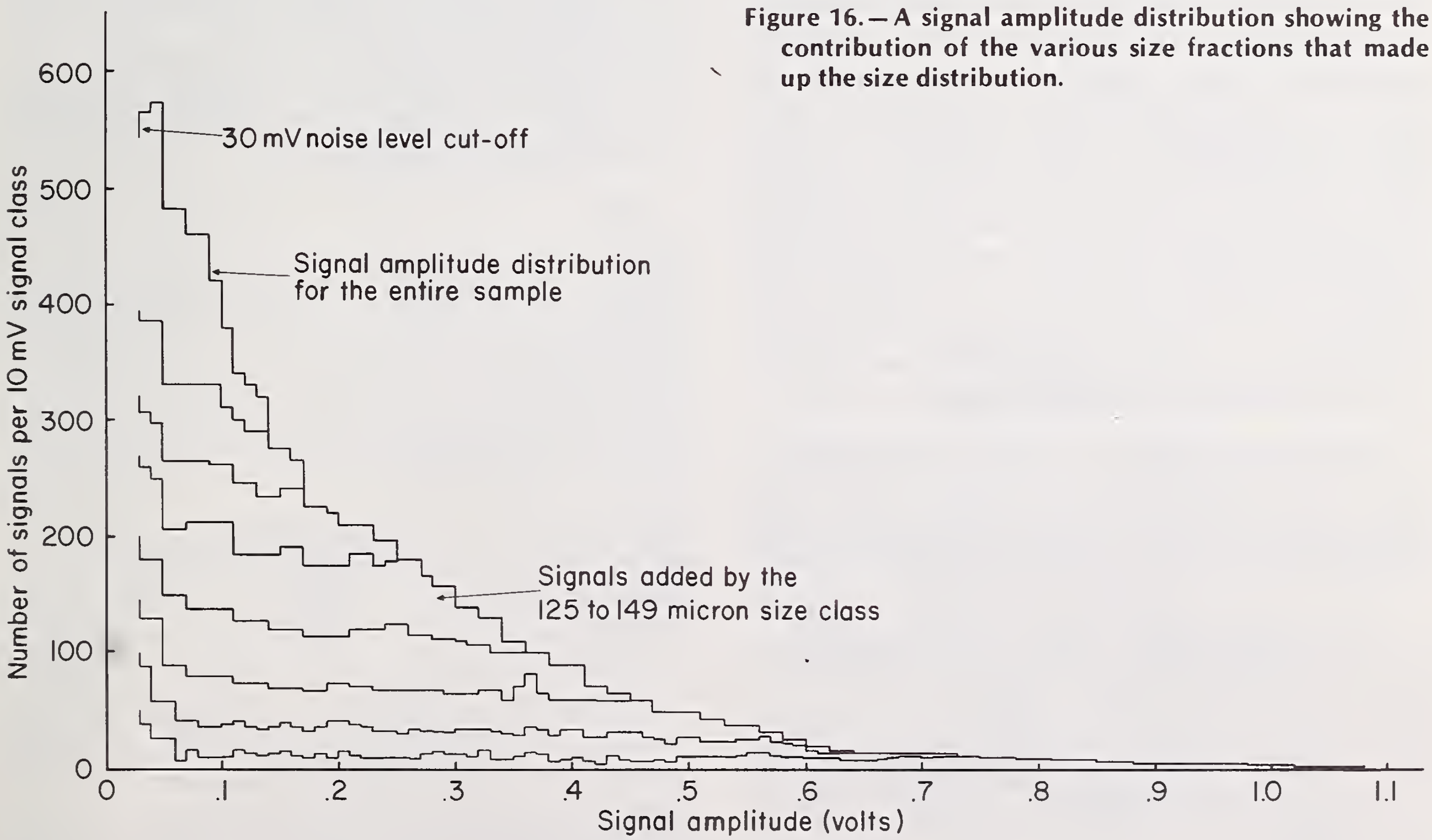

Figure 16.—A signal amplitude distribution showing the contribution of the various size fractions that made up the size distribution.

Figure 17.—Trapezoidal approximations to the areas for each size class in figure 16.

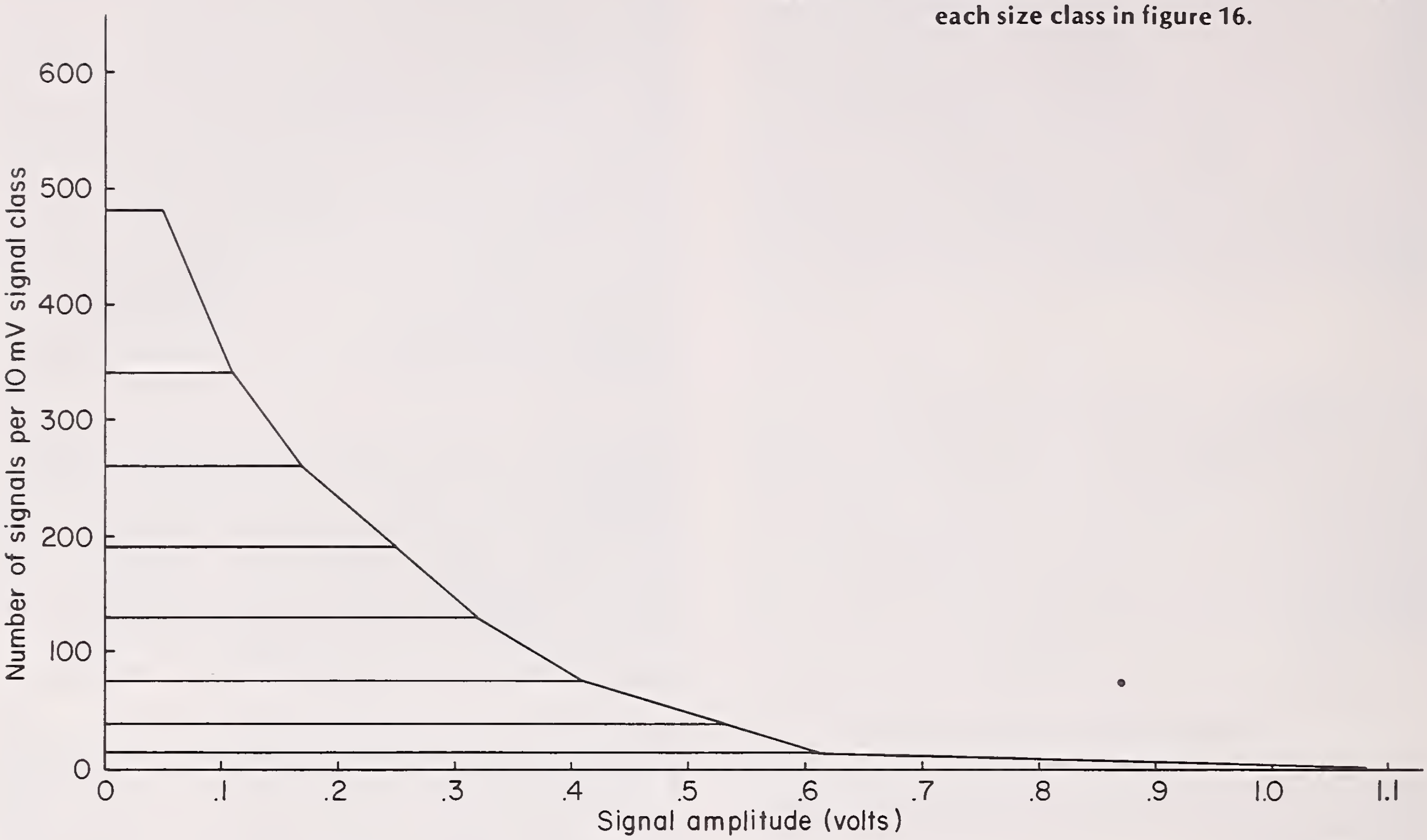

hypothesis, the number of particles N in the class is proportional to the product of the two: N = KLD. A variation in the proportionality constant, K, was expected because the width of amplitude classes decreased geometrically to give size classes that approximated the geometric progression of sieve openings. So, for each size class in five test distributions, the particle count N was divided by the amplitude L at which the signal curve was read for the lower size limit, and the difference D between this reading and the reading at the upper class limit. Values of K = N/LD, plotted in figure 18, were approximated by the two line segments shown.

Computer Program for Size Distribution.— From any signal amplitude distribution stored in the computer file, the following procedure estimated a corresponding particle size distribution:

a. the signal amplitude for which only 0.1% of signals were larger, was obtained by summation of the filed data;
b. beginning with this value, the curve was read at points corresponding to successively smaller voltage increments and the number of particles estimated by N = KLD;
c. using the relationship between "read" voltage L and sieve size, particle size classes were determined from the corresponding voltage classes; and
d. number of particles in each size class was tabulated and the mean diameter of the distribution computed.

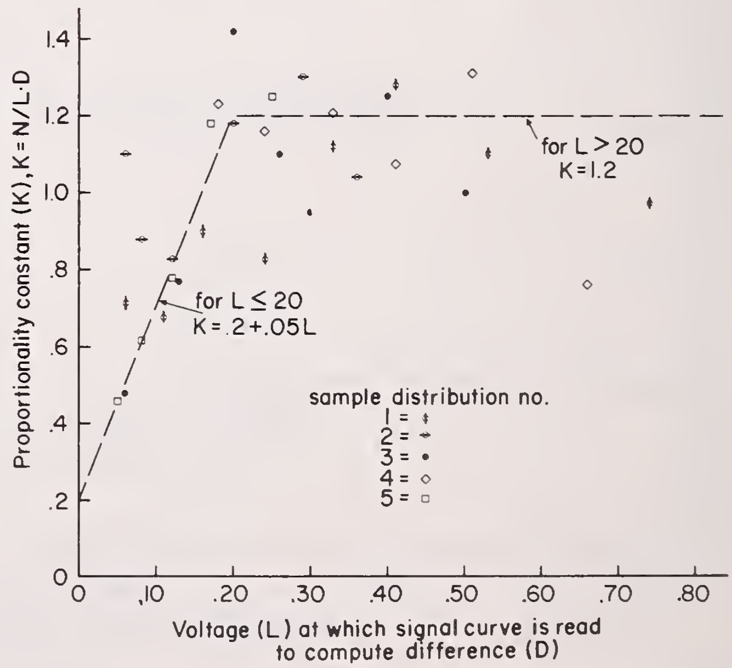

Figure 18.—A plot to determine the variation in K with the "read" voltage for each size class.

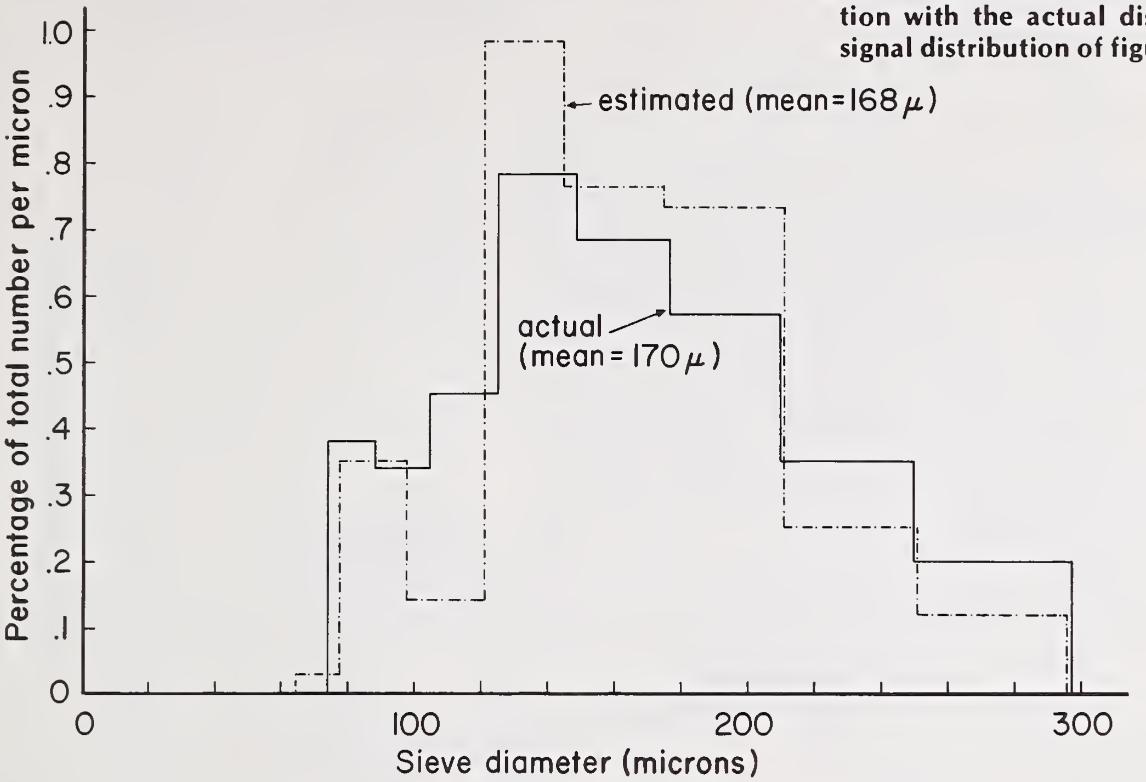

Figure 19.—A comparison of the computed size distribution with the actual distribution that generated the signal distribution of figure 16.

Since the test distributions were used to develop the computer program, it is not surprising that the procedure works pretty well for those cases. Figure 19 compares the actual and computed size distribution used as an example in figure 16. This procedure estimated the mean particle sieve diameter for five test distributions with a maximum error of 3 μm. Figure 20 shows the computed size distributions for a single size class and a bimodal distribution. The program gave at least a rough approximation even for these extreme cases.

Tests on Sieved Snow.—Because the tests reported by Schmidt and Holub (1971) showed that sand gave a signal amplitude response very similar to snow, our working hypothesis was that the procedure for estimating sand size distributions from particle counter signals would give results of similar accuracy for snow signals.

Therefore, the test particle counter apparatus was installed in a cold room, and the signal transferred to the electronic analysis equipment outside the test chamber. At temperatures near -10°C, samples of snow were crushed in a mortar and pestle, and then brushed through sieves to get particles separated into different size classes. Then, a size class was returned to the sieve through which it had been brushed, and the sieve was held above the glass funnel.

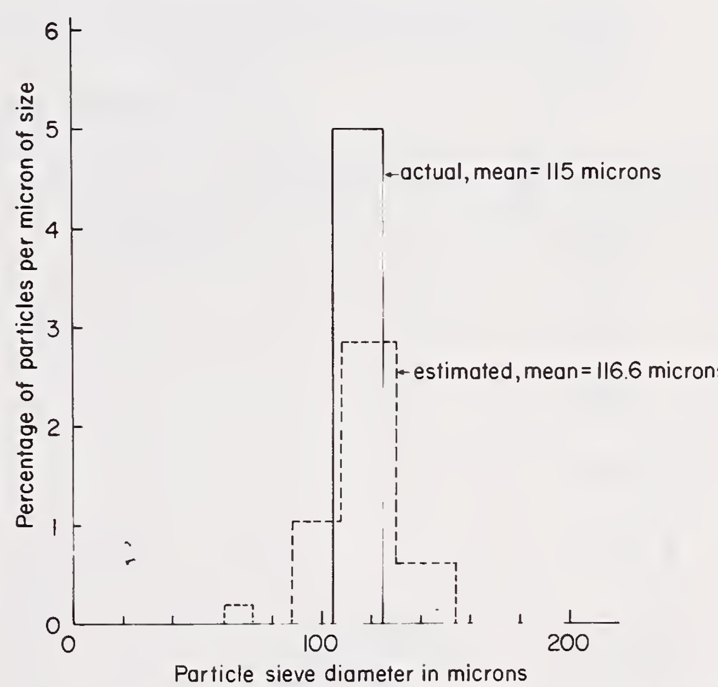

Figure 20a.—Computed size distributions for extreme cases of a single size class.

Brushing the particles gently through the sieve assured that they fell separately.

Signal amplitude distributions for various sieved snow size classes were processed by the computer program developed from tests with sand (fig. 21). Because of particle cohesion, and also the possibility of particle breakage, the sieved snow was more difficult to divide into size classes than sand. Sieved samples of snow

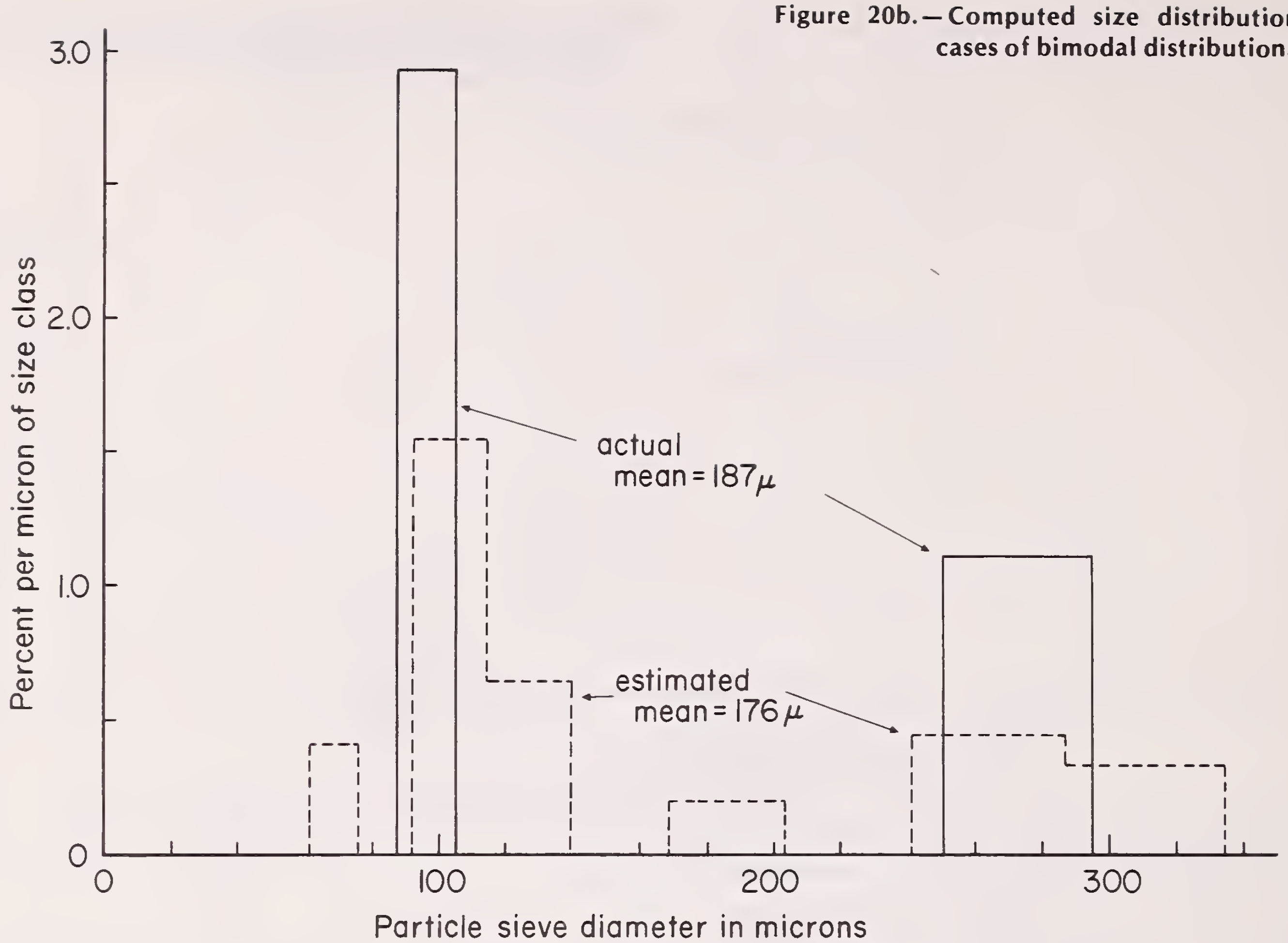

Figure 20b.—Computed size distribution for extreme cases of bimodal distribution.

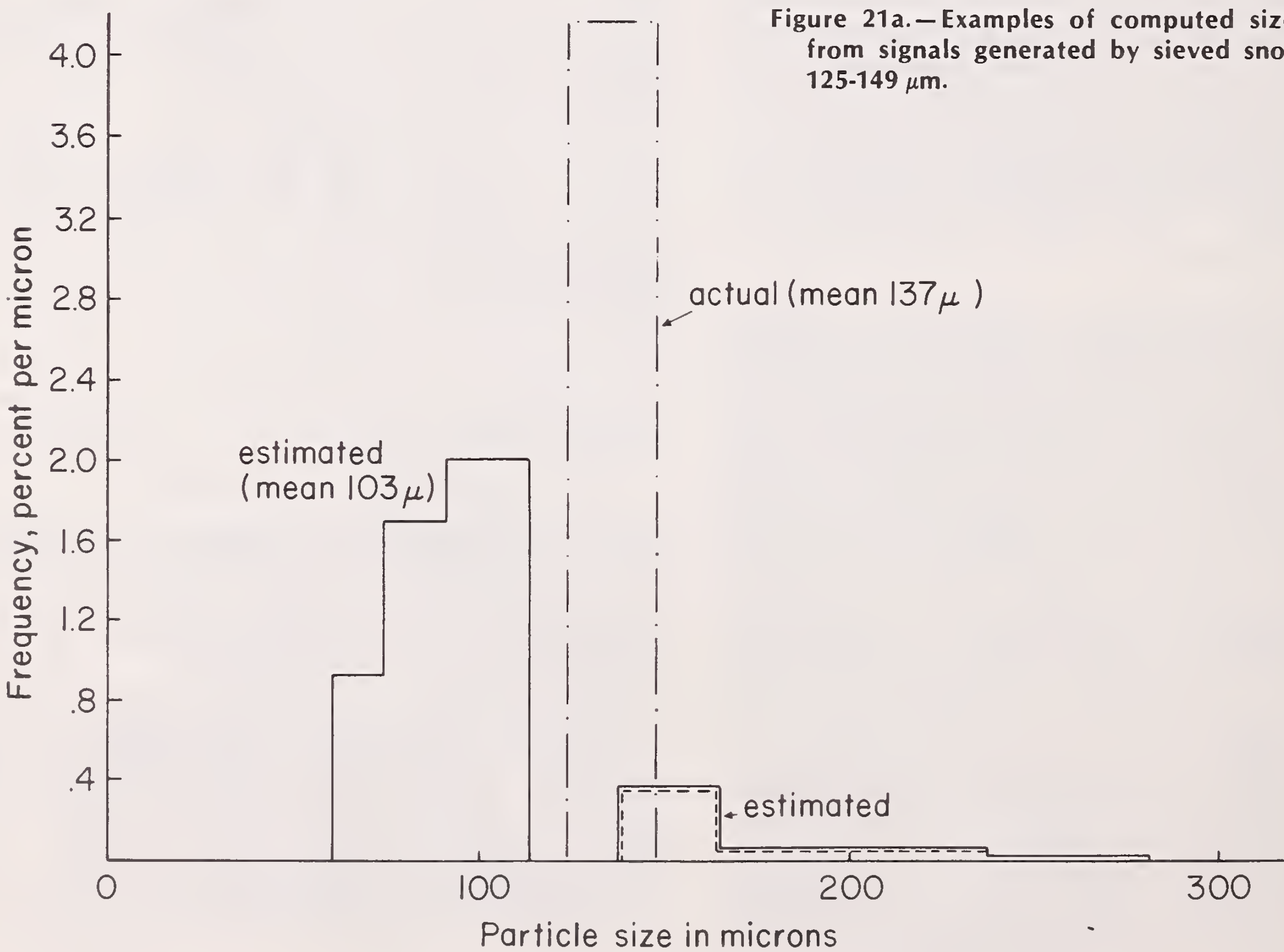

Figure 21a.—Examples of computed size distributions from signals generated by sieved snow particles (a) 125-149 μm.

Figure 21b.—Examples of computed size distributions from signals generated by sieved snow particles (b) 149-177 μm.

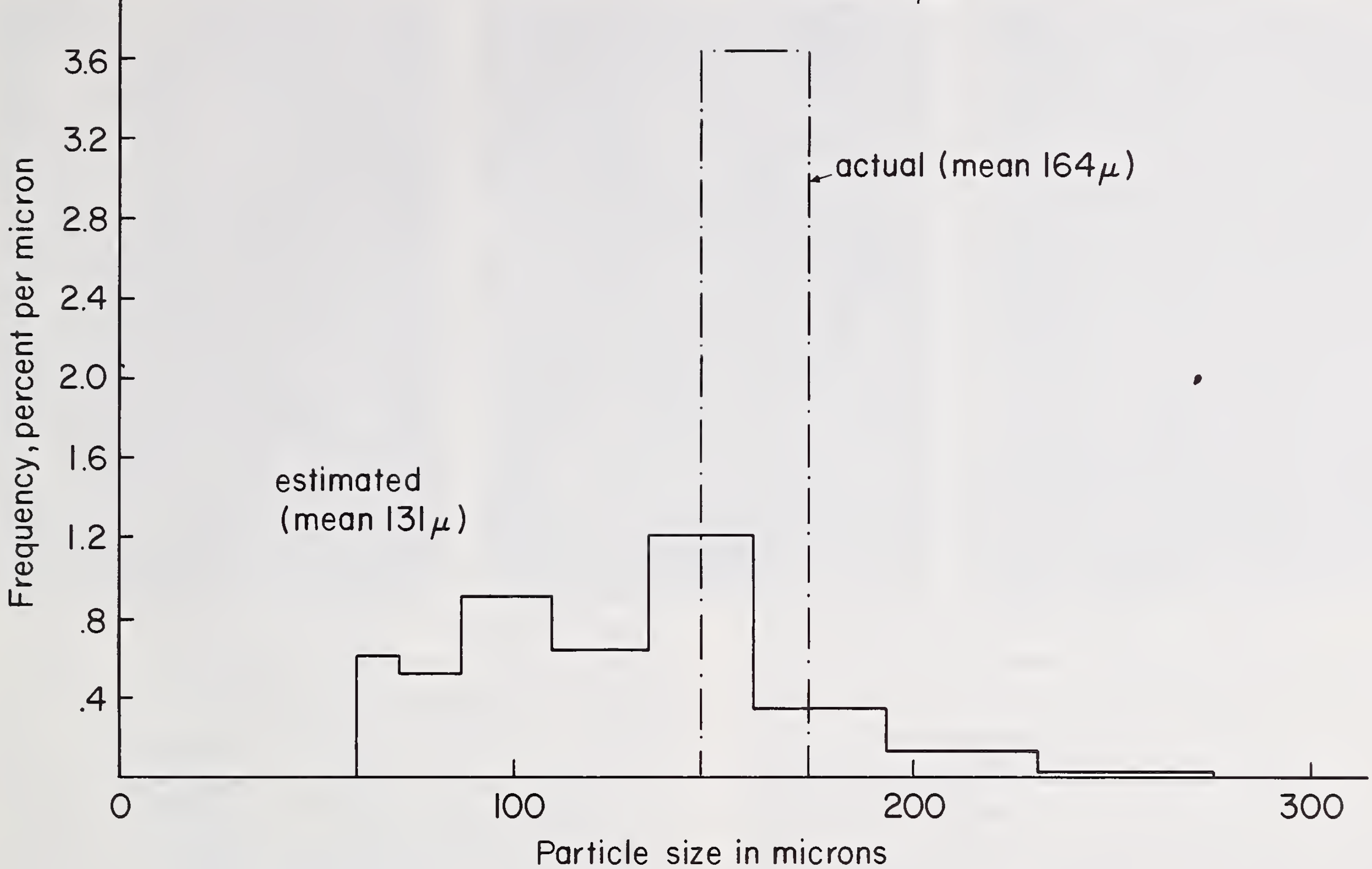

Figure 21c.—Examples of computed size distributions from signals generated by sieved snow particles (c) 177-250 μm.

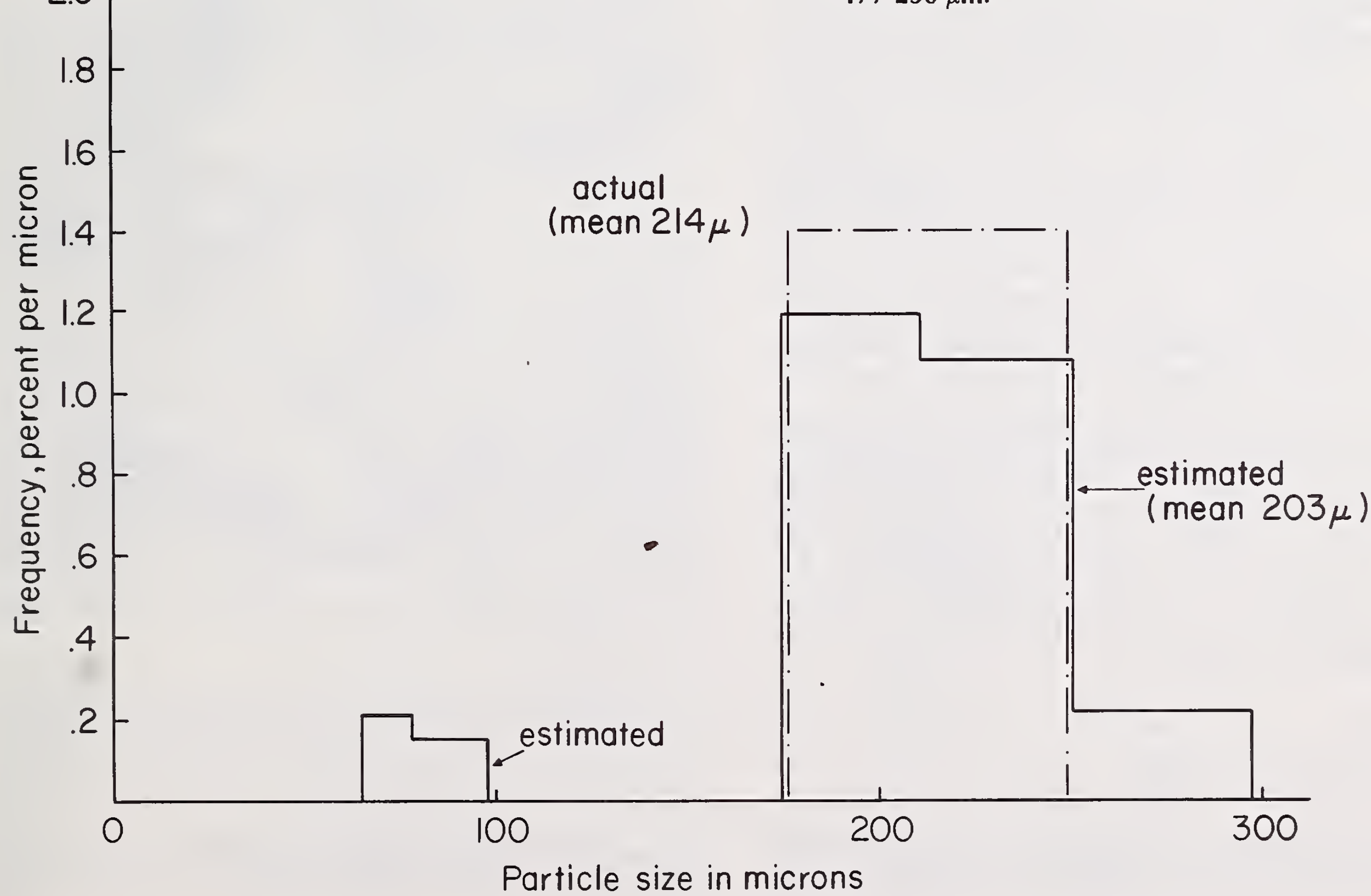

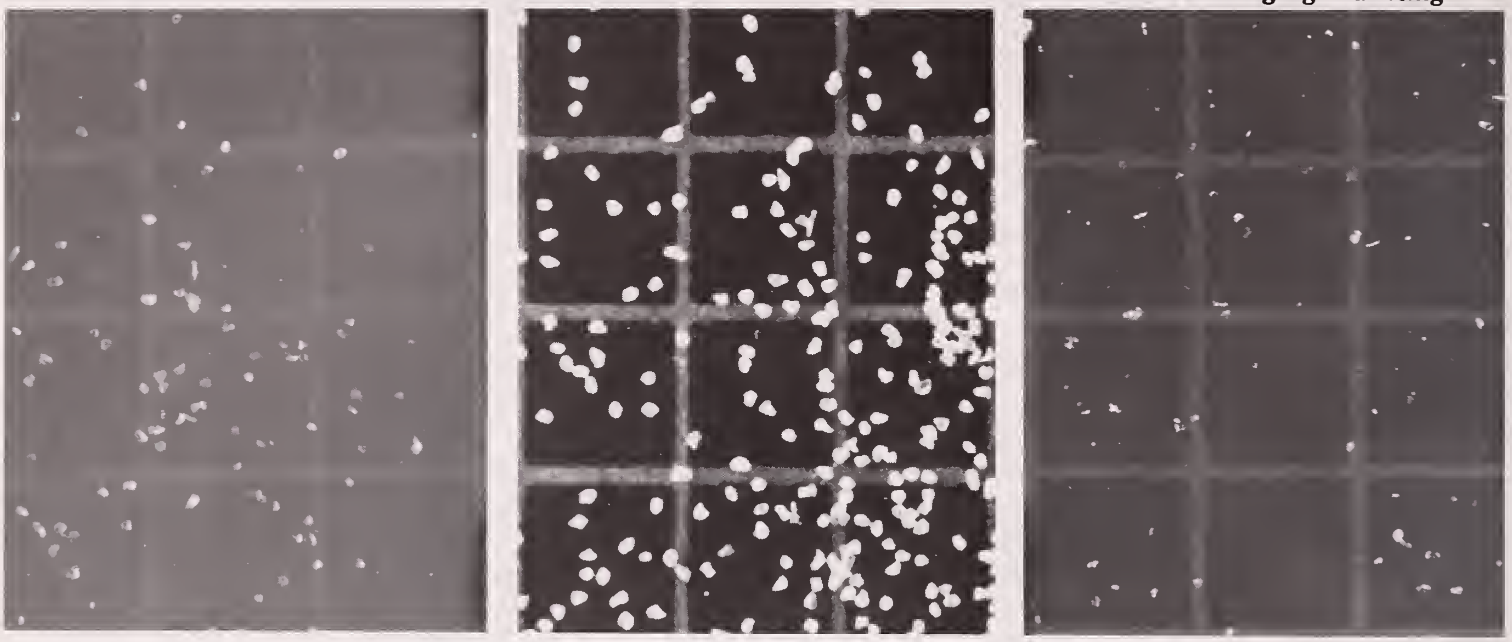

Figure 22.—Samples of sieved sand and snow photographed on a 2 mm grid, for comparison with a sample of natural blowing snow.

appear to be less uniform in size than the sand, with more particles of small diameters (fig. 22). This lack of experimental precision explains the discrepancy between the estimated results for snow in figure 21. Although it is possible that the particle counter responds differently to snow than sand, and more differently at smaller diameters, perhaps because of snow's greater optical transmissivity, the fact remains that measured maximum signals are very similar for both sand and snow (fig. 14), which would not be expected if the sensor responded to the two materials differently. No further experimental work has been done to resolve this question. The procedure for sand has been used to analyze field measurements of blowing snow, but with the reservation that estimated mean snow particle diameters may be somewhat smaller than true values.

As a final note on estimating particle size, experiments described in the next section demonstrated no interaction between particle speed and signal amplitude. The time response of the phototransistors and the amplifier was apparently sufficient to follow the shadow, at least at speeds up to 10 m/s.

Particle Speed Estimates

Tests reported by Schmidt and Holub (1971) provide the calibration data (fig. 23) for particle speed estimates. To estimate particle speed, the time interval between positive and negative pulses is measured, either from an oscilloscope trace or, preferably, by an electronic time interval counter. This time interval, together with the known separation of the sensor windows, provides the data required, but the estimate is only of the horizontal velocity component (assuming the particle counter is oriented with the long axis of the windows in the vertical).

The data in figure 23 was obtained in two ways. One was merely to vary the speed of rota-

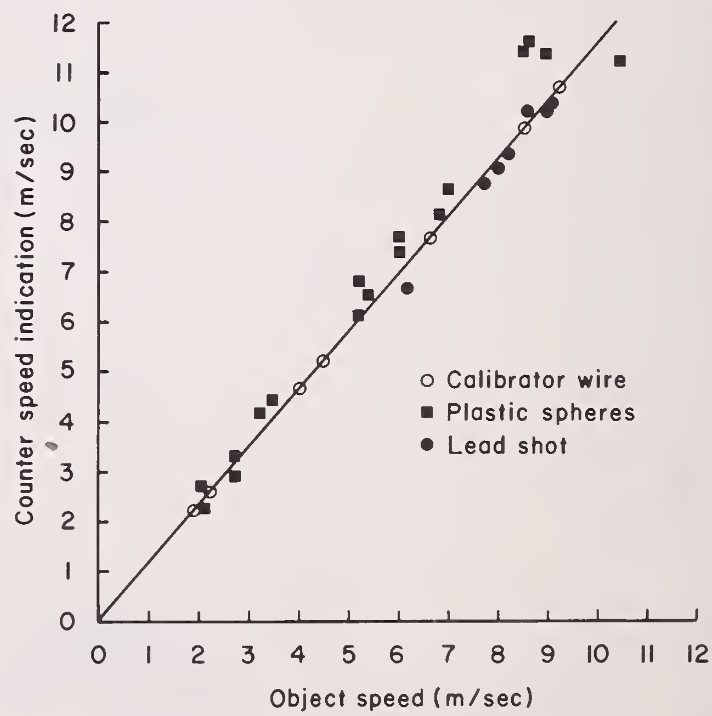

Figure 23.—Particle speed calibration (Schmidt and Holub 1971).

tion of the calibrator wire (fig. 24) through the counter, and measure pulse frequency to get the angular speed. This was converted to a tangential speed by carefully measuring the radius from the center of the calibrating wheel to the top of the sensing windows. Then, to more closely simulate particles, lead and plastic spheres were injected into an air jet which blew them through the counter near the center of the sampling area. A variable frequency strobe light produced multiple exposures of individual particles on photographic film. By measuring the image displacement, the speed was calculated from the known lamp firing frequency.

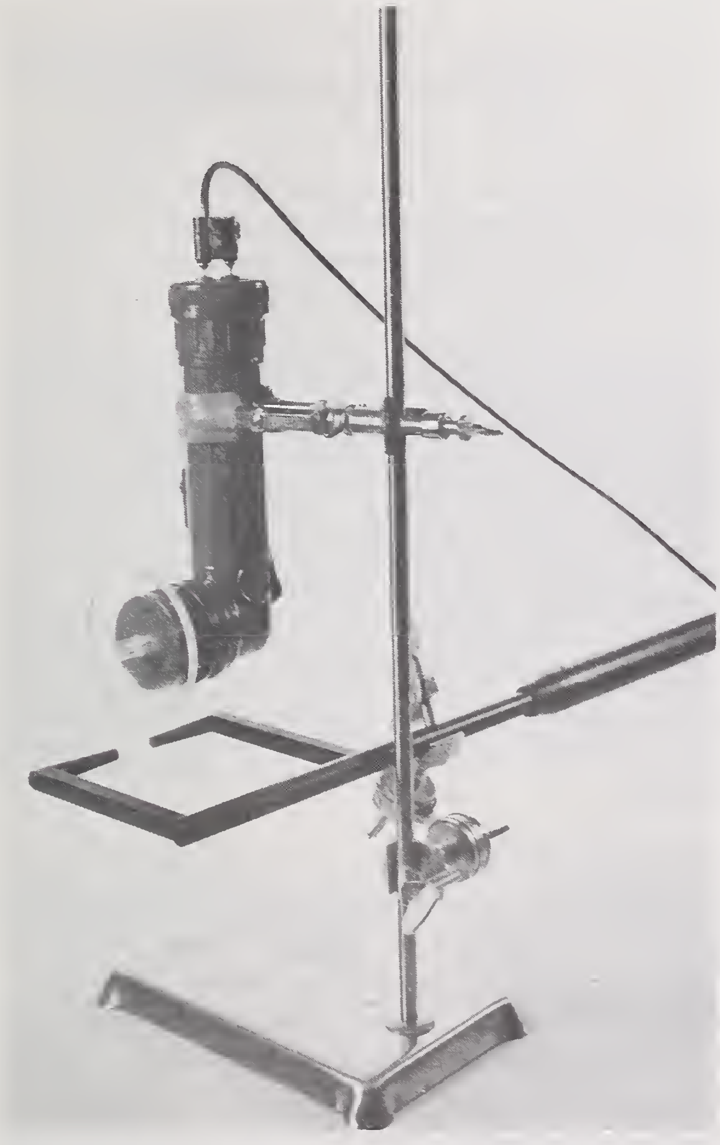

Figure 24.— Particle speed calibration apparatus.

Speed measurements depend to some extent on the voltage levels at which the electronic time interval counter is triggered on and off. Values in figure 23 were measured between +0.1 V on the rising limb of the positive pulse, and -0.1 V on the falling limb of the negative pulse. For these conditions, the horizontal component of particle speed is estimated by $S = 1730/t$, where t is the time interval in microseconds and S is in meters per second.

Because the shadows, and therefore the pulses, are less distinct near the lamp than near the windows, the indicated time interval along the light path varies by about 10%. As with the particle size estimates, data from the center of the path represent an average, and mean particle velocity should be estimated quite well. The variance of particle speeds would be overestimated, however.

Particle Frequency Estimates

Variations in sensitivity also make particle frequency measurements somewhat more complicated. If the peak signal generated by a particle is less than about 30 mV, then it is difficult to distinguish from the normal electrical noise generated by the sensor (fig. 8). Since small particles generate small signals, a greater percentage of signals from small particles are uncountable. Thus, for example, the frequency of blowing snow particles 50 cm above the surface will be underestimated more than particle frequency estimated at 10 cm; both will be underestimates of the true particle frequency.

From the response pattern at the center of the light path (fig. 11), the ratio of cutoff amplitude E_T to maximum signal E_M will give a corresponding sample area in which signal peaks will be greater than the trigger voltage E_T. Figure 14 gives the particle size corresponding to E_M, and the result (fig. 25) is a graph of effective sampling area for different particle sizes. Curves are plotted for both 30 and 40 mV trigger levels. From these curves, it is possible to correct particle number flux for the effect of trigger level, by the following procedure:

a. Determine particle size, for example 150μm;
b. Determine E_m from figure 14 (0.4 V for 150μm size);
c. Compute E_T/E_M where E_T is the trigger level (for $E_T = 0.04$ V, the 150μm example gives $E_T/E_M = 0.04/0.4 = 0.10$);

d. Enter the abscissa of figure 11b with this value of E_T/E_M and read the percentage of total sampling area from the ordinate (150μm particles should give signals above the trigger level over 70% of the sampling area);
e. Divide the measured flux, by this value (so, if 150μm particles were giving a measured signal frequency of 1,000 per second, the best estimate of particle flux would be 1,000/.70 or 1,430 particles/s/cm², assuming the total sensor sampling area was 1 cm²).

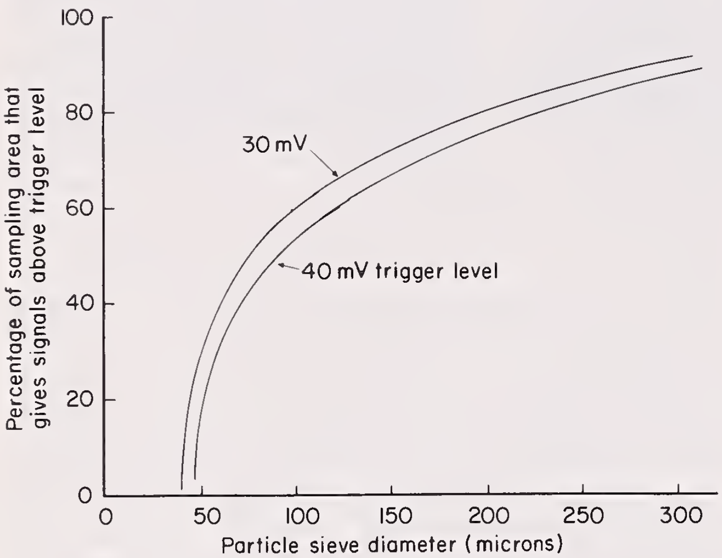

Figure 25.—Effect of trigger level on estimates of frequency, due to reduced sensitivity near the edges of the sampling area.

The snow particle counter gives estimates of particle frequency, size, and speed under conditions of natural blowing snow. It tends to underestimate particle frequency, and this tendency is more pronounced at greater heights above the surface. By additional processing, mean particle diameters for natural size distributions appear to be estimated within 10 μm. There is some trend toward underestimates, again, at the smaller sizes (greater instrument height). Particle speed is estimated quite well, at least in the mean.

The instrument is temperature compensated and will operate for a week or more without adjustment. The extent of the sampling volume limits its use, very near the surface, to low windspeeds, if single particle sampling is required.

Further development of the SPC will be directed toward (1) better measurements of particle size distributions, and (2) improved compensation to reduce long-term output drift. In cases where particle speed need not be measured, the sensor may be designed with only one slit, which should help realize these objectives. Eliminating the second slit would not only permit a better optical design and automatic gain control, but would also improve the sensor's single-particle frequency response, and thus provide better measurements near the surface. Mounting the SPC on a wind vane will also reduce measurement errors and attention required of the user.

The Blowing Snow Monitor

Developing an electronic system that produced continuous records of particle counter output gained much impetus from the work of Dr. R. D. Tabler. His recognition of the importance of sublimation from windblown snow led to a very successful design technique for drifting snow control (Tabler 1975). A close look at the sublimation process indicated temperature, humidity, and particle size were key factors (Schmidt 1971). Estimates of average temperature and humidity during wind-transport were facilitated by records from a drift trap that weighed drifting snow in a recording precipitation gage (Tabler and Jairell 1971). However, hope of gaining a measurement of average particle size caused us to pursue the electronic monitor.

Because the frequency response necessary to accurately record particle counter signals by frequency modulation on magnetic tape required fast tape speeds, recordings were limited to about 10 minutes on each tape. As a design objective, the desired monitor electronics would average particle counter signals, so, the results could be recorded on strip charts run as slowly as 1½ inches per hour. In concept, the blowing snow monitor would amplify the particle counter signal, and feed the amplified signal to an A.C. voltmeter and a frequency meter simultaneously. Outputs from these meters would be recorded on a two-channel strip chart (fig. 26). A prototype monitor system, tested during the 1971-72 blowing snow season in southeastern

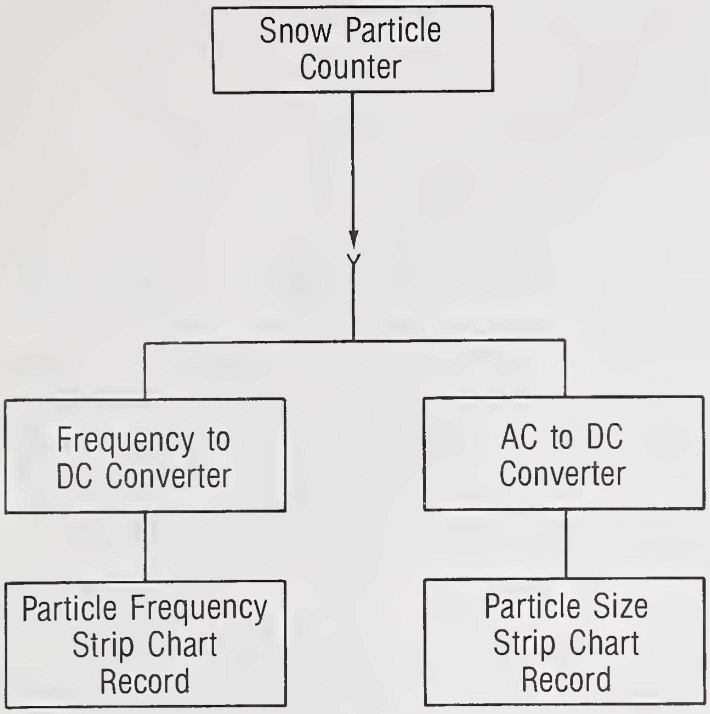

Figure 26.—Block diagram showing concept of the blowing snow monitor.

Wyoming, with the help of Tabler and Jairell, showed several weak points, including those already mentioned concerning the sensor. Nevertheless, an entire winter season of blowing snow records were obtained, and the concept of the monitor system was deemed sound. Design changes that adjusted averaging time and threshold or trigger level solved those problems associated with the monitoring electronics. The remainder of this section describes the electronics that were developed for the 1972-73 season and have been used since.

Particle Size Monitoring

That portion of the blowing snow monitor that produces a measure of average particle size consists of an input amplifier, an alternating-to-direct current converter, and a low pass filter to smooth the output (fig. 27). These operations are accomplished by three linear integrated circuit amplifiers. Diagram B1 in Appendix I, shows details of this circuit. The particle counter signal line is terminated by a 2K resistor, and coupled by capacitor to the input amplifier, thus blocking any direct current component of the signal that might result from an improper balance adjustment at the sensor. Voltage gain at the input amplifier is adjusted to 20, and the amplified signal is processed by both the particle size and particle frequency electronics.

The alternating pulses generated by the particle counter are rectified at amplifier A2 by a standard operational amplifier technique (Graeme et al. 1971). The low pass filter, A3, produces a slowly varying direct current output proportional to the particle counter amplitudes. Output at A3 is adjusted to a particular voltage when the particle counter signal is replaced by a sine wave of specific amplitude. This output is insensitive to input frequency over the range of particle frequencies measured.

Direct current output from a given peak or root-mean-square input is quite well predicted by the transfer functions of the circuit, as long as the input wave form is sinusoidal or at least uniform. For the pulse trains of variable amplitude and frequency generated by natural blowing snow, however, it was more expedient to deter-

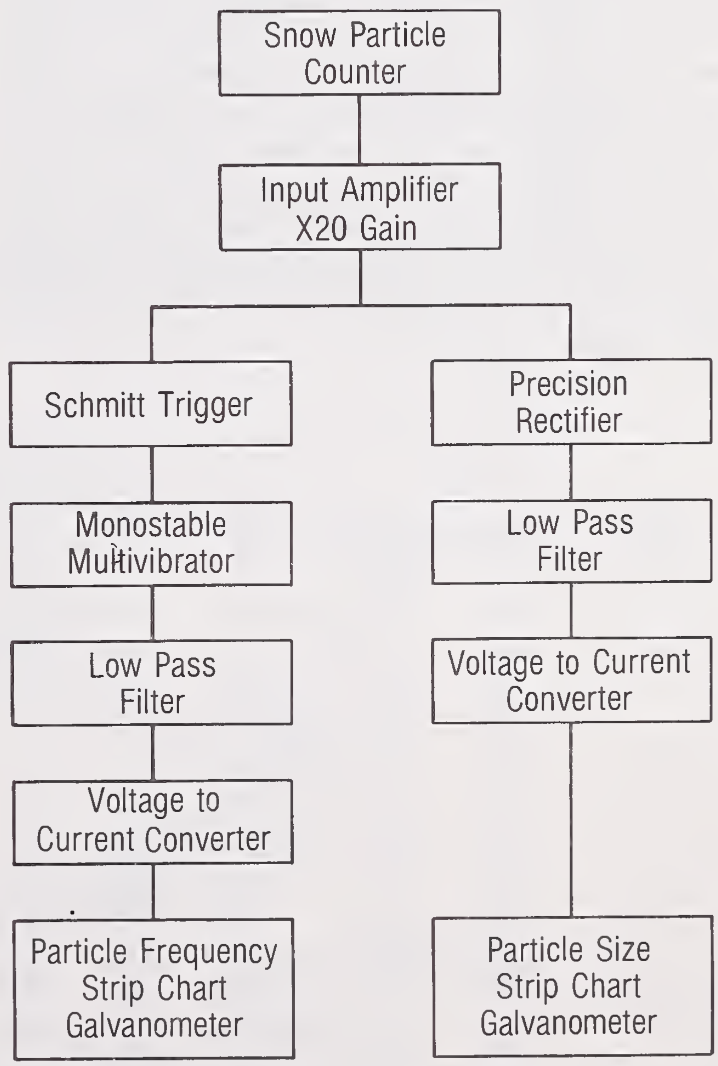

Figure 27.—An expanded block diagram showing the functions of the blowing snow monitor.

mine the relation of output voltage and mean particle diameter empirically. During 19 runs of about 10 minutes duration, the signals from two particle counters were recorded on magnetic tape, while corresponding outputs of the monitor electronics were recorded on strip charts. The particle counters, at 10 and 50 cm above the surface, sampled a variety of snow conditions during several blowing snow events in January and February 1972, in southeastern Wyoming. Average windspeeds at 10 m ranged from 9 to 22 m/s.

Experience with the prototype system determined the output level that allowed most blowing snow events to be recorded without exceeding full scale on the strip chart. Voltage gain at A3 was set to give a 1.0 V output when a 300 mV peak-to-peak sine wave replaced the particle counter signal. Tests verified a linear relation between sine wave amplitude and strip chart reading. For each 10-minute period of tape recording, an average strip chart indication was estimated by eye. Tape recorded signals from each particle counter were processed to yield estimates of mean particle diameter over the same 10-minute interval by the analysis procedure described in the first section of this paper. Data for all runs and both particle counters have been plotted in figure 28a. Table 2 presents dates, average windspeed 10 m above the surface, and remarks on conditions during these events.

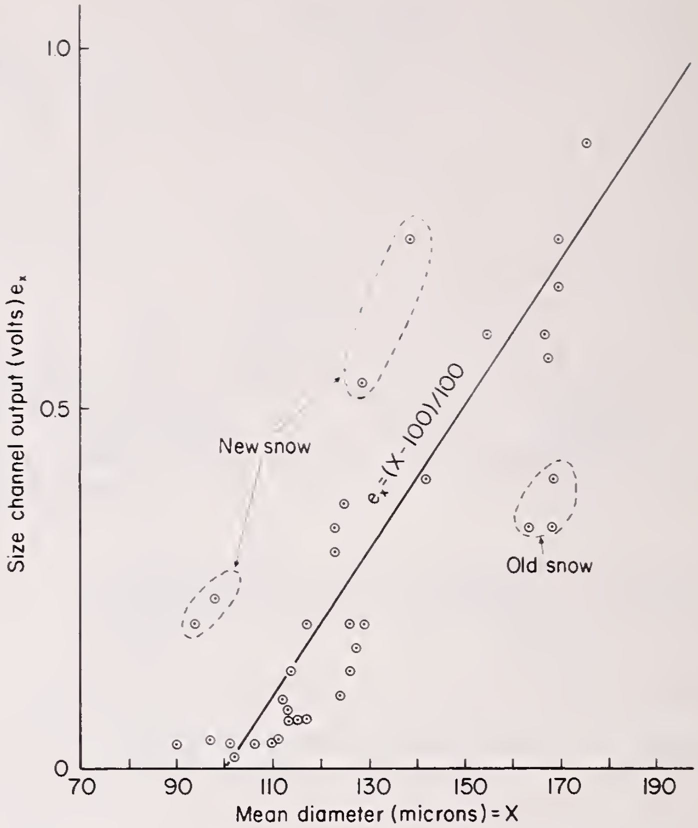

Figure 28a.—Initial calibration data for the size channel of the blowing snow monitor, based on 10-minute means of the strip chart record.

Although it is less precise than we hoped it would be, the strong relation of monitor output to estimated mean size appeared useful, and the line in figure 28a was chosen as a convenient approximation. Until average estimated size

Table 2.—Monitor system size calibration data

Day/Run	Start	Length	Mean windspeed	At 10 cm level: Total signals	At 10 cm level: Mean size	At 10 cm level: Level output	At 50 cm level: Total signals	At 50 cm level: Mean size	At 50 cm level: Level output	Remarks
	Hours	Seconds	m/s	10^3	Micron	Volts	10^3	Micron	Volts	
Jan. 13										
1	1645	790	15 7	865	142	0 37	231	113	0.07	Blowing snow, 24 hours old
Jan. 27										
1	1410	570	8 9	121	117	.07	30	102	02	Blowing snow only
2	1507	600	10 3	379	127	17	86	106	03	Less than 24 hours on ground
3	1522	660	11 2	467	129	.20	129	109	.03	Less than 24 hours on ground
4	1540	615	11 2	420	126	20	116	111	04	Less than 24 hours on ground
5	1605	585	8 9	310	114	13	112	97	04	Blowing snow and precip.
Jan. 28										
1	1700	800	15 6	943	155	60	414	117	20	Blowing snow only
2	1722	600	17 9	872	168	57	360	129	.20	Almost 48 hours since fall
3	1739	645	17 9	1163	167	60	433	126	20	Almost 48 hours since fall
4	1813	540	19 2	1239	170	67	622	123	30	Almost 48 hours since fall
5	1825	500	20 1	1271	170	73	637	123	.33	Almost 48 hours since fall
6	1842	540	22 3	1522	176	87	923	125	37	Almost 48 hours since fall
Feb 11										
1	1717	600	15 6	673	163	33	188	115	07	Old snow looks and sounds like
2	1740	800	15 6	932	168	33	247	113	07	sand
3	1804	900	16 5	1112	167	40	304	112	08	
Feb 14										
1	1715	680	14 3	1533	129	53	778	94	20	About 2 cm new snow on ground
2	1736	850	15 6	2740	139	73	1467	98	23	blowing
3	2150	760	8 9	364	126	13	111	101	03	Blowing snow and precip
Feb 25										
1	1644	660	8 9	191	124	10	34	90	03	Low level with precip

reaches 100 μm, the monitor output is slight. Above this, output increases in a somewhat linear fashion to a full-scale indication at an estimated 200 μm average diameter. Not all scatter in the data can be attributed to lack of experimental precision. Remarks in table 2 show that the snow being transported was notably different for runs giving the greatest scatter. Extreme points below the line (fig. 28a) were recorded from snow that subsequent examination showed to be like sand, both in the sounds it generated during transport and its size and granular quality. Points above the line tend to be from freshly fallen snow, which gives a large percentage of very small particles. Figure 29 compares the estimated size distributions for extreme data at 10 cm during two runs of equal average windspeed.

Tabler[2] suggested that a 10-minute sample time might be too long to show the expected parabolic relationship between mean particle diameter and size channel output voltage. New automatic data processing equipment provided average size and output voltage for 1-minute intervals of tape recorded particle counter signal, made during a single blowing snow event in 1974. Particle counter heights ranged from 5 to 100 cm. Tabler's suggestion was correct, and figure 28b gives a parabolic equation fitted by the method of least squares. The linear relation (fig. 28a) plotted as the dashed line in figure 28b, remains a good approximation and is used in analog computation of visual range.

[2]*Personal communication. 1971. USDA For. Serv., Rocky Mt. For. and Range Exp. Stn., Fort Collins, Colo.*

Particle Frequency Monitoring

A technique called time average frequency demodulation works well to produce a voltage proportional to particle frequency from the sensor signal (Graeme et al. 1971). Figure 27 (lower half) shows the concept of the technique in a block diagram, and schematic diagram B2 in Appendix I gives the circuit details. A linear integrated circuit amplifier, A1, and the Schmitt

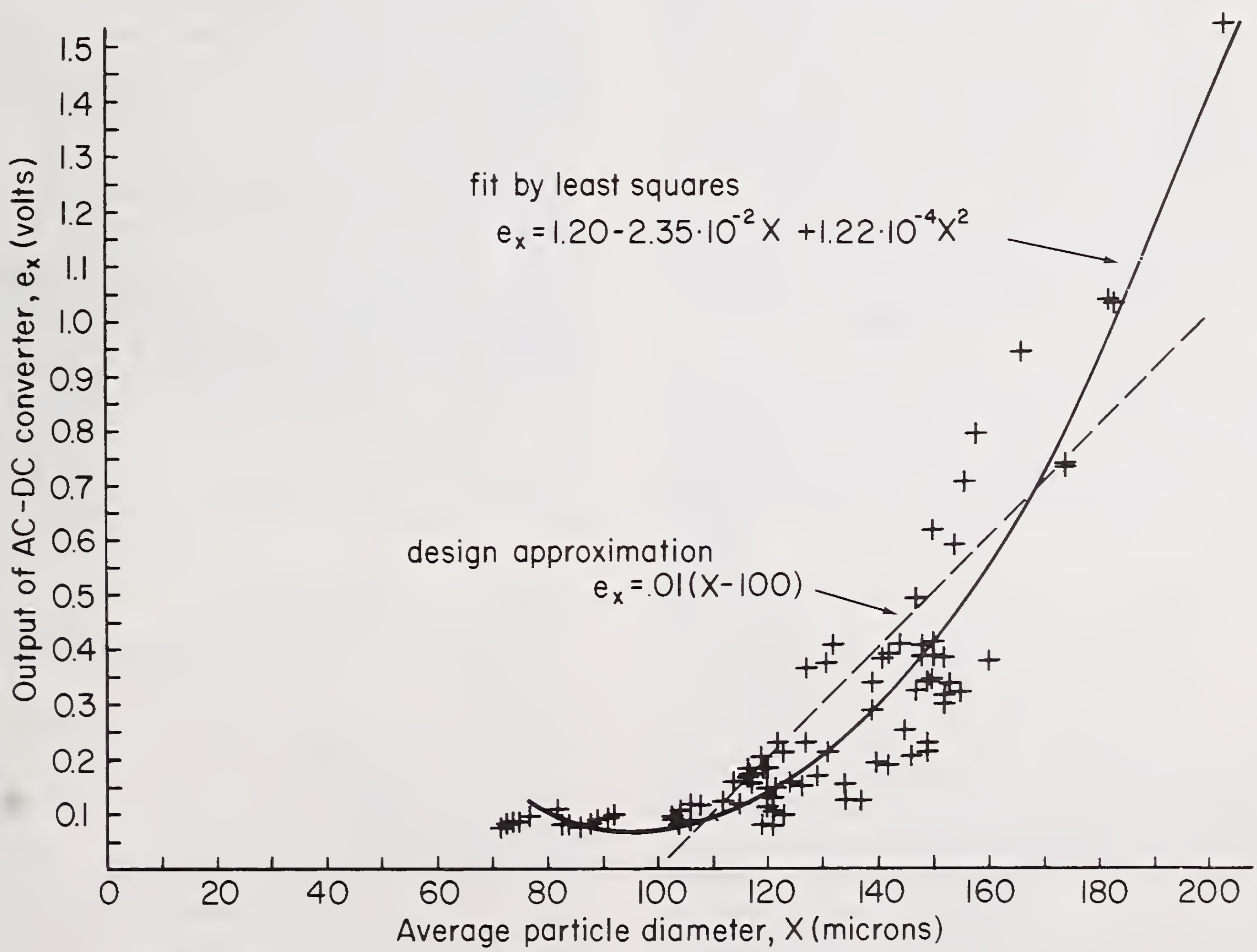

Figure 28b.—Revised calibration of the size channel output, using 1-minute means.

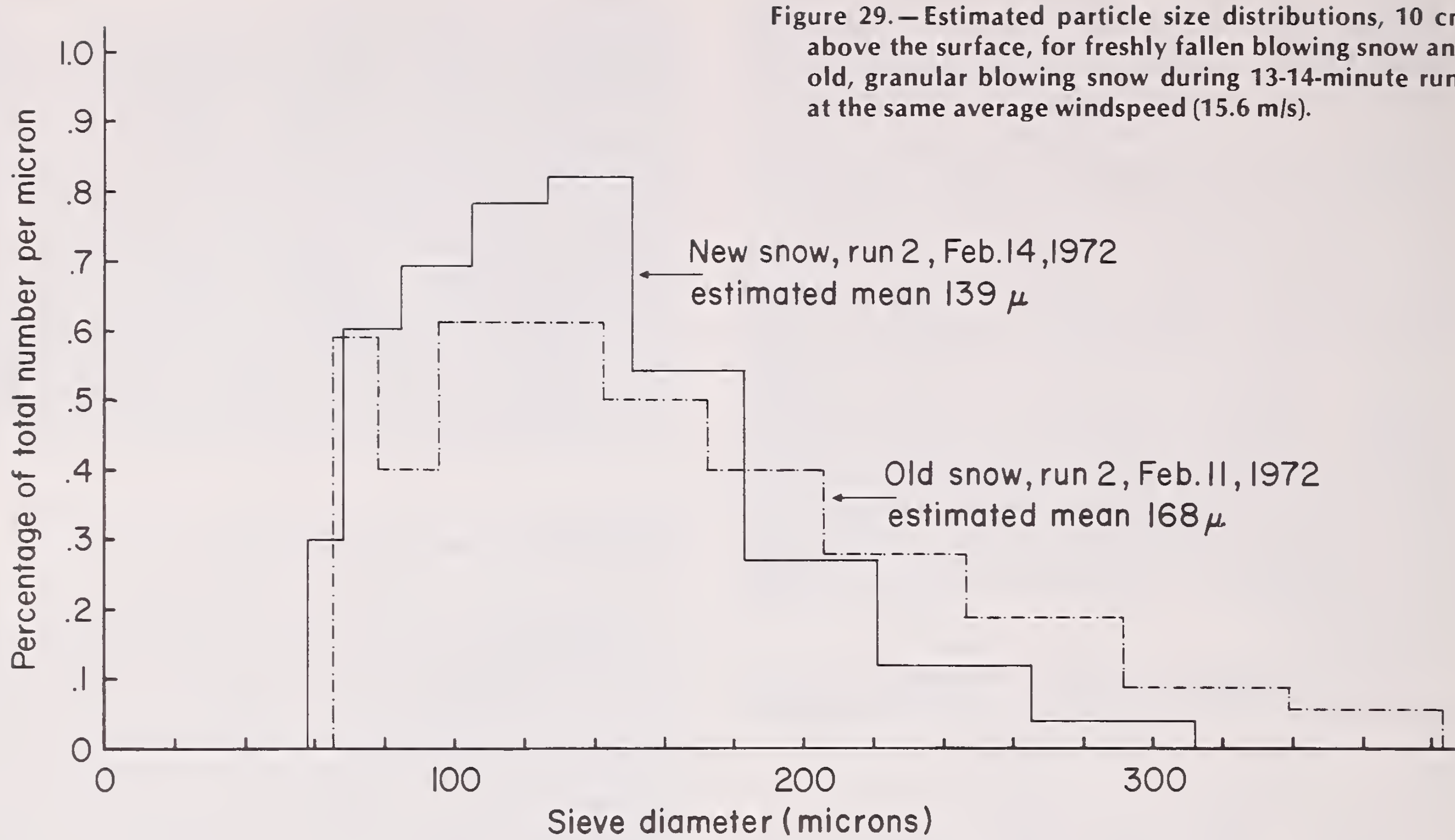

Figure 29.—Estimated particle size distributions, 10 cm above the surface, for freshly fallen blowing snow and old, granular blowing snow during 13-14-minute runs at the same average windspeed (15.6 m/s).

trigger U1 generate a pulse train corresponding to all signal pulses above the adjustable trigger level (reference). Each pulse from U1 triggers the monostable multivibrator U2, which generates a corresponding pulse of uniform width. The low pass filter A2 averages these pulses and produces a smoothed voltage that is a linear function of the input signal frequency. Amplifier A3 allows the output to be adjusted to zero when all signals are less than the threshold voltage.

Although monitor output voltage is a well-defined function of input signal frequency, the relationship with actual snow particle frequency is again complicated by the nonuniform sensor response, and the necessity of setting a threshold level for counting pulses. Average particle frequency estimated from the monitor strip chart appears to be just about twice the frequency computed by dividing the length of a tape recorder run into the total number of signals analyzed (fig. 30). It appears that the monitor electronics count double pulses caused by amplifier overshoot, while the MCA, with an adjustable rise time, ignores most of the double pulses. These data are from the same experiments that provided the data in table 2. Monitor frequency output was adjusted for a full-scale chart reading of 10,000 particles per second from the 10-cm sensor, and 5,000 particles per second at 50 cm. These settings gave less than full-scale indications for all but the most severe blowing snow conditions.

The particle counter does not give countable signals for all particles passing through the sensor area, and the monitor electronics apparently overestimates the true particle frequency. The degree to which these factors compensate depends on the distribution of particle sizes. If the monitor output voltage for particle

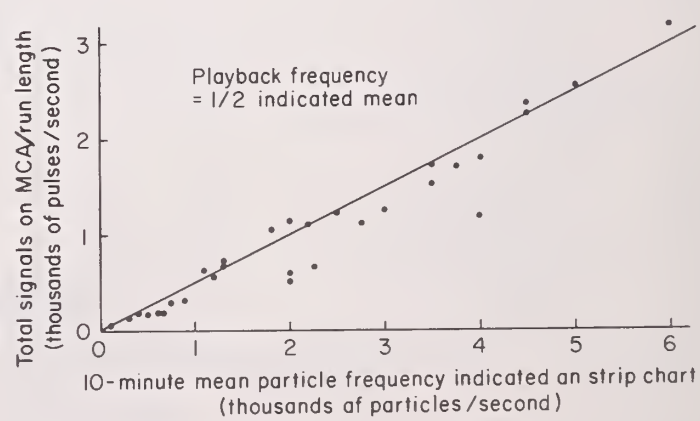

Figure 30.—Calibration data for the frequency channel of the blowing snow monitor.

frequency is denoted by e_f, and if e_f is adjusted to 10 volts for a calibration signal of 5 kHz, then the pulse frequency from the sensor is $f = (e_f \cdot 10^3)/2$. The corresponding estimate of particle number flux (number per second per square centimeter) must take account of the effective sampling area, A for different sizes of particles, so $F = f/A = (e_f \cdot 10^3)/2A$. Values of A are estimated from figure 14b, as fractions of the total sampling area (fig. 14a), as outlined in the procedure of the first part of this paper.

For example, if a blowing snow monitor is adjusted to measure frequency of signals above 40 mV then the trigger level is $E_t = 0.04$ V. By the equation for maximum signal (fig. 14), at 100 μm, $E_m = 0.2$V; at 150 μm, 0.41, and for 200 μm, $E_m = 0.63$. Tabler has pointed out that for small values of relative response, the curve in figure 14b is approximated by $A = .9927 \exp(-3.514\ E_t/E_m)$. The fraction, A of the total sampling area that gives signals above the noise level is 0.53, 0.69, and 0.82 for 100, 150, and 200 μm particles, respectively.

In the summary, the sensor sampling area is closer to a square centimeter than the 0.75 cm^2 assumed from the design geometry, so that $F = 1.33f$. But only part of this area gives countable pulses, depending on particle size, or $F = 1.33f/A$. Further, according to figure 30, the monitor voltage e_f predicts about twice the actual mean value of F, and since $f = (e_f \cdot 10^3)/2$ is predicted, $2F = 1.33\ (e_f \cdot 10^3)/2A$ or $F = 1.33 e_f \cdot 10^3/A$. When $A = 0.66$, the predicted value of f would correspond to the best estimate of particle frequency per unit area F. This would be expected for particles with diameters near 150 μm. Estimates would be about 10% high for 200 μm diameter particles and about 12% low for 100 μm particles.

Applications of the Blowing Snow Monitor

In spite of the limitations described in this section, the blowing snow monitor has been a useful research instrument that led us to formulate several new hypotheses, and provided data to test some old ones. The system records, first of all, the start, duration, and relative intensity of blowing snow. When combined with a record of windspeed, some picture of the interaction between snow particle size, frequency and windspeed can be sketched. But the most important application of this system was foreseen by Tabler. He suggested that measures of particle size, frequency, and windspeed could be combined to estimate visual range in blowing snow. With his encouragement, and that of the Wyoming Highway Department, I undertook development of a visual range monitor for blowing snow.

Monitoring Visual Range in Blowing Snow

If Interstate Highway 80 between Laramie and Rawlins, Wyo. had not presented such problems of traffic control caused by blowing snow, it is doubtful that the system described in this section would have come about. However, with the prospect of immediate research application, development and testing proceeded rapidly. The Wyoming Highway Department gave both encouragement and financial support. Circuit design began in November 1972, and field tests of a prototype system started in early February 1973 at a study site on I-80, 55 km west of Laramie, Wyo. Changes and improvements were made during the summer of 1973, and a system, of the form described here, was constructed during the fall of that year. On January 11, 1974, this system was installed near Arlington on I-80. Data continuously transmitted to Laramie were recorded in the radio dispatcher's office of the Wyoming Highway Department. The fact that conditions indicated on the chart agreed with the impressions of patrolmen and maintenance people led to use of visual range data in traffic control decisions on I-80.

Theory of Visibility in Blowing Snow

Middleton (1952) provides an interesting review of work on visibility. Both Lillesaeter (1965) and Mellor (1966) report measurement of visual attenuation by falling snow. For blowing snow, Liljequist (1957) observed visibility in relation to windspeed. By assuming the same distribution of particle sizes for all cases, he developed the hypothesis that visibility was in-

versely proportional to drift density (the mass of snow per unit volume of air), at eye level. Budd et al. (1966) used direct measurements of drift to verify Liljequist's hypothesis, and reported that as an average, $V = 100/n_{200}$ where V is visibility in meters and n_{200} is the drift density in grams per cubic meter, 2 m above the surface.

As Mellor (1966) points out, the attenuation of light by blowing snow is actually proportional to the scattering cross section of the particles, which is equal to their projected area, and the relation to mass is only valid if the size distribution remains the same. The Byrd data (Budd et al. 1966) indicate that this relation is valid. However, the situation changes when snowfall occurs with blowing snow, and also when snow available for transport is limited. The argument presented below (Middleton 1952, Mellor 1966) takes account of possible variability in particle size.

The attenuation of visible light by blowing snow lies within the domain of geometric optics, since

$$X/\lambda >> 1$$

where X is particle diameter, and λ is wavelength (snow particles are typically of the order of 100μm in diameter, while the visible light spectrum encompasses wavelengths of 0.4 to 0.7μm; therefore, $X \doteq 100\lambda$). Absorption of light is significant only when $X/\lambda >> 1$.

If each particle within a parallel beam of light with cross-section area A has an "attenuation cross-section" a, then the fraction of the light flux removed by each of the particles is a/A, assuming $A >> a$. If the sum of all particle cross-sections per unit volumes

$$\sigma = \Sigma a$$

then the sum of particles over length dL along the beam is σ A dL. When P is the light flux per unit cross-section of the beam, then the total flux PA will be reduced in distance dL by

$$\frac{\sigma A\, dL}{A} \cdot PA = \sigma PA\, dL$$

Therefore, $dP = -P\,\sigma\, dL$

and integrating, $P = Po\, e^{-\sigma L}$

where Po is the flux at zero distance from the light source. Signal level at any distance L relative to the signal level at zero distance is

$$P/Po = e^{-\sigma L}$$

The contrast C between an object of luminance B and a background with luminance B′, as viewed from a given point, is expressed as

$$C = \frac{B' - B}{B'}$$

Assuming attenuation by absorption to be negligible, Middleton (1952, p. 104) gives the contrast of a black object viewed against the horizon sky as

$$C_L = e^{-\sigma L}, \text{ or } \ln C_L = -\sigma L$$

where L is the distance between observer and object, and σ is the total cross-section per unit volume.

Liminal contrast (C_e) is defined as the observer's threshold of contrast, below which the object is not discernible against the background. This value is reported by Middleton (1952) to be between 0.01 and 0.03. The "observer's (maximum) visual range," V, is defined as that distance at which $C = C_e$, thus,

$$V = \frac{-\ln C_e}{\sigma}$$

Assuming spherical particles of uniform diameter

$$\sigma = na = n\,\pi X^2/4$$

where n is the number of particles per unit volume, and X is the particle diameter. Therefore,

$$V = \frac{-4 \ln C_e}{\pi n X^2}$$

For a liminal contrast equal to 0.02, then

$$V = 5/(n X^2)$$

Particle frequency F (number of particles per second per unit area) may be expressed as

$$F = nU_p$$

where U_p is particle speed. Assuming U_p equal to windspeed U,

$$V = 5 U/(F X^2)$$

Visual range is thus seen to be inversely proportional to particle frequency and the square of particle diameter.

The Visual Range Computer

Our objective was to design an electronic system that would compute visual range in blowing snow from the particle counter signals and the output of an anemometer (fig. 31). The desired result was a slow-speed strip chart record that could aid in traffic control. It seemed expedient to use analog techniques for our purposes. Thus, from voltages proportional to windspeed, particle size, and frequency, visual range would be computed by the relationship developed from theory. The system would be field tested to verify the usefulness of this analogy.

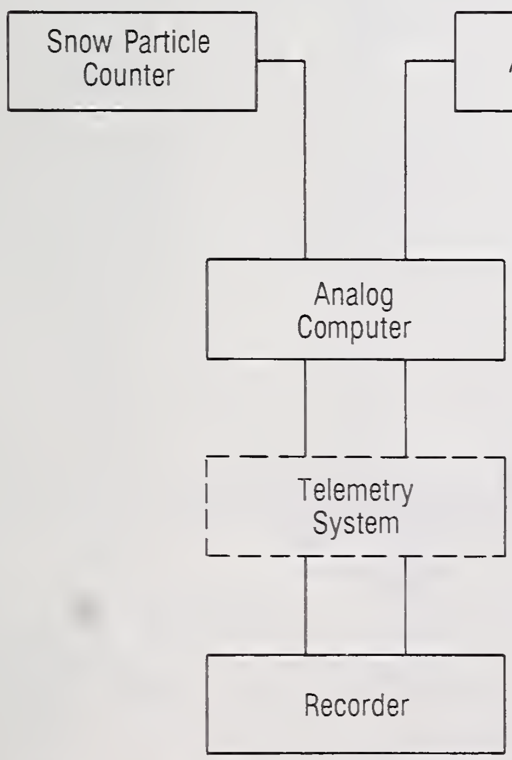

Figure 31.—Conceptual block diagram of the visual range monitor for blowing snow.

Visual range can vary from zero to infinity by definition and in actuality, from less than a meter to 100 km or more. The range of greatest interest for traffic control, however, is from about 30 to 300 m. To display this range effectively on a strip chart, it is convenient to produce a voltage proportional to the reciprocal of visual range. For our visual range monitor, then, a voltage $e_v = K/V$ was the desired output. Particle size was estimated by the output voltage e_x from the blowing snow monitor. Since this voltage is roughly proportional to particle size X from 100 to 200 μm, the relationship is $X = 100 (e_x+1)$. The analog voltage e_f, proportional to particle frequency F is also produced by the blowing snow monitor electronics.

An electrical analogy to the reciprocal visual range in blowing snow is thus

$$e_v = \frac{C\, e_f(e_x + 1)^2}{e_u}$$

where C is a scale factor, or proportionally constant. For microcircuit analog computation, a 0 to 10-V operating range is standard. Some scaling was required to keep outputs within the range the analog function modules used to perform the squaring, multiplication, and division. Further scaling is necessary to compensate for the difference between theoretical and optimum instrument heights, and to allow adjustments in cases where a sensor location later proves to be unrepresentative of conditions in the area to be monitored.

The following description of the circuits that perform the visual range computation proceeds from simple to detailed in three levels. The first level of understanding is aided by a simplified block diagram (fig. 32) that shows how the two sensor signals are combined to produce a voltage representing the reciprocal of visual range. Then this description is expanded to show the control, calibration, and recording functions (fig. 33). Finally, actual circuit details are explained using schematic diagrams included in the appendix.

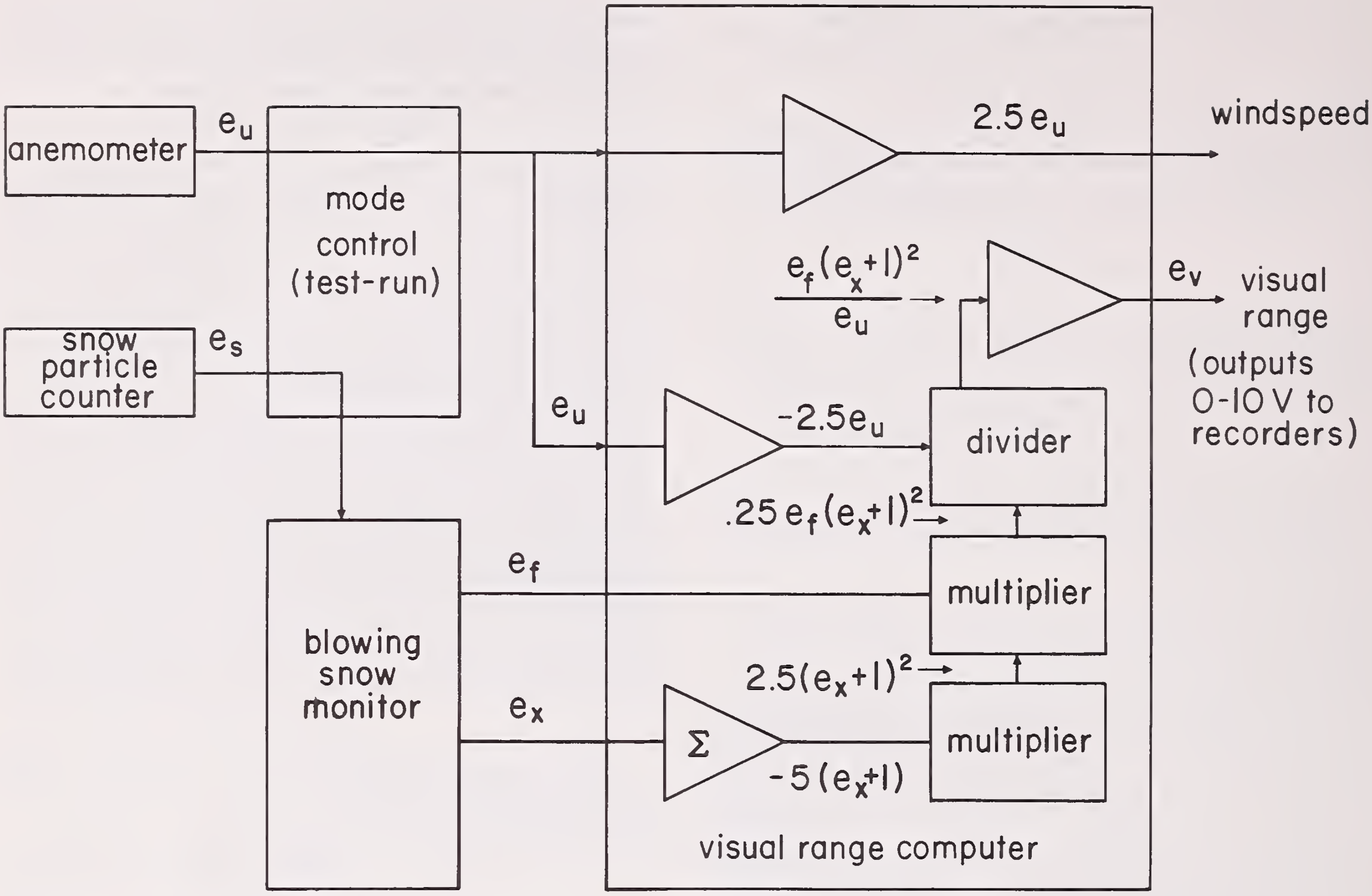

Figure 32. — Simplified block diagram of the VRM.

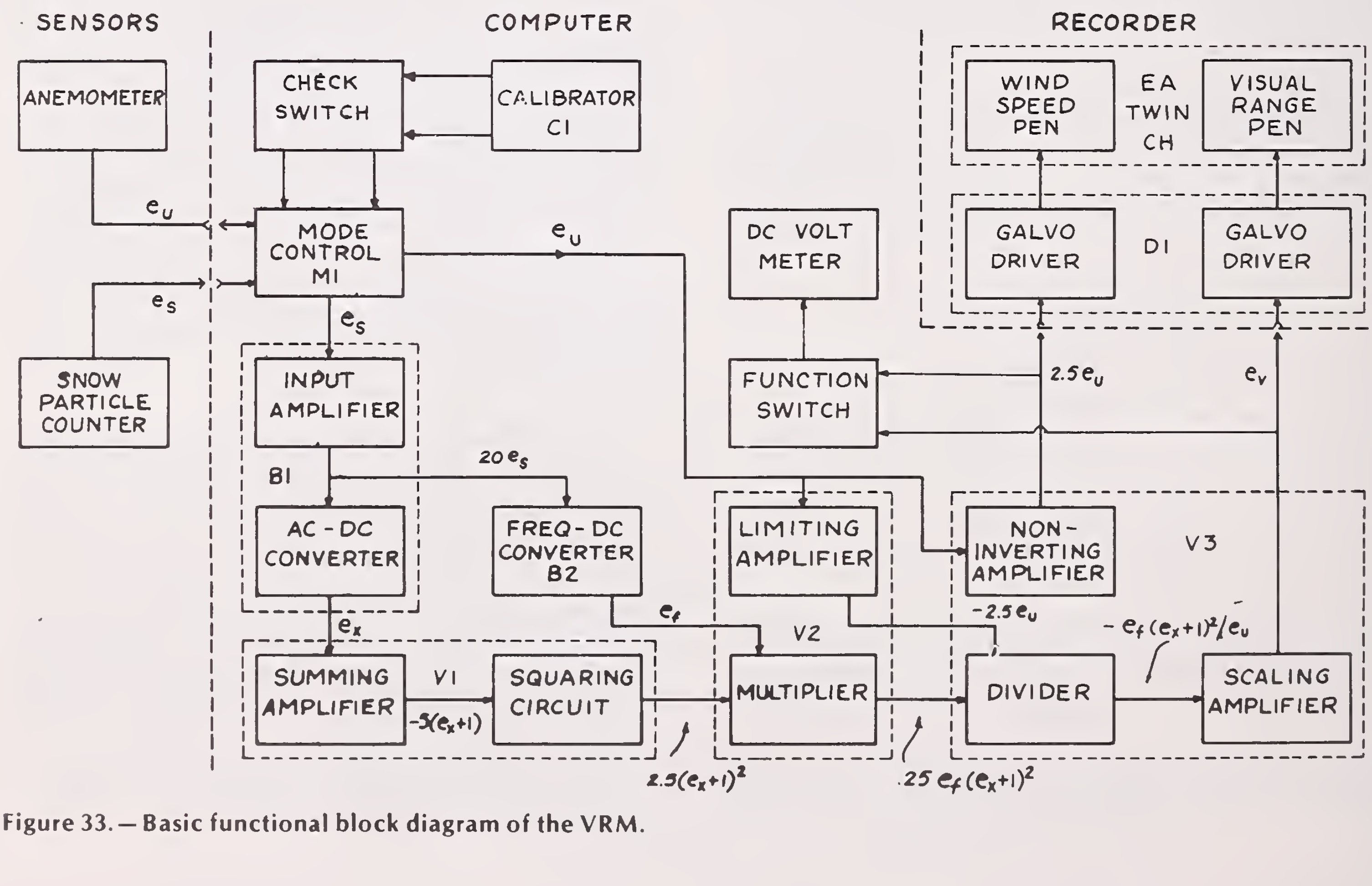

Figure 33. — Basic functional block diagram of the VRM.

In figure 32, the particle counter signal e_s is processed by the blowing snow monitor (printed circuits B1 and B2) which produces particle size and frequency signals (e_x and e_f, respectively). This operation was described in the preceding section. These signals, and the windspeed voltage from the anemometer e_u, enter the VRM computer. Its first operation is to add 1 volt to e_x and square this sum, using a multiplier. This result is multiplied by e_f. To make e_u an input compatible with the divider function module, the windspeed voltage is multiplied by -2.5 with an inverting amplifier. The divider produces the ratio, which is scaled by a final amplifier to give the desired reciprocal.

The second level of detail is shown by the expanded block diagram (fig. 33). To provide a self-calibration feature, the sensor signals are channeled through a mode control card (M1) which disconnects these signals and replaces them with internal calibrator signals in the "test" mode. The function switch connects the computer outputs to a voltmeter to help the operator check system performance. Windspeed and visual range output voltages are converted to current outputs by the galvanometer drivers (D1) to drive the pens of the strip chart recorders.

The summing and squaring circuit is printed circuit card V1. The wiper of R3 is adjusted to provide 1.0 V at test point 3. Amplifier A1 simultaneously sums this fixed voltage and the particle size voltage e_x, and amplifies the result by -5 to give the voltage $-5(e_x+1)$ at the squaring module M1. This multiplier gives the output voltage $2.5(e_x+1)^2$, which is proportional to the average particle scattering area.

Two functions are performed by printed circuit V2. Multiplier V2M1 produces the product of the frequency voltage e_f and the $2.5(e_x+1)^2$ output from V1, internally scaling by 1/10 to give $0.25\ e_f(e_x+1)^2$. The second function is amplification of the windspeed voltage to provide $-2.5\ e_u$ as output at A1. The circuit limits the output to -1.0 V as e_u goes to zero, to avoid the undefined operation of division by zero at the final divider V3M1. The anemometer response time is also damped by V2C1, to match the time response of circuits B1 and B2.

Printed circuit V3 computes the voltage $-e_f(e_x+1)^2/e_u$ at the output of V3M1. This ratio is scaled by the final coefficient at V3A1 to give the voltage proportional to the reciprocal of visual range, e_v. To provide a windspeed output that is not limited and damped, amplifier V3A2 provides $2.5\ e_u$ for recording.

Response of several parts of the computer to a set input is shown by figure 34. The matching of

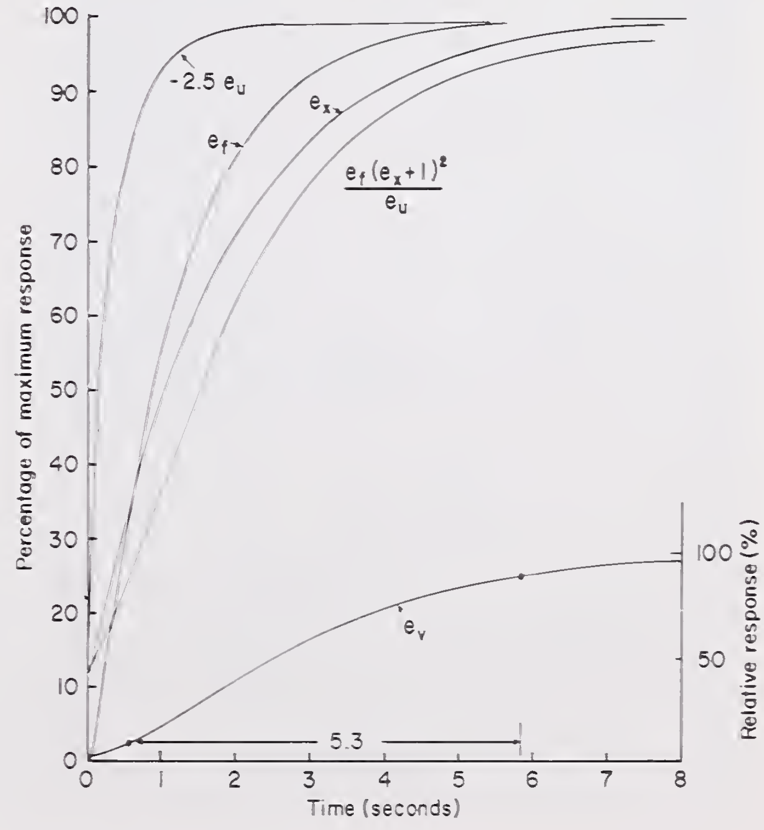

Figure 34.—Computer response times to step input.

windspeed to particle size and frequency signals is important to accurate computation. The figure shows that rise time from 10 to 90% of final output is about 5 seconds, with e_x the most damped of the input signals. Although closer matching could be obtained between rise times of the input voltages, in practice, the computer seems to perform well.

The VRM computer was designed to give an output voltage e_v related to the input voltages by

$$e_v = C\, e_f\, (e_x + 1)^2 / e_u$$

Scaling factor C can be predicted from the theoretical relationship for visual range

$$V = 5U/FX^2$$

and the calibrations that relate factors U, F, and X to corresponding input voltages e_u, e_f, and e_x. Since $e_v = K/V$,

$$C = \frac{K}{V} \; \frac{e_u}{e_f\,(e_x + 1)^2}$$

or

$$C = \frac{K}{5} \; \frac{F/e_f \quad X^2/(e_x + 1)^2}{(U/e_u)}$$

Assuming the particle counter estimates frequency f for a 0.75-cm^2 area, then the frequency per square centimeter, F is f/0.75. The monitor electronics provides the voltage e_f equal to 10 V when f = 5,000 particles per second, so that $f/e_f = (500/0.75)/cm^2/s/V$ or $F/e_f = 667/cm^2/s/V$. If the linear approximation for the particle size calibration is used, average diameter X (in centimeters) is related to voltage e_x by $X = 0.01\,(e_x + 1)$. The value of U called for by the equation is the windspeed at the observer's eye level. However, the standard measurement height (10 m) is desirable to reduce the influence of local small scale obstacles on the windspeed, and to make this data comparable with other meteorological stations. At the same time, experiments with the blowing snow monitor indicated that the snow particle counter responded to the widest range of drifting intensity when it was positioned at 50 cm above the surface. For the theoretical evaluation of the scaling factor, C, the windspeed measured at 10 m was reduced according to the 1/7 power law profile to give the wind speed at 50 cm. If U_{10} is the measured windspeed, then $U_{10}/U_{0.5} = (10/0.5)^{1/7}$, so the value of U is $U = 0.652U_{10}$. For the anemometer used, the calibration was linear with 4.0 V output at 100 miles per hour, so $U_{10}/e_u = 1{,}118$ (cm/s)/V. Thus $U/e_u = 729$ (cm/s)/V. Substituting these calibrations into the equation for C gives a predicted value of $C = 1.12\ (V^{-1})$ when the value, K = 610 (meter volt) is chosen to give an output voltage $e_v = 10.0$ V when visual range is reduced to V = 61 m (200 feet).

Designing a system according to these criteria was equivalent to formulating the following hypothesis: An observer's visual range in blowing snow can be measured by an electronic system that solves the equation $V = 5U/FX^2$. This equation is derived by assuming:

a. light attenuation in blowing snow follows the laws of geometric optics;
b. particles are ice spheres of uniform diameter;
c. snow particle frequency and size are adequately represented by a snow particle counter at 50 cm above the surface; and
d. windspeed can be measured at the 10-m level.

Given these assumptions, and the errors associated with electronic circuitry, we were very anxious to calibrate the system.

Field Tests of the VRM

To determine the proper constant of proportionality, and the reliability of this system, we ran a series of experiments with a set of black visual targets, each about 1.5 m high (fig. 35). Target width increased with distance from the instrument building so that visual angle was constant at about ½ degree. The distance between targets increased geometrically along a line nearly perpendicular to the average wind direction during snowdrifting events. Anemometer height was 10 m, and blowing snow was measured with the SPC at 50 cm above the snow or ground surface. The instruments were supported on separate masts, about 30 m apart.

Visibility in blowing snow gives an impression somewhat like the view through a white

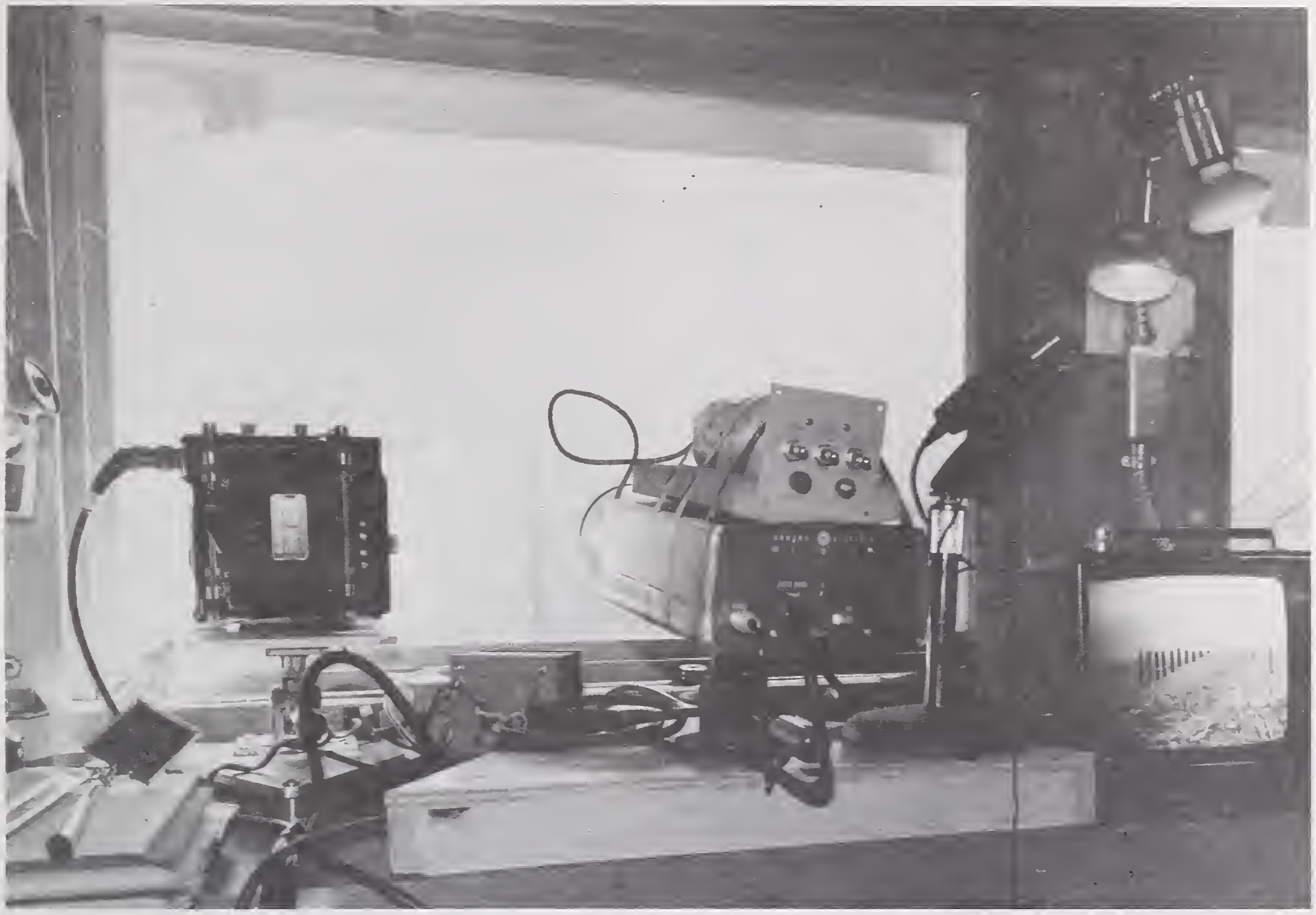

Figure 35.—Photograph of VRM calibration array from the instrument building.

picket fence, while riding a bicycle down the sidewalk. That is, the snow moves in plumes that obscure vision momentarily, so that visual range is a rapidly varying function of time. With the observer's optical senses doing a lot of averaging, and perhaps introducing some persistence to the observation, it is difficult to compare the average output of the VRM with true visual range of an observer.

A closed circuit television system helped in making this comparison, since the video tape could be replayed and stopped. First, to ascertain that the camera's visual range in blowing snow was comparable to an observer's, Tabler recorded his observations of maximum visible target on the audio track of the video tape, and compared these with the visual image during playback. Since the television range was almost identical with his observations, the camera was used to record visual range while he read values of the input voltages e_x, e_f, and windspeed onto

the audio track. During replay, the values were tabulated, and averaged to provide the data in figure 36. From these observations, a design point was chosen at $e_f(e_x + 1)^2/e_u = 7.0$ volts for $V = 200$ feet. The desired computer output was $e_v = 10.0$ volts at $V = 200$ feet.

$$C = \frac{e_v}{e_f(e_x + 1)^2/e_u} = \frac{10.0}{7.0} = 1.43$$

This value is about 1.3 times that estimated from the theoretical analysis and electronic scaling equations. The reasons for this difference are still being investigated, primarily out of academic concern. The fact that the theoretical curve in figure 36 falls outside the estimated maximum probable error computed for values at 525 feet is of more consequence, since the computer indicates visual range is about 200 feet less than the actual observed value. Although this difference could be minimized by statistically determining the design point, estimated visual range at 200 feet was deemed more critical, so, the system was tested operationally with the calibration shown.

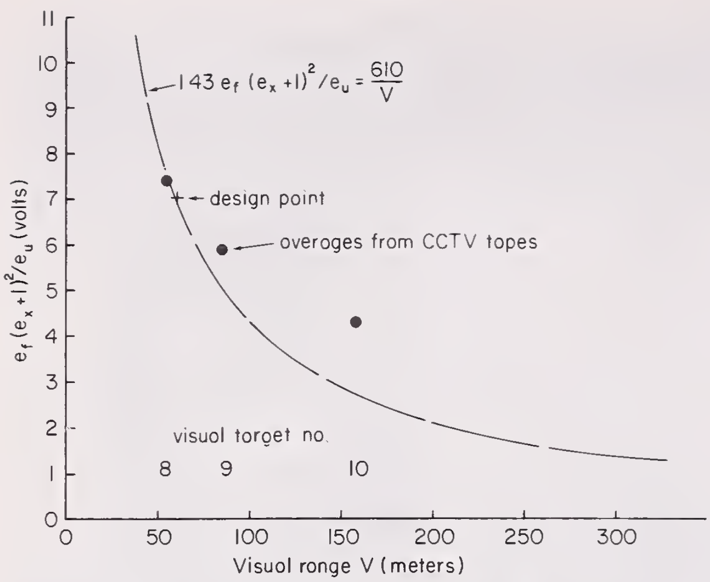

Figure 36. — Initial data for scaling the VRM output.

Comparisons of indicated and observed visual range during the remaining 1972-73 snowdrifting season showed the computer estimates were much better than expected from figure 36. More recent analysis of VRM records

Figure 37. — Arlington visual range monitor station. The SPC is on a short pipe mast on the extreme right of the picture.

shows that the system gives results very comparable to the observations of Liljequist (1957) and Budd et al. (1966), under similar conditions of snow availability. However, because particle size is included as input to the system, better estimates of visual range during snowfall are obtained. Further, the system may provide some possibilities for forecasting changes in visibility.

Application of the VRM System

In January 1974, the Wyoming Highway Department installed an operational VRM system on Interstate Highway 80 near Arlington, about 60 km west of Laramie. Their objective was to test the usefulness of the system for providing input data to traffic control and highway maintenance decisions. Data from the instrument site (fig. 37) were telemetered by radio, microwave, and telephone land line to the district maintenance office in Laramie. Frequent calibration checks showed the system was very stable, and required little adjustment. Calibration of the snow particle counter at 2-week intervals and lamp replacement once a month appeared to be sufficient maintenance.

Reports from patrolmen and snowplow operators were noted on the VRM strip charts by the radio dispatcher. Analysis of this record over 3 years indicates that the system gives a reliable indication of road conditions in the vicinity of the monitor station. A second station, near Elk Mountain, extended this type of monitoring, beginning in 1975.

As with most instruments, experience in evaluating the record is required before a person can make the best use of this system. Examples of several records show how VRM data are interpreted.

Figure 38 follows an actual drifting event (February 18-19, 1973; I-80, mile post 231) from beginning to end. During this case study, both lanes were closed to traffic due to poor visibility and hazardous driving conditions.

Moderate snowfall and light winds (9 to 12 m/s) were observed prior to the event. The VRM signal, showing only occasional low-level spikes, is typical while snow is falling with little accompanying wind. At about 5:30 p.m. on February 18, windspeed began a steady increase, reaching about 40 mi/hr by 6 p.m. New (fresh) snow particles are relatively large in diameter until they are mechanically abraded during relocation by the wind. Because they are usually quite delicate in their intricate form, however, they quickly fragment into a tremendous number of small ice particles. As a result, severely reduced visual range accompanied stronger winds; visibility was reduced to as little as 225 feet with a wind gust of only 45 mi/hr. The conditions recorded between 5:50 and 6:40 p.m. were sufficiently severe to cause the road to be closed to traffic (this statement should not be construed as implying a standard for traffic control decisions, however).

Figure 38 suggests the fresh snow particles had been mechanically reduced to a quasi-equilibrium size by about 6:40 p.m., some 50 minutes after the event began: from this point on, the relationship between visual range and windspeed was constant.

As a qualitative reference only, visibility conditions between 6:40 and 7:50 p.m. (fig. 38) would be termed hazardous, or marginal with respect to satisfactory traffic flow. The event ended at about 1:30 a.m. on February 19 because winds diminished rather than due to a lack of snow on the ground.

Figure 39 is an example of the VRM record when visibility improves as the snow on the ground is depleted. Air temperatures during this example ranged from −1° to +2°C, and skies were clear.

Conclusions

The visual range monitor (VRM) system is a useful, reliable indicator of visual range in blowing snow that already has been applied to highway maintenance and control operations. Tabler is presently developing a forecasting procedure to be used for a system in which two VRM's provide input to a computer that analyzes conditions, alerts road maintenance personnel to forecast wind and visibility problems, and, with the operator's approval, relays warnings and control decisions to the highway users via large, remotely controlled signs.

Detailed studies of the interrelations among particle frequency, size, and windspeed indicate

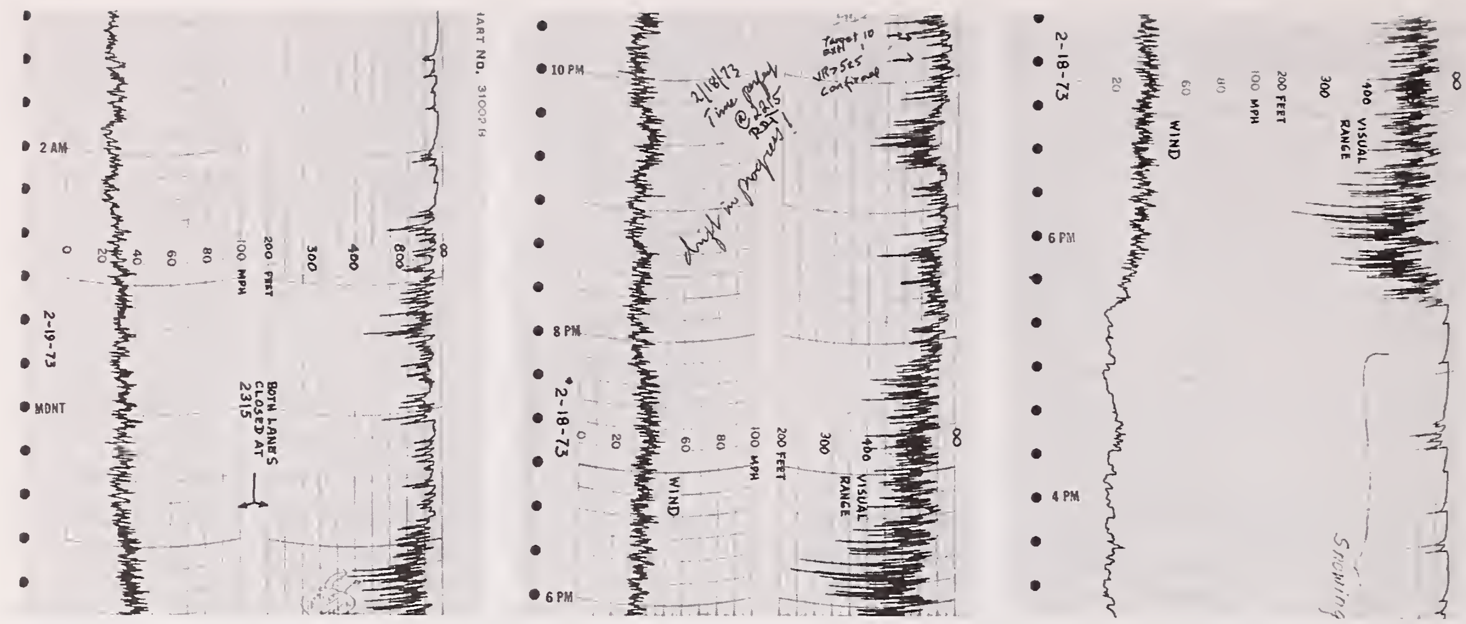

Figure 38.—Record from VRM during a blowing snow event, February 18-19, 1973 at Cooper Cover, Wyo.

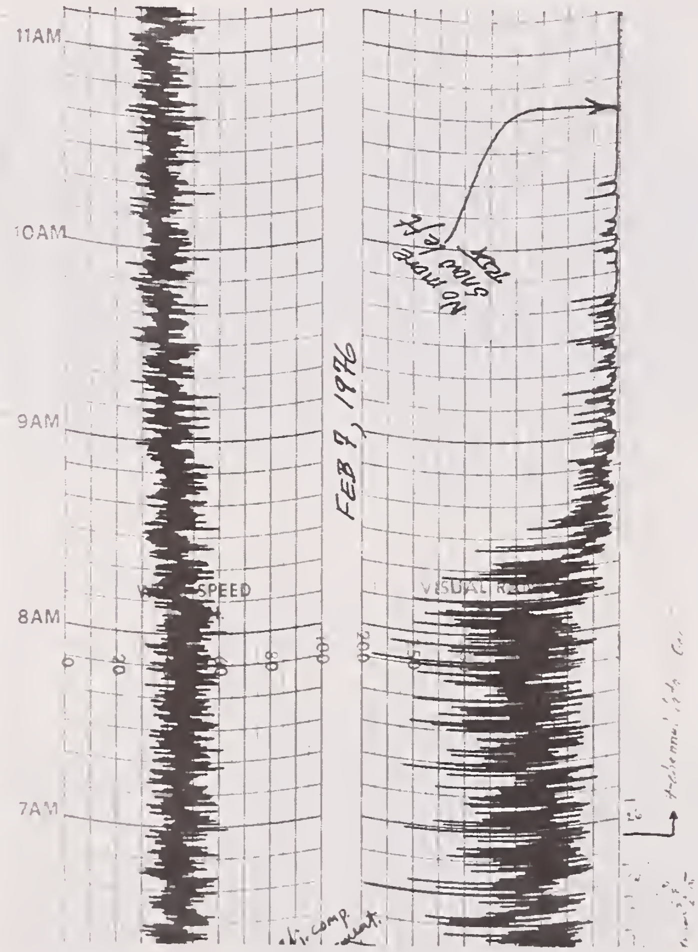

Figure 39.—An example of the VRM record when visibility improves even though windspeed remains high (note gust of 55 to 60 mi/hr between 9 and 10 a.m.). In this case, the visual range increase coincided with an increase in air temperature to near 0°C levels. Similar records are produced when either the ground or hard old snow surface is uncovered.

that the snow particle counter (SPC) may be used to detect precipitation during blowing snow. If this expectation becomes a reality, the device will find still more uses in blowing snow research and management. Prediction of avalanche "loading" by windblown snow is one exciting example.

Literature Cited

Bliss, J. 1971. Theory and characteristics of phototransistors. Application Note 440, 12 p. Motorola Semiconductor Prod., Inc.

Budd, W. F., W. R. J. Dingle, and U. Radok. 1966. The Byrd snowdrift project. Outline and basic results. *In* Stud. in Antarc. Meteorol. vol. 9. Antarct. Res. Ser. NAS-NRC Publ. 1482. Am. Geophys. Union, Wash., D.C.

Graeme, J. G. 1972. Op amp boosts phototransistor speed. Electron. Design. March 2.

Graeme, J. G., G. E. Tobey, and L. P. Huelsman (eds.). 1971. Operational Amplifiers, Design and Applications. 473 p. McGraw-Hill, N.Y.

Hollung, O., W. E. Rogers, and J. A. Businger. 1966. Development of a system to measure the density of drifting snow. Joint Tech. Rep., Dep. Elec. Eng., Dep. Atmos. Sci., Univ. Wash., Seattle. 54 p.

Landon-Smith, I. H., and B. Woodberry. 1965. The photoelectric metering of windblown snow. Interim Rep. Series A(IV), Glaciol., Publ. 79, 18 p. Antarctic Div. Dep. External Aff., Melbourne, Australia.

Liljequist, G. 1957. Energy exchange of an Antarctic snowfield, Borwegian-British-Swedish Antarctic Expeditions 1949-1952. Sci. Results, vol. II, part 1C. Oslo, Norway.

Lillesaeter, O. 1965. Attenuation of a parallel beam of light, particularly by snow. Stormy Weather Group. Sci. Rep. MW-43 McGill Univ.

Mellor, M. 1966. Light scattering and particle aggregation in snow storms. Cold Reg. Res. and Eng. Lab. Res. Rep. 193, 16 p. Corps Eng., U.S. Army, Hanover, N.H.

Middleton, W. E. K. 1952. Vision through the Atmosphere. 250 p. Univ. Toronto Press, Toronto, Can.

Rogers, W. E., and R. A. Sommerfeld. 1968. A photoelectric snow particle counter. Am. Geophys. Union Trans. 49:690. (Abstr.)

Schmidt, R. A. 1971. Processing size, frequency, and speed data from snow particle counters. USDA For. Serv. Res. Note RM-196, 4 p. Rocky Mt. For. and Range Exp. Stn., Fort Collins, Colo.

Schmidt, R. A., and E. W. Holub. 1971. Calibrating the snow particle counter for particle size and speed. USDA For. Serv. Res. Note RM-189, 8 p. Rocky Mt. For. and Range Exp. Stn., Fort Collins, Colo.

Schmidt, R. A., and R. A. Sommerfeld. 1969. A photoelectric snow particle counter. West. Snow Conf. [Salt Lake City, Utah, April 1969] Proc. 37:88-91.

Sommerfeld, R. A., and J. Businger. 1965. The density profile of blown snow. J. Geophys. Res. 70:3303-3306.

Tabler, R. D. 1971. Design of a watershed snowfence system, and first-year snow accumulation. West. Snow Conf. [Billings, Mont., April 1971] Proc. 39:50-55.

Tabler, R. D., and R. L. Jairell. 1971. A recording gage for blowing snow. USDA For. Serv. Res. Note RM-198, 7 p. Rocky Mt. For. and Range Exp. Stn., Fort Collins, Colo.

Tabler, R. D. 1975. Estimating the transport and evaporation of blowing snow. *In* Snow Manage. on the Great Plains Symp. (Bismarck, N. Dak., July 1975) Proc. Great Plains Agric. Council, Publ. 73 p. 85-104.

Wishart, E. R. 1965. A new photoelectric drift snow gauge. Interim Rep. Ser. A(IV), Glaciol., Publ. 79, 6 p. Antarctic Div. Dep. External Aff., Melbourne, Australia.

APPENDIX I

A Visual Range Monitor for Blowing Snow
Operating and Service Manual

Contents

Page

Figures

Tables

This section outlines the purpose and scope of the manual, provides a brief description of the system, and lists the range of environmental operating conditions for the subsystems.

Scope and Purpose

Instructions for installing, operating, and maintaining an electronic system that monitors windspeed and visual attenuation by blowing snow are provided by this manual. A discussion of the design theory provides information to aid interpretation of the record for traffic control decisions. The purpose of this manual is to help assure effective use of the system.

Brief System Description

This visual range monitor system (VRM) contains two sensors, a small analog computer, and a strip chart recorder. Windspeed is measured by a direct current generating anemometer. A snow particle counter (SPC) photoelectrically detects size and frequency (number of particles per second) of windblown snow. The analog computer processes electronic signals from the two sensors to produce output voltages proportional to windspeed and visual range. These signals may be connected directly to the recorder, or transmitted to another location for recording.

Environmental Conditions

Both sensors will withstand the severe weather conditions they are designed to measure; that is, temperatures to –30°C, windspeed to 50 m/s and relative humidity approaching 100%. However, both the analog computer and recorder subsystems must operate at temperatures above freezing, and with relative humidity below 80%.

Best performance of these subsystems will be obtained if relative humidity is below 50% and a temperature range of 20° to 25°C is maintained. Temperatures greater than 100°F may cause damage. Vibration of all subsystems should be minimized by proper installation.

Installation

Power and grounding requirements, instructions for mounting the sensors and subsystem connections are contained in this section.

Power Requirements

A source of 115-V (± 10%) power at 50 to 400 Hz frequency is required by both the analog computer and recorder. Power to the SPC is provided by the analog computer subsystem, which dissipates about 15 W. The recording subsystem requires approximately 2 W.

Grounding

Both computer and recorder should connect to earth potential through the ground wire of the three-conductor power cord. The computer ground plug should conduct through at least #12 AWG wire to one or more copper grounding rods driven near the instrument building at the measurement site. The telemetry system should be connected to the same reference potential.

Sensor Installation

To reduce the influence of local topography, windspeed is measured 10 m (33 ft) above the surface. Considering ease of maintenance, probably the best mounting method is to place a crossarm at the appropriate height on a radio or TV tower of triangular cross section (fig. 2-1). This type of mast may be climbed to remove the sensor, and may also support a transmitting antenna for telemetry. Orient the crossarm so the tower causes interference only for the least important wind direction.

The particle counter is exposed 50 cm (20 in) above the ground surface. Blowing snow intensity changes rapidly with height, so it is essential to locate this sensor where drifting snow does not accumulate. Of course, the instrument site should be selected so as to be representative of the area to be monitored. Smooth, uniform terrain is preferable. If possible, site selection should be made in winter to ensure that the in-

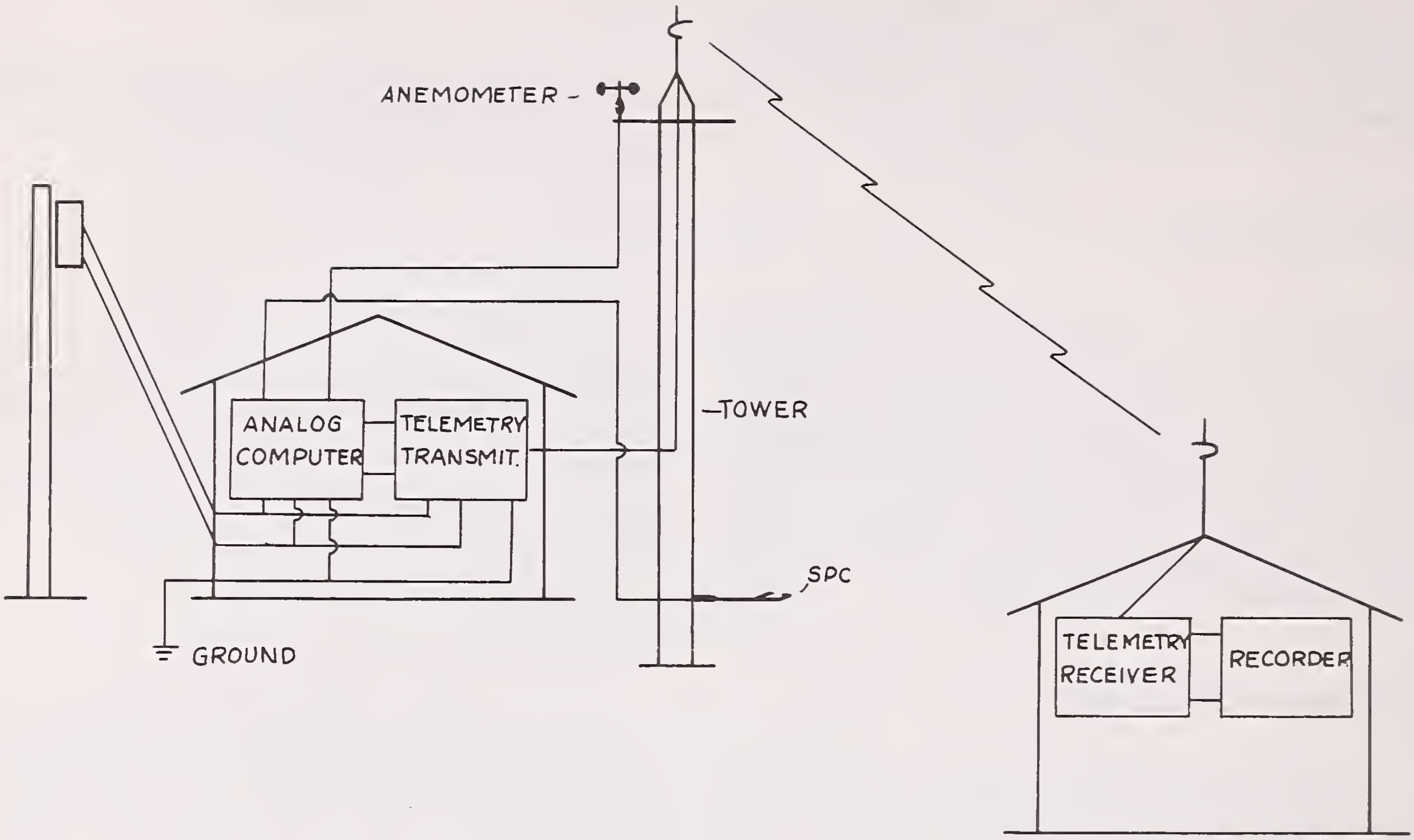

Figure 2-1.—Typical installation.

struments will not be placed in a snow accumulation area. The particle counters should be oriented with the light beam normal to the prevailing winds during drifting events; however, experience has shown that the wind angle can vary up to about 20° without significant effects on the VRM output. Any vibration of the support will contribute to electronic noise in the signal oscillation. The particle counter may be clamped to the anemometer mast if the above conditions are met; otherwise, use a separate mast of 2.5-inch pipe set about 2 feet in concrete.

Hookup

The analog computer and recorder may each be used on a bench or in a standard electronic rack. Figures 3-1 and 3-2 show connector locations. Installation is accomplished by the following steps:

a. Mount sensors at proper heights on mast(s).
b. Connect the snow particle counter to the rear panel of the VRM computer, using the six-conductor shielded cable.
c. Connect anemometer and computer using the two conductor line.
d. Couple the outputs from the rear of the panel of the computer to the recorder inputs, either directly or via the telemetry system.
e. Plug the computer and recorder power cords into the line power source.

The system should now be ready for testing and operation.

Operation Instructions

As a monitoring system, the VRM is designed for continuous operation with only occasional checks and maintenance. This section describes the turn-on procedure, and those function checks that assure proper system operation.

Controls, Indicators, and Connectors

The location of all external controls, indicators and connections on the analog computer and recorder are shown in figures 3-1 and 3-2.

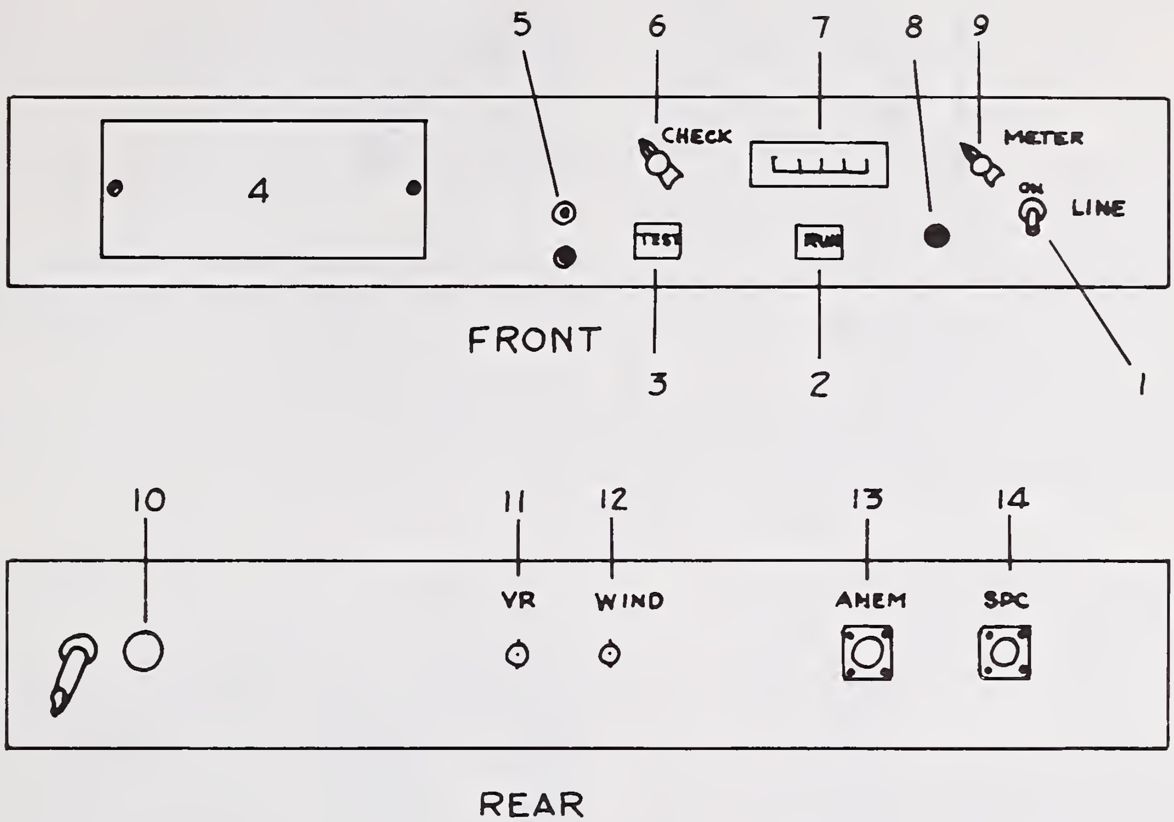

No.	DESCRIPTION
1	Line power switch
2	RUN mode switch
3	TEST mode switch
4	Printed circuit access cover
5	External input jacks
6	CHECK selector switch
7	Voltmeter
8	External input jack to meter
9	METER selector switch
10	Fuse
11	Visual range output BNC
12	Wind speed output BNC
13	Anemometer input
14	Snow particle counter connector

Figure 3-1. — VRM computer, front and rear view.

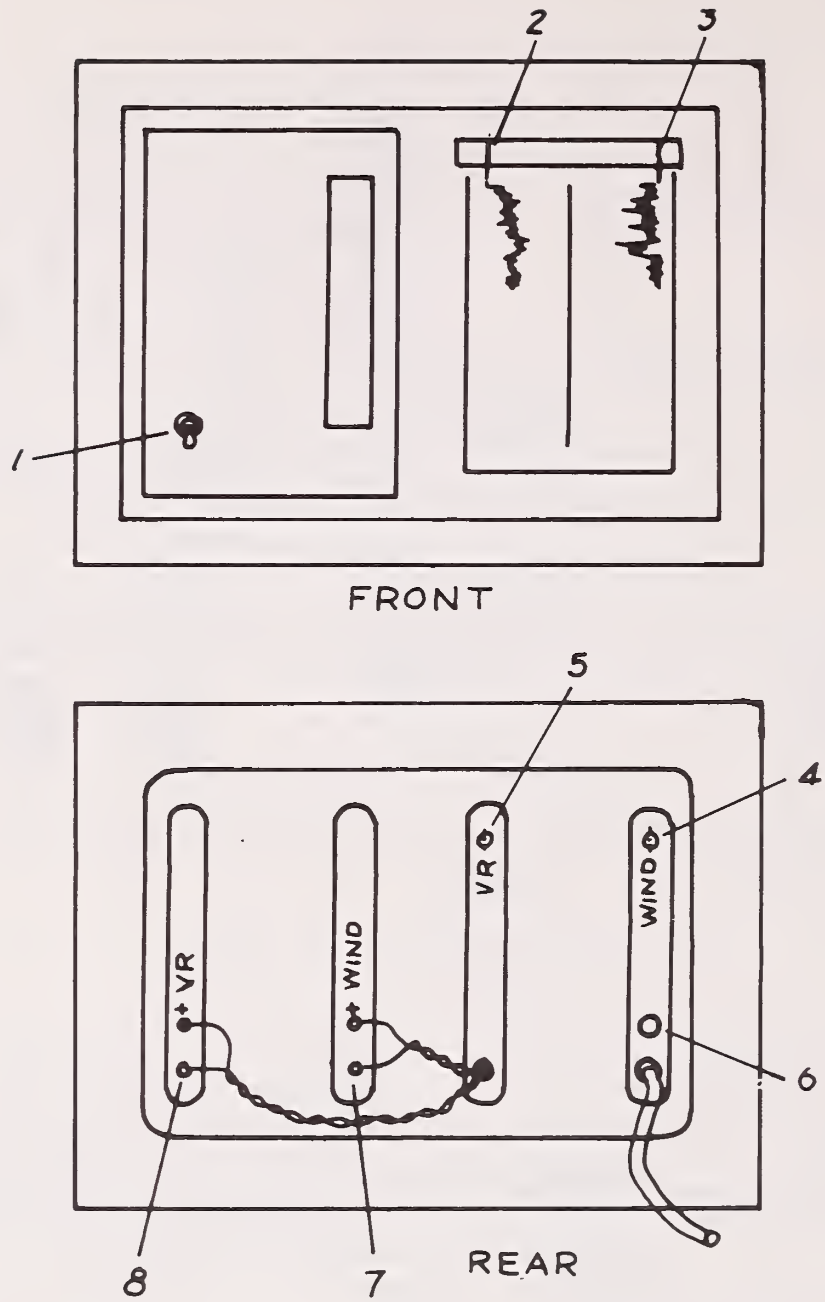

No.	DESCRIPTION
1	Line power switch
2	Wind speed pen
3	Visual range pen
4	Wind speed recorder input
5	Visual range recorder input
6	Fuse
7	Wind speed galvonometer input
8	Visual range galvonometer input

Figure 3-2. — VRM recorder, front and rear view.

Turn-on Procedure

With all instruments installed and connected as described, the following procedure will bring the system up to operation.

a. Turn light switch ON. Check that RUN switch is illuminated.

b. If a telemetry system is used between the computer and recorder, turn it on and allow the required warmup time.

c. Press the recorder POWER ON switch. The indicator should light.

Function Checks

The following procedures may be performed immediately after turn-on, or at any time during operation, to assure the operator that system operation is nominal. If any of these checks give negative results, refer to the troubleshooting procedures in the maintenance section. Complete system calibration is also covered under maintenance.

These checks are made with the system in RUN mode, and will not interrupt data.

a. Visually check to see that the SPC lamp is lit. This assures the lamp is not burned out and the sensor and computer are connected.

b. The visual range output may be checked during operation by checking that the recorder gives a reasonable indication of existing conditions. This output may also be checked at the computer by setting the METER switch to VR. If snow is blowing, the voltmeter on the computer should give a variable reading between 0 and 10 V. As visual range decreases, this voltage should increase. Without drifting, the reading should be zero.

c. To check the windspeed, set the METER switch to WIND and read the voltmeter. The reading (1V = 10 mi/hr) should be reasonable for the existing conditions. Check that this reading is being recorded.

The following checks are made with the computer in the TEST mode, which disconnects the sensor signals at the computer. Data will be interrupted during these checks.

d. Set METER switch to VR and CHECK switch to ZERO. Press TEST switch. RUN light should be off, TEST light on, and the voltmeter should indicate zero after about 30 seconds. Check that the recorder indicates visual range is infinite. (Pen records at right-hand margin).

e. Turn METER switch to WIND. The voltmeter should read zero volts and the recorder pen should ink on 0 mi/hr (left-hand margin).

f. Set CHECK switch to FULL SCALE. The computer voltmeter should indicate +10 V and the recorder should indicate 100 mi/hr windspeed.

g. Set METER switch to VR and check that voltmeter reads 14.2 V and recorder indicates less than 200 feet on visual range channel (pen to left of left-hand chart margin). These checks ascertain that computer and recorder are functioning, and that data from these sensors is being recorded. If the system accuracy is in doubt, refer to calibration procedures in the next section.

Maintenance

This section includes performance checks, calibration procedures, and a troubleshooting guide, to aid in maintaining proper system operation.

Test Equipment

The following equipment is required for checking performance and calibration of the VRM system.

a. A d.c. voltmeter with 1% accuracy and ranges of 0-1 V and 0-15 V.

b. An oscilloscope with vertical sensitivity of 50 mV/cm and frequency response of 100 kHz. (HP 120, 122, 130, or equivalent).

c. A sine wave test oscillator with calibrated output frequency from 0 to 5 kHz and variable amplitude to at least 300 mV p-p.

d. A d.c. voltage source variable from 0 to 4 V.

e. Anemometer calibration requires an a.c. synchronous motor with 600 or 900 r/min output and a means of coupling to the anemometer shaft.

f. A small d.c. motor with a wire attached perpendicular to its shaft. Such a unit is included with the VRM system to generate a calibration signal from the snow particle counter. (The wire that intercepts the light beam should be at least 0.5 mm (0.02 in) in diameter.

Performance Checks

The procedures outlined below are intended to check the VRM system accuracy. They should be performed upon initial system installation, after repairs, or any time proper system performance is doubted.

Snow Particle Counter Output Test.—

a. Check that system is properly connected.

b. Check that power is on to all subsystems.

c. Check that lamp in particle counter is on.

d. Attach the calibrator motor to the particle counter and check that the wire is centered in the sensing gap. Check that the wire shadow completely blocks each slit as it rotates. Turn the motor on. (If the sensor is in bright sunlight at the time of this test, shading the sensor will give a more accurate check.)

e. Remove the printed circuit access cover from the computer front panel.

f. Set the oscilloscope time base for 0.1 ms/div. and the vertical sensitivity to 1 V/div. Connect the vertical input to TP1 on B1 (fig. 4-1). (The low side of the scope input should be strapped to system ground.) Adjust the scope for a good display and check that the SPC signal has a +(3.0 ± 0.2) V pulse followed by a -(3.0 ± 0.2) V pulse (fig. 4-2).

Anemometer Output Check. —The following steps will check the output from the windspeed generator for excessive noise. The anemometer should be exposed to a wind greater than 10 mi/hr for this check.

a. Set computer to RUN.

b. Set the oscilloscope to display 1 ms/div. with a vertical sensitivity of 1 V/div. Connect the vertical input to TP5 on M1 and adjust the scope for a clear display. The wave form should be similar to that shown in fig. 4-3. Check that no large noise spikes occur.

Internal Oscillator Calibration Check.—This procedure checks the output frequency and amplitude of the internal oscillator and reference voltage source that provide full-scale calibration inputs to the computer.

a. Place the computer in TEST mode.

b. Set the oscilloscope vertical sensitivity to 100 mV/div. and the time base to 0.1 ms/div. Connect the scope input to TP1 on the C1 printed circuit.

c. Check that the scope displays exactly 5 cycles of a sine wave with 300 ±10 mV peak-to-peak amplitude.

d. Connect the d.c. voltmeter to TP2 on the calibrator card and check that the voltage is + 4.00 ± .05 V.

Computer Alinement Checks.—Both zero and full-scale outputs of each PC card are checked by the following procedure. Refer to fig. 4-1 for the location of test points.

a. Place the computer in TEST mode and set CHECK switch to ZERO. (This step disconnects the sensors and ground the input to B1 and the anemometer input at V2.)

b. Check that the voltages at each test point listed in table A-1 are within the specified range. (All are d.c. voltages measured with reference to the system ground.)

c. With the computer in TEST mode, set CHECK switch to FULL SCALE. (This step applies to sine wave output of the calibrator card to the input of B1 and the 4 V d.c. calibrator output to the anemometer input.)

d. Test points in table A-1 should be rechecked in the order listed. If voltages are not within the specified range, refer to the calibration procedure.

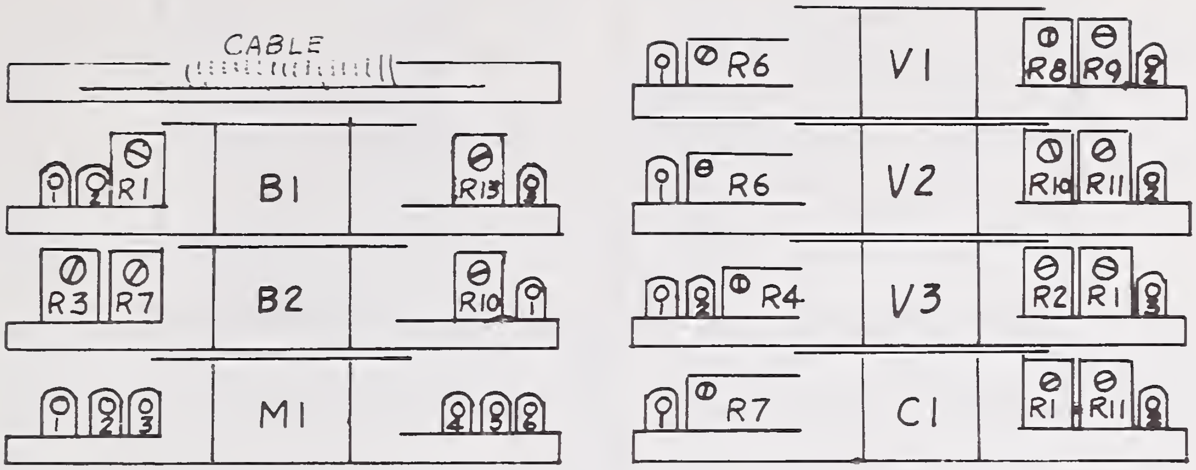

Test point	Description of signal	Adjustment for "Zero"	Adjustment for "Full scale"
B1TP1	SPC input	none	SCP R10
B1TP2	Attenuated input	none	B1R1
B1TP3	e_x	B1R7	B1R13
B2TP1	e_f	B2R10 1/	B2R7
V1TP1	$-5(e_x + 1)$	V1R7 (side)	V1R6
V1TP2	$2.5(e_x + 1)^2$	V1R9	V1R8
V2TP1	$-2.5e_u$	V1R9 (side)	V1R6
V2TP2	$.25e_f(e_x + 1)^2$	V2R11	V2R10
V3TP1	$2.5e_u$	none	V3R7
V3TP2	e_v	none	V3R4
V3TP3	$-e_f(e_x + 1)^2/e_u$	V3R1	V3R2
C1TP1	sine wave	C1R1 (freq.)	C1R7
C1TP2	dc reference	none	C1R11
M1TP1	+15v dc supply	none	none
M1TP2	-15v dc supply	none	none
M1TP3	+5v dc supply	none	none
M1TP4	+27v dc supply	none	none
M1TP5	anemometer	none	none
M1TP6	ground	none	none

1/ These adjustments are located on the left-hand side of the board when viewed from the front or handle end.

Figure 4-1. — Location of test points and adjustments.

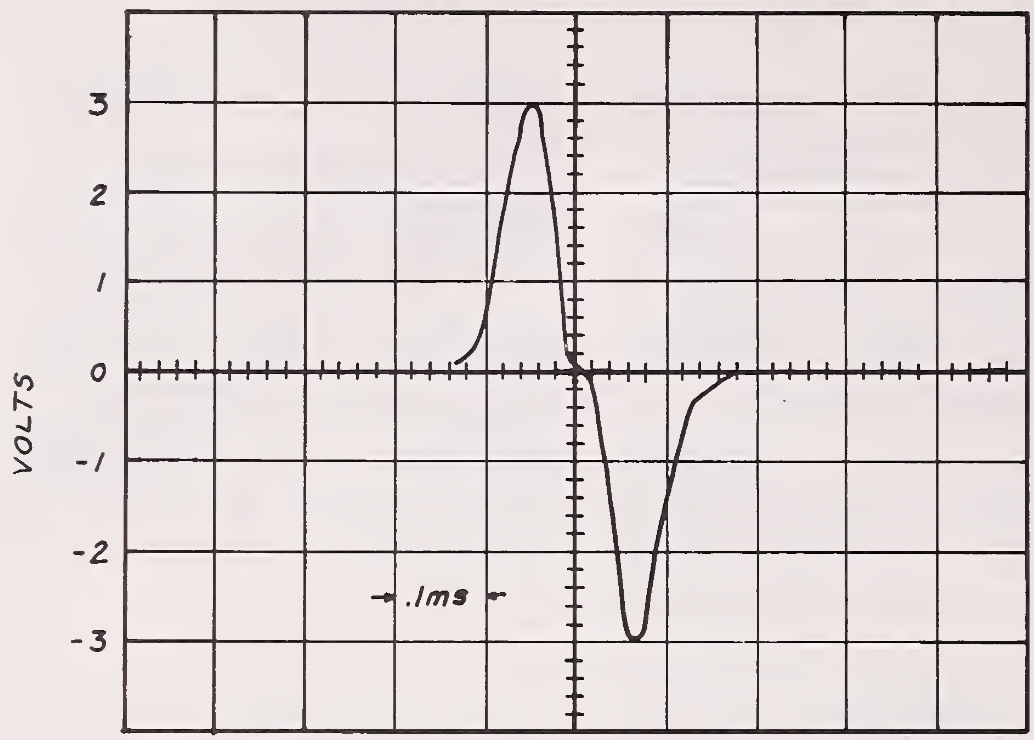

Figure 4-2. — SPC calibration signal.

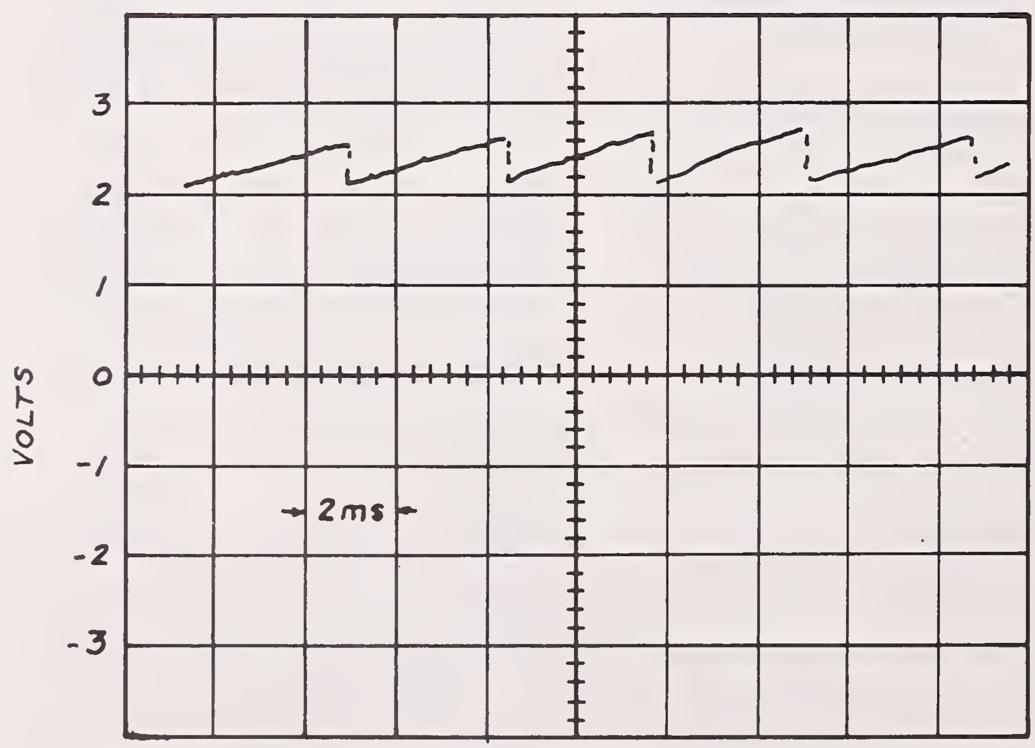

Figure 4-3. — Anemometer output signal.

Table A-1. Test point calibration voltages

Test point	Description	"Zero"	"Full-scale"
B1TP1	Input	(grounded)	(cal. sig.)
B1TP2	Attenuated input[1]	(grounded)	(cal. sig.)
B1TP3	e_x	0 ± .01	1.00 ± .01
B2TP1	e_f	0 ± .01	10.00 ± .05
V1TP1	$-5(e_x + 1)$	-5.00 ± .01	-10.00 ± .05
V1TP2	$2.5(e_x + 1)^2$	2.5 ± .01	10.00 ± .05
V2TP1	$-2.5e_u$	-1.00 ± .01	-10.00 ± .05
V2TP2	$.25e_f(e_x + 1)^2$	0 ± .01	10.00 ± .05
V3TP1	$2.5e_u$	0 ± .10	10.00 ± .10
V3TP2	e_v	0 ± .05	$(14.20 \pm .10)^2$
V3TP3	$-e_f(e_x + 1)^2/e_u$	0 ± .05	-10.00 ± .10
C1TP1	sine wave	0	300 mV p-p, 5 kHz
C1TP2	d.c. reference	0	4.00 ± .01
M1TP1	+15 V d.c. supply		+15.00 ± .10
M1TP2	-15 V d.c. supply		-15.00 ± .10
M1TP3	+5 V d.c. supply		+5.00 ± .10
M1TP4	+28 V d.c. supply		+28.00 ± .10
M1TP5	anemometer signal	0 ± .05	4.00 ± .01
M1TP6	Ground		

[1]*Normally the input is not attenuated.*

[2]*The calibration procedure described in the subsection on adjusting V3 is used to set the value of e_v to 10.00 ± .10 V with a special input.*

Recorder Performance Check.—This check requires that both the computer and the telemetry system (if used) be properly alined.

a. Set computer to TEST, CHECK ZERO.
b. Turn on recorder.
c. Check that windspeed pen records 0 mi/hr (left-hand margin) and that visual range reading is "clear" (right-hand margin).
d. Set computer to TEST, CHECK FULL SCALE.
e. Recorder should indicate 100 mi/hr on windspeed channel and less than 200 feet (to left of left-hand margin on visual range channel).

Adjust the recorder (see calibration procedure) only if the computer and telemetry subsystems are properly alined.

System Linearity Check.—This procedure checks performance of the computer, telemetry, and recorder subsystems. It assures complete system calibration if the SPC and anemometer calibrations have been checked.

a. The test setup is shown in fig. 4-4. Use the external input connectors to connect the test signals at the front panel of the computer.
b. Adjust the test instruments for the values in table A-2 and check the recorder for corresponding outputs. Figure 4-5 shows a strip chart record of this check.

Calibration and Alinement Procedures

The performance checks listed above are designed to locate any subsystem that needs adjustment and to isolate the particular unit in the subsystem that is causing the problem. These calibration procedures should be used only when performance checks indicate a problem with the particular assembly.

Snow Particle Counter Calibration.—When a performance check indicates this sensor does not provide the proper calibration pulse amplitudes (+3.0 ± 0.2 V and -3.0 ± 0.2 V), the following adjustments of sensor "balance" and "gain" should be made.

a. With sensor and computer connected, and computer in RUN mode, attach the calibrator motor to the sensor and check proper alinement of the wire.
b. Connect oscilloscope to B1TP1 on the computer and adjust for clear display of the calibration signal.
c. Loosen the set screws on the SPC and turn the amplifier cover until the adjustment pots are accessible (fig. 4-6).
d. Adjust SPC R1 on the sensor amplifier assembly (fig. 4-6) until the positive and negative pulse amplitudes are equal.
e. Adjust the amplifier gain (SPC R10) for ±3.0 V pulse amplitudes.
f. Remove calibrator from sensor and close amplifier cover. Tighten set screw.

Table A-2.—Test values for linearity check

Run	Voltage Source d.c. volts	Oscillator Hz	Oscillator mV p-p	$2.5e_u$ d.c. volts	e_v d.c. volts
1	+4.00	0	0	+10.00	0
2	3.00	0	0	7.50	0
3	2.50	4.5 k	120	6.25	+10.00
4	2.25	3.5 k	90	5.60	7.50
5	2.05	2.5 k	60	5.10	5.00
6	2.05	1.5 k	30	5.10	2.50
7	1.00	0	0	2.50	0
8	0	0	0	0	0

Anemometer Calibration.—Noisy anemometer signals usually indicate worn brushes and a dirty commutator in the windspeed generator. Worn brushes should be replaced, the commutator cleaned, and the sensor recalibrated. Even though the windspeed signal is not noisy, the following calibration check should be made once a year, before the blowing snow season.

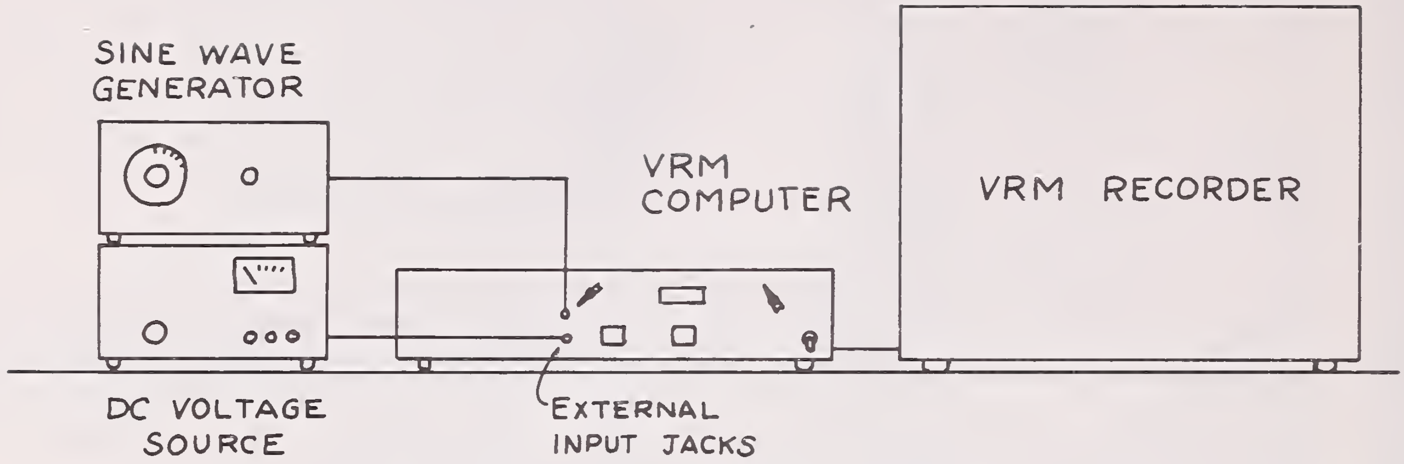

Figure 4-4.—Test setup for linearity check and scaling amplifier adjustment.

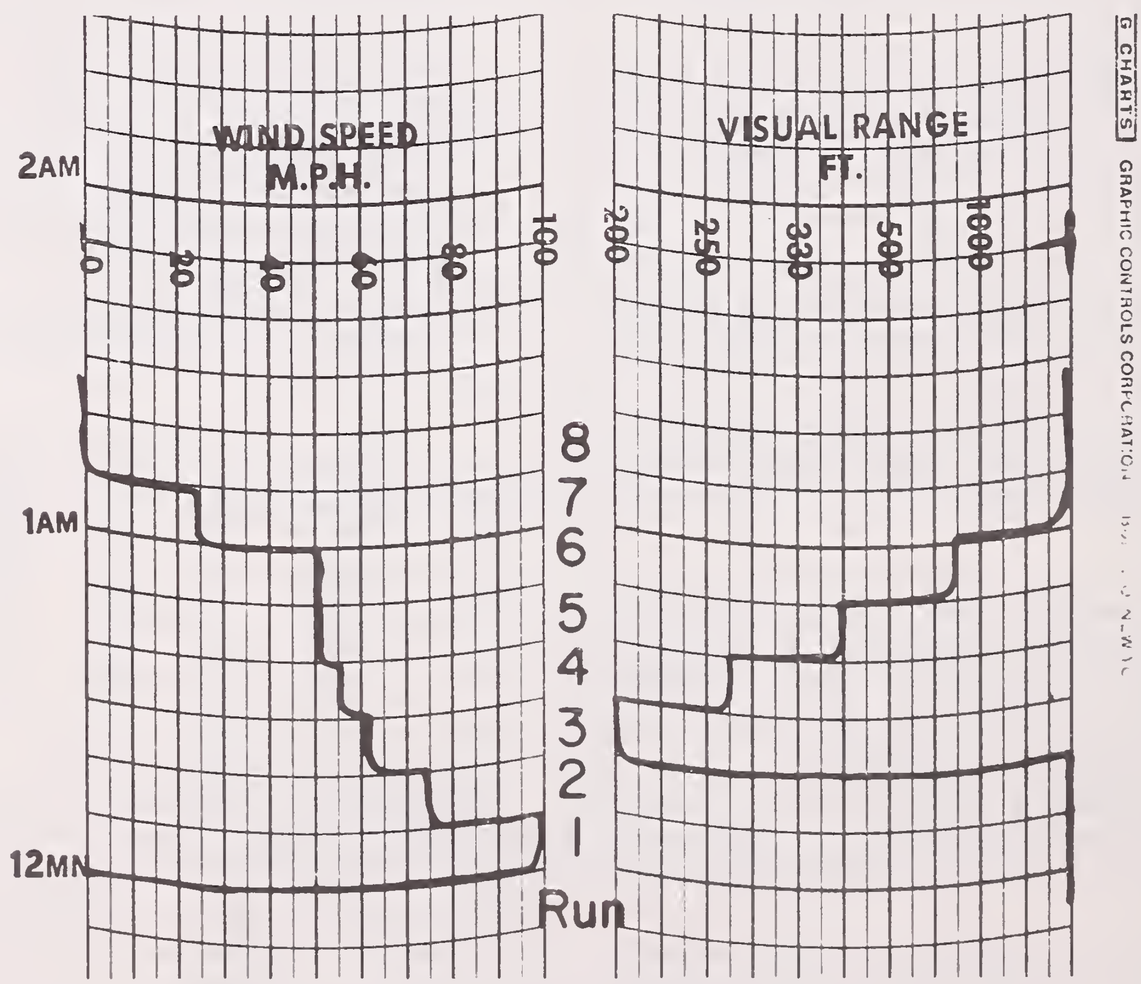

Figure 4-5.—Strip chart record of linearity check.

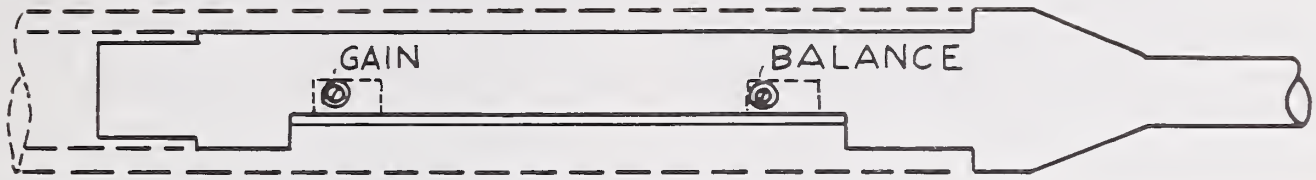

Figure 4-6.—Location of BALANCE and GAIN adjustments on SPC amplifier.

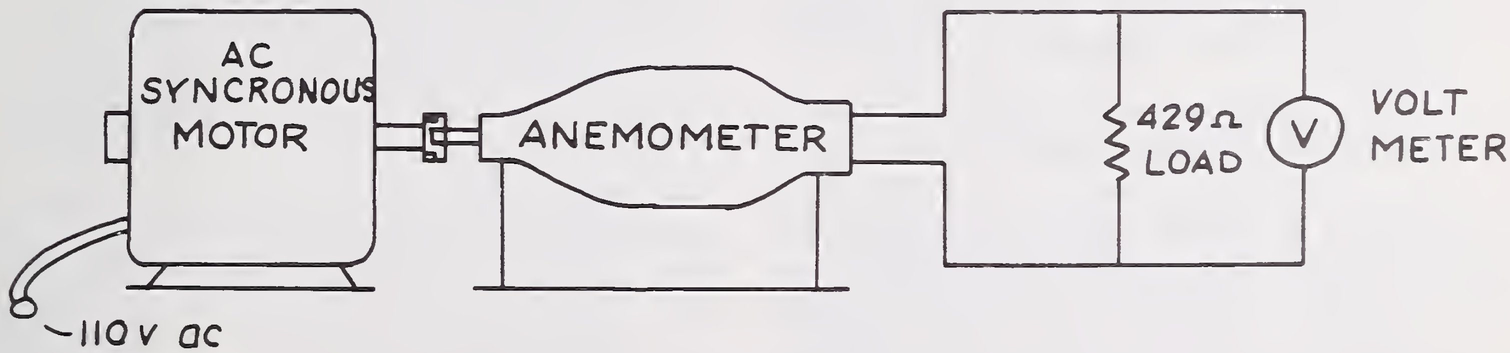

Figure 4-7.—Anemometer calibration setup.

a. Couple the anemometer shaft to a synchronous motor of 600 to 900 r/min output (fig. 4-7).
b. Connect a 429 ohm dummy load across the anemometer output.
c. Read the d.c. voltage across the load with the motor turned on.
d. Adjust the anemometer field as explained in the anemometer service manual until the appropriate value is obtained (600 r/min = 62.5 mi/hr, e_u = 2.50 V; 900 r/min = 92.4 mi/hr, e_u = 3.70 V).

Computer Alinement.—Since the computer is alined by adjusting the zero and full-scale outputs of each pc card, the internal calibrator must first be properly adjusted. Then, adjustment of the computer boards should be made in the order listed below.

Remove and install printed circuits ONLY when power is OFF. Otherwise, damage to the integrated circuits may result.

Internal Calibrator Adjustment.—The calibrator consists of a sine wave oscillator to simulate the SPC signal and a d.c. reference voltage source to replace the anemometer signal. Frequency and amplitude of the oscillator, and output level from the voltage source are adjusted by the following procedure.

a. With the power off, extend the calibrator card C1 using the card extender.
b. Turn computer power on and set to TEST mode. (No power is applied to C1 in RUN mode.)
c. Set oscilloscope vertical sensitivity to 0.1 V/div. and time base to 0.1 ms/div. Connect the vertical input to C1TP1. Adjust R1 so exactly 5 cycles are displayed in 10 cm on the scope (5 kHz ±50 Hz). Adjust R7 for 300 mV(±10 mV) peak to peak oscillator amplitude. Since these adjustments interact, it is necessary to readjust R1 and R7 until the 5 kHz, 300 mV p-p signal is obtained.
d. Connect the voltmeter to C1TP2 and adjust R11 for 4.00 V (±.05 V).

Adjusting B1 Input Amplifier and A.C.-D.C. Converter.—These procedures adjust the zero offset and gain of the input amplifier and the full-scale output of the a.c.-d.c. converter.

a. With power off, reconnect B1 through card extender.
b. Turn computer on and set to TEST, CHECK ZERO.
c. Connect voltmeter to TP4 (fig. 5-3) and adjust B1R7 for 0.0 V output. Disconnect voltmeter.
d. Set CHECK switch to FULL SCALE.
e. Connect vertical input of scope to B1TP1 and check that C1 oscillator signal is present at the input.
f. Connect scope to TP2. Input attenuator R1 is normally set fully clockwise so the input is not attenuated and the signal at TP2 should be 300 mV p-p.
g. Connect scope to TP4 on the card and adjust R6 for 6.0 V p-p signal. (X20 gain).
h. Set B1R13 so the full-scale output voltage at B1TP3 is 1.00 ± 0.01 V.

Adjusting B-2, Frequency to D.C. Converter.—These adjustments include setting zero and full-scale outputs, and the trigger level.

a. With power off, place B2 on the card extender and reconnect.
b. Turn computer on, and set to TEST, CHECK FULL SCALE. Adjust B2R7 for +10.0 V d.c. at B2TP1.
c. Set CHECK switch to ZERO and adjust B2R10 for 0.0 V at TP1.
d. Repeat steps b and c until both zero and full-scale outputs are correct.
e. To check and adjust the trigger level at which the converter starts to operate.
f. Connect a 30 mV p-p, 5 kHz sine wave from the test oscillator to the SPC external input jack.
g. Connect the scope to multivibrator output B2TP2 (fig. 5-5) and set display for 1 V/div, 0.1 ms/div. A train of +3.2 V pulses of about 50 ms width and 5 kHz rate should appear (fig. 4-8).
h. Turn B2R3 counterclockwise until the pulses disappear. Then turn slowly clockwise until the multivibrator just starts to fire again.
i. Check this sensitivity adjustment by reducing the test signal amplitude. The pulses should disappear and reappear only when the amplitude is increased to 30 mV p-p.
j. Turn power off, remove card extender and reconnect.

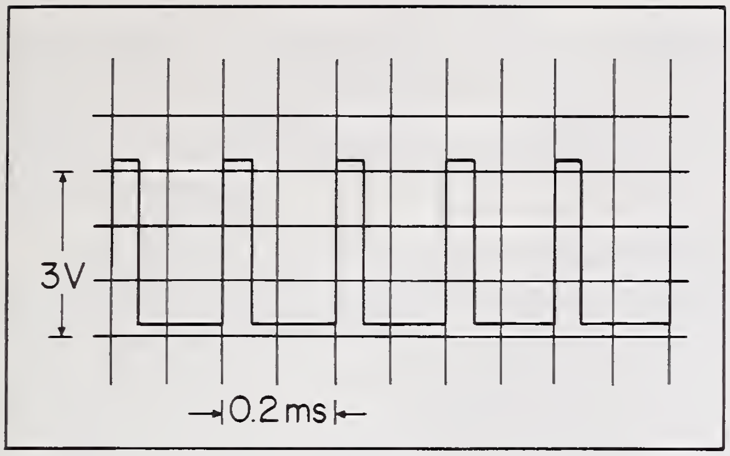

Figure 4-8.— Multivibrator pulse train output at B2TP2.

Adjusting V1, Analog Squaring Circuit.—Steps for adjusting the reference voltage, amplifier gain, zero and full-scale outputs follow.

a. With power off, connect V1 through the card extender.
b. Turn power on, and set computer to CHECK ZERO in TEST MODE.
c. Connect the voltmeter to R4 lead and adjust R3 for +1.00 V d.c. (±.005).
d. The summing amplifier V1A1 generates the output, $-5(e_x + 1)$. When $e_x = 0$, the output should be –5.00 at TP1. Adjust R7 for this value (± .01 V).
e. Adjust the multiplier zero R9 for +2.50 V (± .01) at TP2.
f. Set CHECK to FULL SCALE, and adjust amplifier gain V1R6 for –10.00 V (± .01).
g. Adjust multiplier gain, R8, for +10.00 V at TP2.
h. Shut power off and remove the card extender.

Adjust V2, Windspeed Amplifier and Multiplier.—This procedure adjusts the gain of the windspeed amplifier and the zero and full-scale outputs of the multiplier that generates $0.25\ e_f(e_x + 1)^2$.

To avoid output noise at the divider (V3), the output of the anemometer amplifier is limited by the circuit R7, R8, R9, and CR1 of V2. This prevents the output from going to zero as windspeed drops. Figure 4-9 shows that windspeed amplifier output is $-2.5e_u$ for windspeeds greater than 15 mi/hr. The breakpoint is adjusted by R9 so that amplifier output is –1.0 V when $e_u = 0$. Normal alinement proceeds as follows:

a. With power off, connect V2 through card extender.
b. Turn on power and set computer to TEST, CHECK ZERO.
c. Adjust R9 for –1.00 V (± .01) at V2TP1.
d. Adjust R11 for 0 V (±10 mV) at V2TP2.
e. Set CHECK to FULL SCALE and allow 30 seconds before adjustments.
f. Adjust windspeed amplifier gain R6 for –10.00 V (± .05 V) at TP1.
g. Adjust multiplier gain R10 for +10.00 V at TP2.
h. Turn power off, remove extender and replace card.

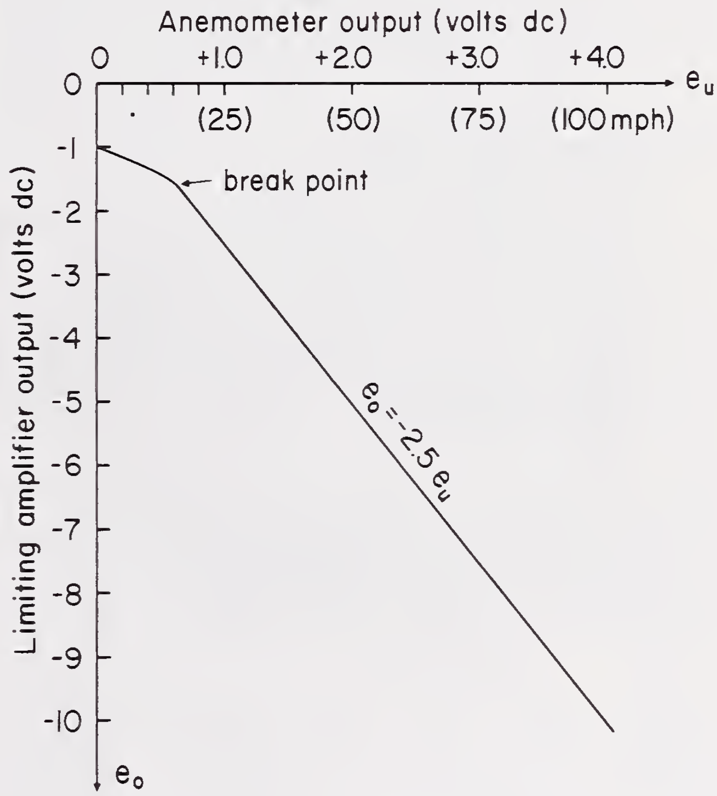

Figure 4-9.— Limiting amplifier output for windspeed.

Adjusting V3, Analog Divider, and Windspeed Amplifier.—Zero and full-scale outputs from the divider are alined by the following procedure.

a. With power off, reconnect V3 through the extender.
b. Turn power on and set computer to TEST, . CHECK ZERO.
c. Adjust R1 for 0 V d.c. (+50 mV) at TP3.
d. Set computer to TEST, CHECK FULL-SCALE and adjust R2 for –10.0 V d.c. at TP3.
e. Adjust R7 for +10.00 V (± .01 V) at TP1 (Windspeed output, $+2.5e_u$).

Adjusting V3, Final Scaling Amplifier.—This procedure should be followed only if components in the V3A1 amplifier are replaced, and only after all of the above calibration procedures have been properly accomplished. **Adjusting the gain of the scaling amplifier changes the empirical calibration of the VRM system.**

a. With power off, disconnect the sensors at computer rear panel.
b. Set up test equipment as indicated in figure 4-4.
c. Reconnect V3 through card extender.
d. Turn power on. Adjust test equipment for the values given in table A-3. These values simulate natural blowing snow conditions in which visual range is 200 feet. If the d.c. voltages are not within the indicated range at any test point, refer to the appropriate calibration procedure.
e. If all test point voltages are within the proper calibration range, check that the VR output, e_v at V3TP1 is +10.0 V d.c. (±50 mV). Adjust V3R4 only if necessary.
f. Turn power off, disconnect all test equipment, remove the card extender, and reconnect the sensors.

Table A-3.—Test voltages for scaling amplifier adjustment. Test oscillator sine wave output. Amplitude 120 mV p-p. Frequency 4,500 Hz (±25 Hz). Voltage source +2.50 V d.c.

Test point	Description	Voltage	Range
B1TP1	Test sine wave	(85 mV rms)	*
B1TP2	120 mV p-p 4.5 kHz		
B1TP3	e_x	+ 0.40 V	± 0.01 V
B2 TP1	e_f	+ 9.00 V	± 0.05 V
V1TP1	$-5(e_x + 1)$	- 7.00 V	± 0.05 V
V1TP2	$2.5(e_x + 1)^2$	+ 4.90 V	± 0.05 V
V2TP1	$-2.5e_u$	- 6.25	± 0.05 V
V2TP2	$.25e_f(e_x + 1)^2$	4.41	± 0.05 V
V3TP2	e_v (being adjusted)	10.00 V	± 0.05 V
V3TP3	$-e_f(e_x + 1)^2/e_u$	- 7.05	± 0.05 V

Test signal amplitude may be adjusted slightly to give $e_x = 0.40$ V.

To understand this adjustment, recall the theoretical equations for visual range. We have chosen to let $e_v = 10$ volts when $V = 200$ ft, thus fixing the proportionality constant $K = e_vV$ at 2,000 volt feet (fig. 4-10). By analogy to the theoretical equation for visual range $e_v = Ce_f(e_x + 1)^2/e_u$, and the experiments described show that $e_f = 9.0$ volts, $e_x = 0.4$ volts and $e_u = 2.5$ volts when $V = 200$ ft. These values give $e_f(e_x + 1)^2/e_u = 7.05$ volts so the scale factor C is $10.0/7.05 = 1.42$. This is the gain required at the scaling amplifier.

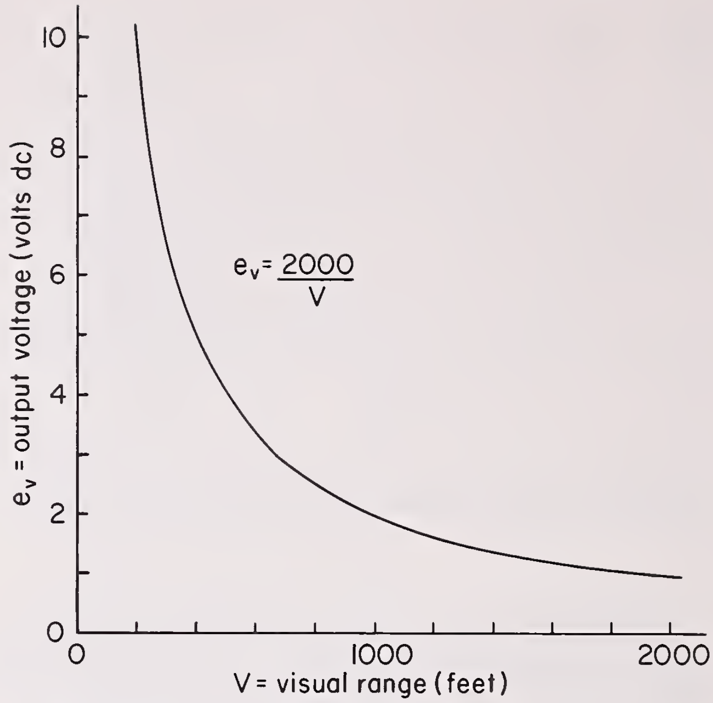

Figure 4-10.—Output voltage as a function of visual range.

Recorder Adjustments

The mechanical zero and full-scale deflection of the recorder galvanometers may be adjusted using either the system, or a separate d.c. voltage source for the full-scale input.

a. Remove the signal input cables from the recorder and ground the recorder inputs at the rear panel connectors. Turn power on.
b. Adjust the mechanical zero of the windspeed channel so the pen tracks the 0 mi/hr chart margin (left-hand zero).
c. Adjust the visual range channel zero to track the right-hand chart margin (marked "00" on scale plate).
d. Remove input grounds and apply +10.00 V d.c. to windspeed input at rear connector.
e. Adjust D1R1 so pen indicates 100 mi/hr on windspeed channel.
f. Place 10.00 V d.c. signal on the VR input and adjust D1R2 so the pen inks the 200-ft line on the visual range chart (left-hand margin).

Troubleshooting

These procedures are designed to isolate system malfunctions by first locating the subsystem, then the assembly and finally the compo-

nent which is causing the problem. A system malfunction may be detected at the recorder, where an illogical record indicates some problem, or at the measurement site, by the performance checks.

Illogical Records.—Figure 4-10 shows normal strip chart records for wind without blowing snow, and wind with blowing snow (reduced visual range). The following illogical records (fig. 4-11) indicate a system malfunction.

a. Both channels steady at zero. This usually indicates that no signal is being recorded, at least on the wind channel. Even during calm conditions, slight variations in windspeed are observed during periods of 1 hour or more.

b. Reduced visual range with little or no wind. Since the threshold wind velocity for blowing snow is about 15 mi/hr, this condition definitely indicates a system malfunction.

c. One or both channels "pegged" full-scale. The normal record shows a great deal of variation even during high intensity drifting. A continuous full-scale record indicates a problem.

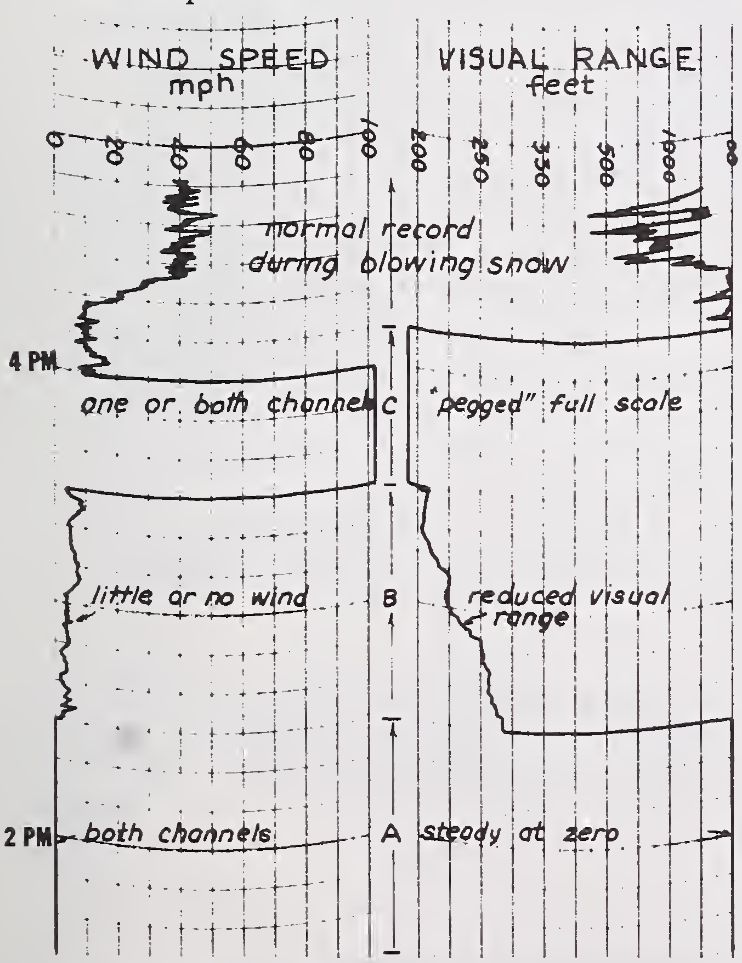

Figure 4-11.—"Illogical" records.

If the malfunction is first detected at the recorder, then the subsystems should be tested in reverse order, starting with the recorder, (then the telemetry system, if used) the computer, and the sensors last.

Troubleshooting the Recorder.—The main assemblies in the recorder subsystem are the two galvanometers that deflect the pens, the dual channel galvo driver board D1, and a ±15 V d.c. modular power supply. Figure 4-12 gives the troubleshooting procedure for each of the problems listed in the preceeding section.

Troubleshooting the Telemetry Subsystems.—There are so many types of telemetry that no specific procedure will be outlined here. In general, the telemetry should be checked first to isolate the problem to either the transmitter or receiver, then to a particular assembly within that unit, and if necessary, to the component.

Troubleshooting the Computer.—The internal oscillator calibration and computer alinement performance checks provide a means of isolating problems to particular boards in the computer. However, some problems may not permit these checks. A scheme to handle most problems with the computer is diagramed in figure 4-13. Troubleshooting individual boards should not be attempted in the field. In most cases, a qualified technician can troubleshoot the pc boards using the schematics in the next section.

Troubleshooting the Snow Particle Counter.—Problems with this sensor will usually be detected during the snow particle counter output performance check. They include the following:

a. No signal.
b. Excessive noise.
c. D.C. offset.
d. Pulse amplitudes won't balance.
e. Gain adjustment not sufficient to give ±3.0 V.

These problems may be either electrical or mechanical in origin. If electrical malfunctions, they may be traced to (1) the lamp, (2) the connections, (3) the amplifier, and (4) the phototransistors. Problems of mechanical origin can usually be traced to vibration, or damage to the slit plate and lens. Figure 4-14 shows a systematic method for troubleshooting the snow particle counter.

PART I

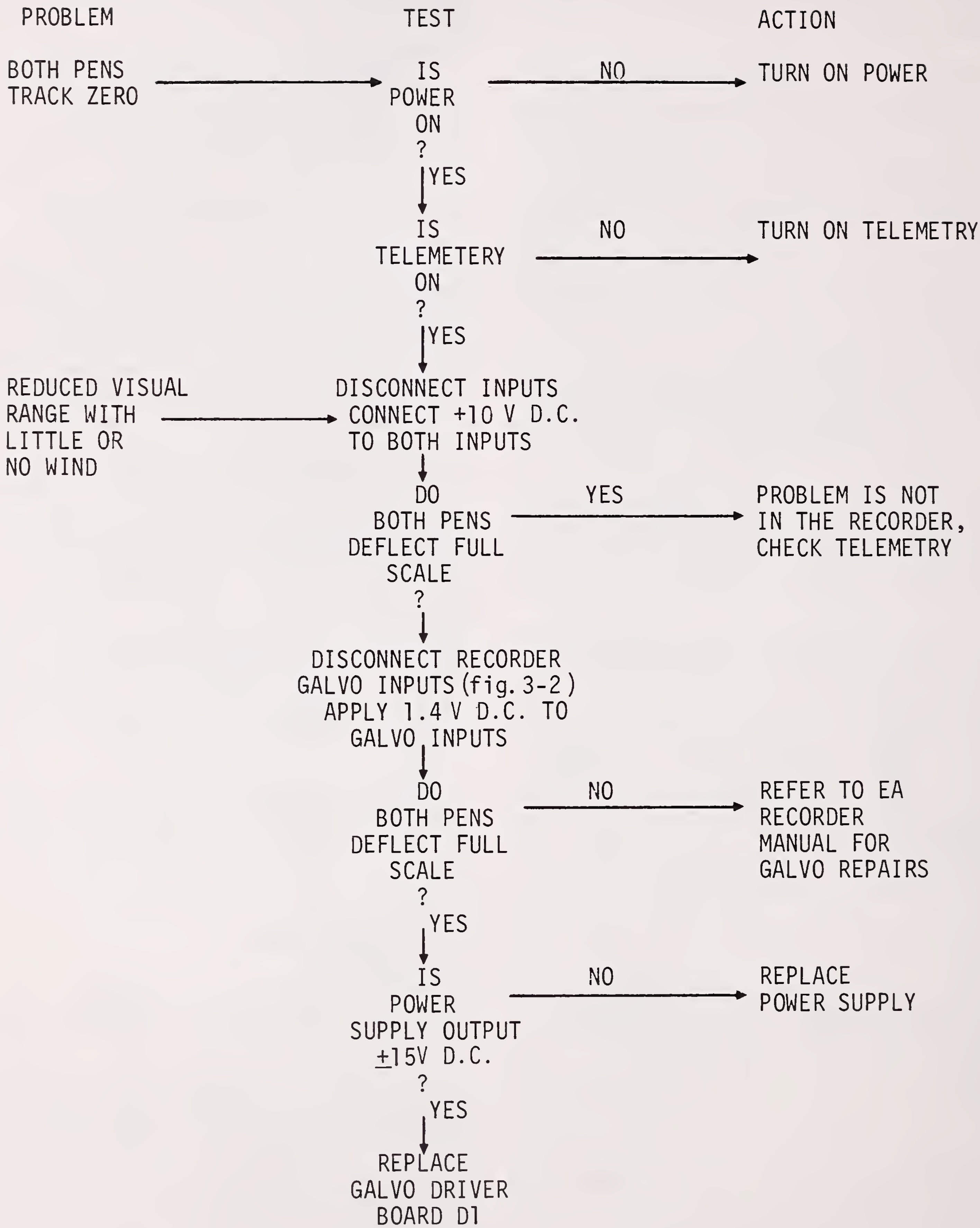

Figure 4-12.—Troubleshooting procedure for the recorder.

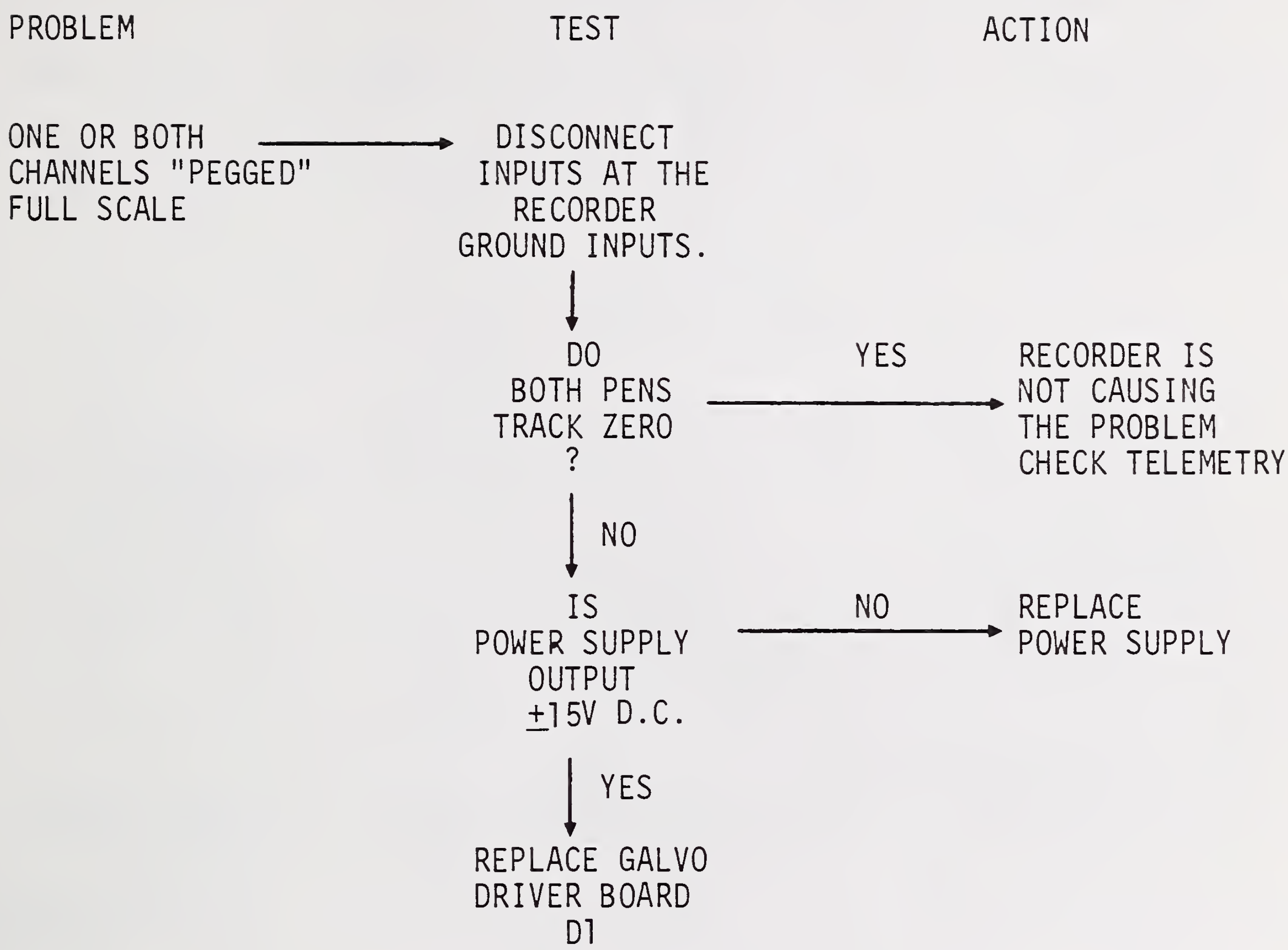

Troubleshooting the Generating Anemometer.—If a malfunction is traced to the wind-speed sensor, the problem is usually one of the following:

a. No output.
b. Low output.
c. Excessive noise.

Figure 4-15 gives a troubleshooting scheme for the generating anemometer.

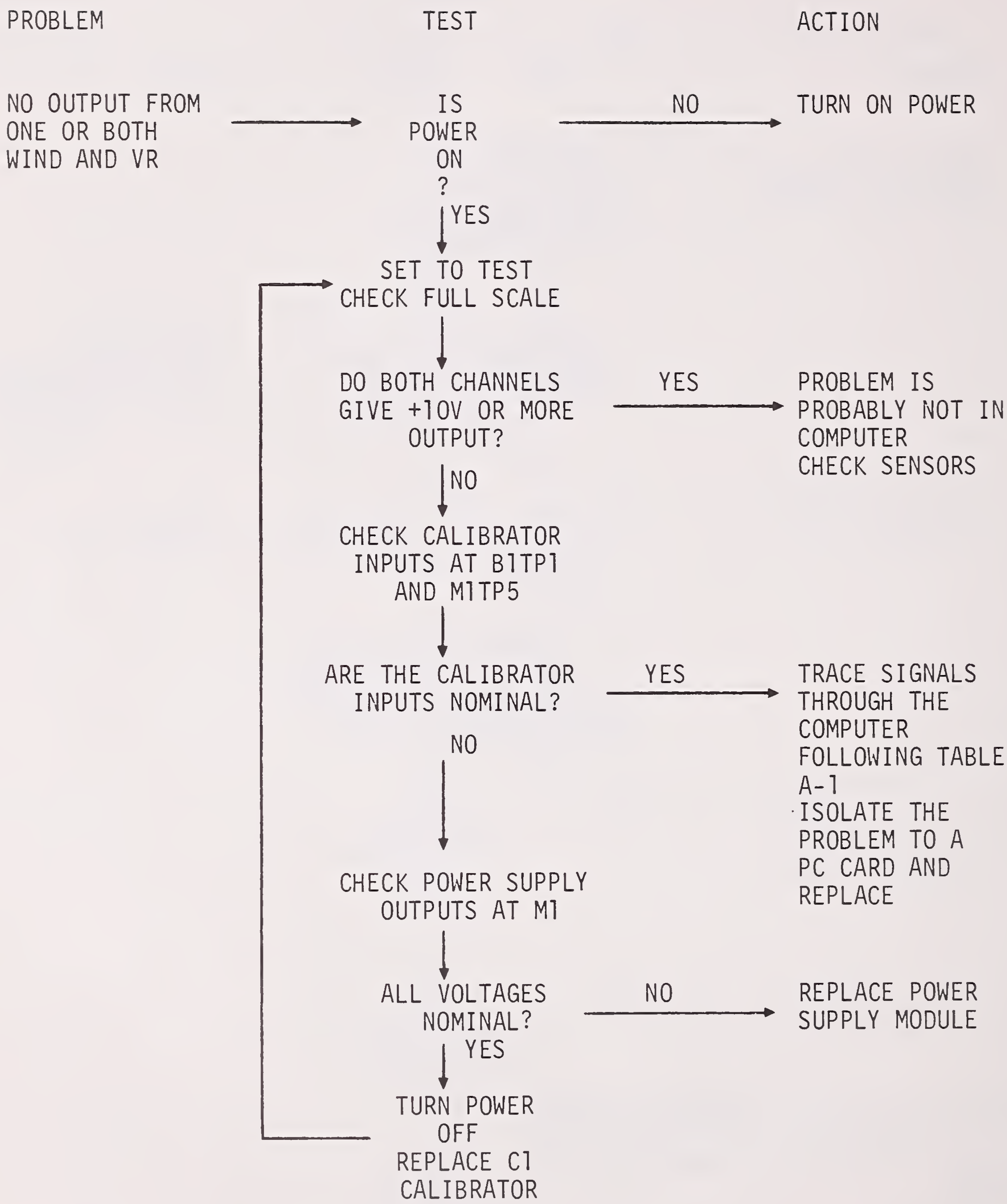

Figure 4-13.—Troubleshooting procedure for the computer.

PART I

PROBLEM	TEST	ACTION
NO SIGNAL AT B1TP1 →	IS COMPUTER ON ? — NO →	TURN ON POWER
	↓ YES	
ADJUSTMENT SPC R1 WON'T BALANCE THE SIGNAL →	IS LIGHT PATH CLEAR ? — NO →	CLEAN SPC WINDOWS REMOVE OBSTRUCTION
GAIN ADJUSTMENT SPC R10 IS INSUFFICIENT FOR ± 3.0 V →	↓ YES	
NOISE IS GREATER THAN 40mV p-p →	IS SPC LAMP ON ? — NO →	EITHER POWER IS NOT CONNECTED TO SPC OR LAMP IS BURNED OUT <u>SHUT OFF POWER BEFORE REMOVING SPC</u> FOR LAMP REPLACEMENT
DC OFFSET IS GREATER THAN 20mV →	↓ YES	
	TURN OFF POWER REPLACE SENSOR	
	↓	
	DOES PROBLEM STILL EXIST? — NO →	REPAIR SPC THAT WAS REMOVED FIG 4-14 PART 2
	↓ YES	
	CHECK CABLING AND CONNECTORS	
	-	
	TURN POWER OFF REMOVE SENSOR TURN POWER ON CHECK THE VOLTAGES AT THE SPC CABLE CONNECTOR WITH A PORTABLE VOM	

PINS +	PINS -	
A	F	0 V A.C. and D.C. SIGNAL LINE TO GROUND
B	F	+15V D.C. AMPLIFIER SUPPLY
C	F	+27V D.C. LAMP SUPPLY
D	F	-15V D.C. AMPLIFIER SUPPLY
E	F	0 V LAMP RETURN TO SIGNAL GROUND
A	F	2,000 ohms ± 200

Figure 4-14.—Troubleshooting the snow particle counter.

PART 2

PROBLEM	TEST		ACTION
NO OUTPUT NOISY OUTPUT UNBALANCED OUTPUT (CAN'T BE ADJUSTED)	REMOVE AMPLIFIER COVER FIX SENSOR TO TEST BENCH CONNECT POWER CONNECT OSCILLOSCOPE TO OUTPUT AT PIN A MOVE A WIRE THROUGH THE LIGHT BEAM AND OBSERVE SIGNAL ON SCOPE ↓		
	CAN SENSOR BALANCE AND GAIN BE ADJUSTED FOR CLEAN SIGNAL OF ± 4.0 V	YES →	SENSOR IS OK RECHECK IN VRM SYSTEM
	↓ NO		
	IS ONLY HALF OF SIGNAL OBSERVED?	YES →	CHECK PHOTO-TRANSISTOR
	↓ NO		
	REMOVE INPUTS 1 AND 2 FROM AMPLIFIER BOARD GROUND INPUT 2 CONNECT A SINE WAVE VOLTAGE OF 1 kHz AND 0.1 V p-p TO INPUT 2 ↓		
	IS OUTPUT A SINE WAVE OF ABOUT 3V p-p?	YES →	PROBLEM IS NOT IN SPC AMPLIFIER CHECK PHOTO TRANSISTORS
	↓ NO		
	REPLACE AMPLIFIER OR TRACE SIGNAL AND REPLACE COMPONENTS		

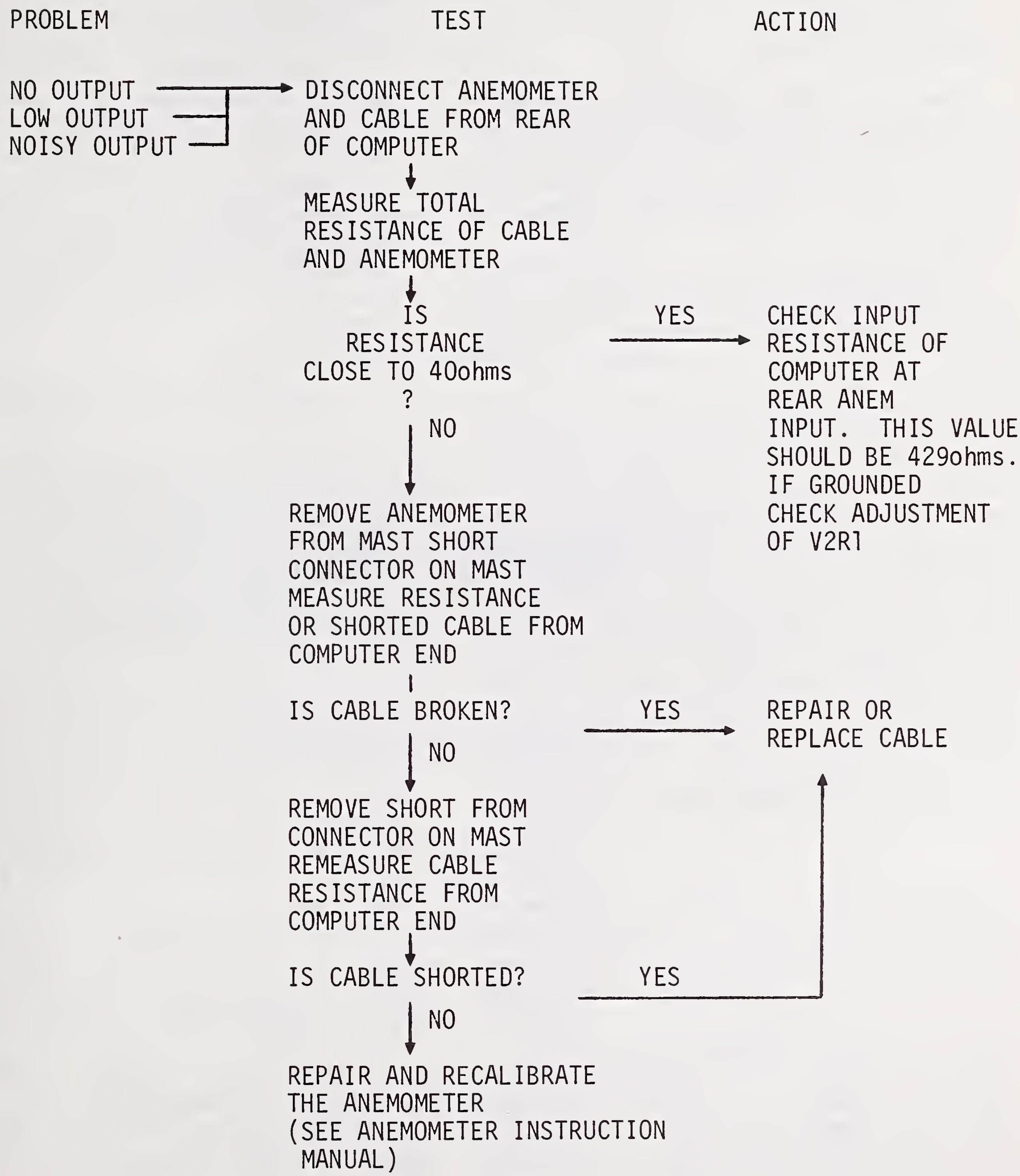

Figure 4-15.—Troubleshooting the generating anemometer.

Schematic diagrams

Each part of this section contains a) a circuit description, b) a component location diagram and description list, and c) the circuit diagram.

Snow Particle Counter

The SPC contains a 28-V lamp circuit and a photodetector and amplifier circuit. These two circuits are electrically isolated; that is, the lamp ground return is separate from the signal amplifier ground and separate supply voltages are used.

The sensing circuit employs two NPN silicon phototransistors, biased with -15 V d.c. Amplifiers A1 and A2 provide low impedance current to voltage conversion, thus improving the response time of the phototransistors. Feedback resistor, R1, provides a means of adjusting the signal from the first slit to match the signal from the second slit, eliminating differences due to transistors.

Differential amplifier A3 combines the two detector outputs with unity gain. Capacitor C1 is an optional blocking capacitor that removes the d.c. component due to unbalanced signals. The voltage gain of output amplifier A4 is adjusted with R10 to give the required output from a calibration wire moving through the light path. The feedback loop of A4 also contains thermistor R9 which automatically increases the output gain to compensate for the decrease in phototransistor output with decreasing temperature.

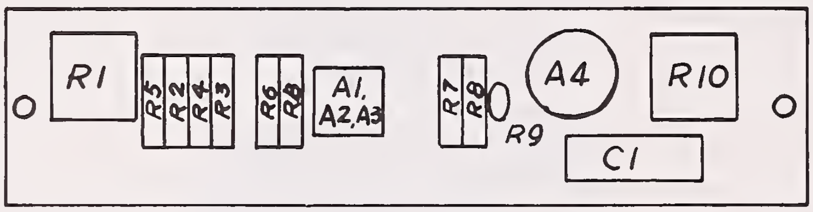

SNOW PARTICLE COUNTER AMPLIFIER

List of Components

No.	
A1, A2, A3	Tripple operational amplifier, siliconix L144AL
A4	Operational amplifier, type 741 military grade
C1	Capacitor, 15uf, 20 wvdc
Q1, Q2	Phototransistor, Motarola MRD 200.
R1, R10	Resistor, variable, 20K, 3/8 sq. wirewound
R2	Resistor, fixed, 10K, 1%, metal film
R3, R4, R5, R6	Resistor, fixed, 5.1K, 1%, metal film
R7	Resistor, fixed, 1K, 1% metal film
R8	Resistor, fixed, 20K, 1% metal film
R9	Thermistor, YS1 44003, 1K @ 25°C
RB	Resistor, amplifier bias, 1 meg, 1%

Figure 5-1.—Component placement on SPC amplifier.

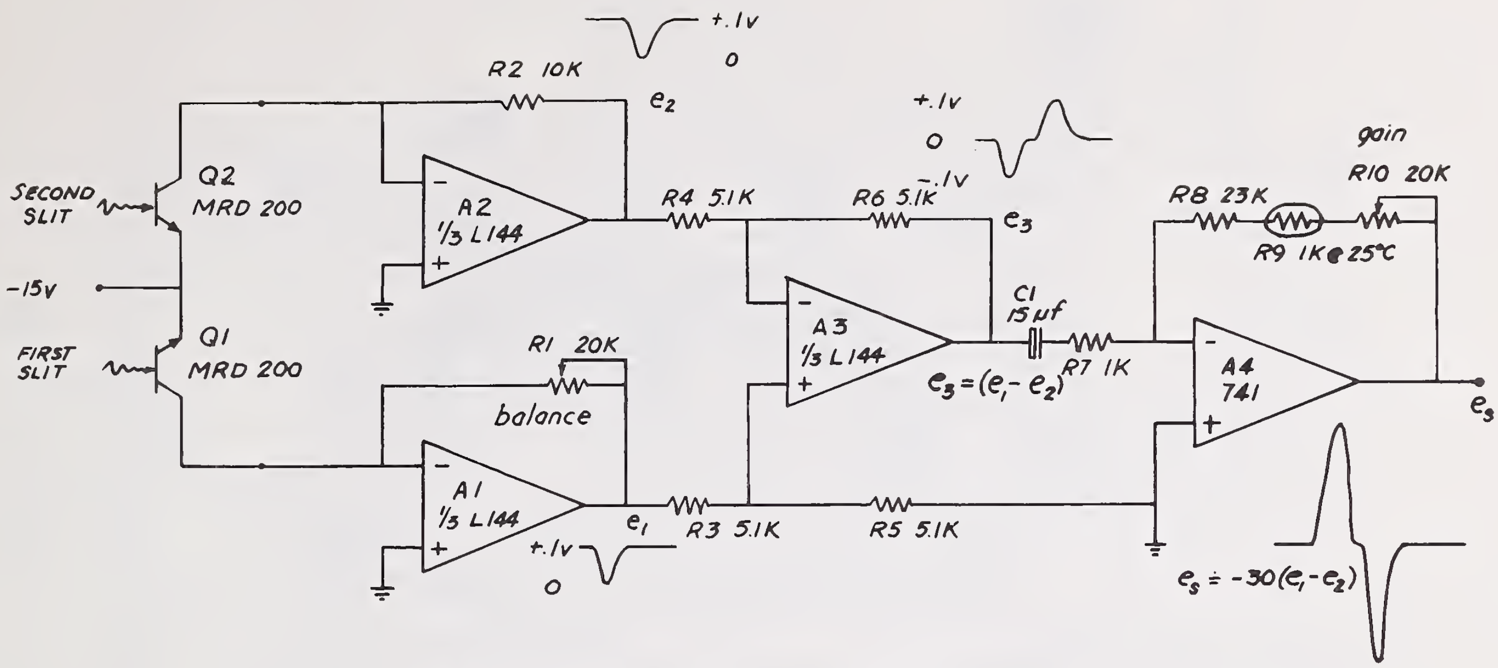

Figure 5-2.—Schematic diagram for SPC amplifier.

B1 Amplifier and A.C.-D.C. Converter

This circuit provides line termination for the SPC, amplifies the signal, and provides a d.c. signal proportional to the average peak-to-peak input. The SPC signal is terminated by R1 and shunted by C1 to reduce high frequency noise. Amplifier A1 is ac coupled through C2 to the wiper of R1. Zero offset of A1 is adjusted by R7 and gain is set to 20 by R6. The amplifier is non-inverting.

Amplifiers A2 and A3 provide the a.c.-d.c. conversion. The positive part of the SPC is inverted by A2 and A3 contains C4 in a feedback loop to provide low pass filtering; the signal is further filtered by R14 and C5. Full-scale output at TP3 is adjusted by R13.

B-2 Frequency — D.C. Converter

This circuit yields a d.c. voltage proportional to the frequency of snow particles passing through the SPC light beam. The amplified SPC signal triggers a "one-shot", or monostable multivibrator that produces a train of uniform pulses equal in frequency to the frequency of particle signals above some minimum amplitude. The energy in this pulse train is averaged to provide the d.c. output.

Integrated circuit U1 contains a Schmitt trigger with very stable threshold levels. The amplified SPC signal ($20e_s$) is further amplified by A1 to trigger the Schmitt trigger at some minimum input voltage e_s. For example, if the SPC noise level of B1TP1 is 20 mV p-p, then the converter might be set to trigger only on signals of 40 mV p-p, providing a factor of 2 safety margin. A sine-wave signal of 40 mV p-p applied to the external input jack would give $20e_s = 800$ mV p-p as input to A1 on pc board B2. Thus, the positive amplitude of the sine wave would be +0.4 V. The Schmitt trigger threshold for positive going pulses is very stable at +1.66 V, so, the gain of amplifier A1 is adjusted by R3 to be just over 4, ($1.66/.4 = 4.15$). Thus, only signals with positive pulses greater than 20 mV will cause the Schmitt trigger to change state. Zener diode D1 limits the input to U1 to about 4.7 V.

The output of U2 triggers the monostable multivibrator, U1. Pulses produced by U2 are of equal amplitude and width, regardless of the snow particle signal amplitude or duration. The pulse width is determined by C4 and R12 which were chosen to give a pulse width of about 40μs.

Amplifier A2 with feedback capacitor C1 provides a low pass filter with d.c. output adjusted by R7. Amplifier A3 is employed in a differential mode to provide a zero adjustment, R10, since the "zero level" output of the one-shot is about +0.2 V. Output is a d.c. voltage $e_f = 2f/10^3$ where f is the frequency of positive signals greater than the adjusted trigger level. Response time for a step input is about 5 seconds.

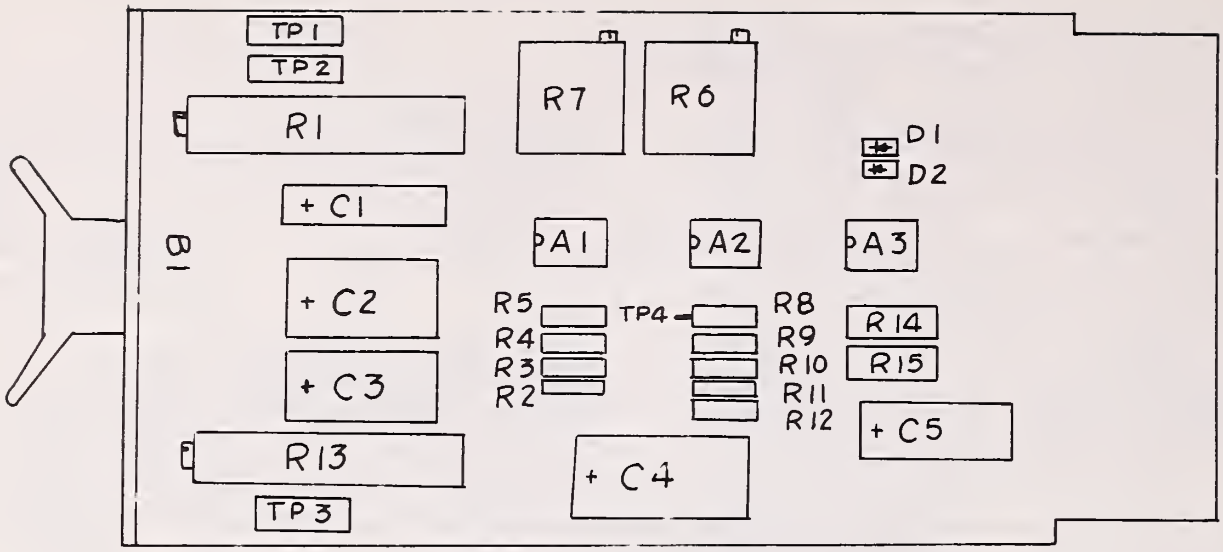

B1 Amplifier and AC-DC Converter

List of Components

No.	
A1, A2, A3,	Operational amplifier, type 741, commerical grade
C1	Capacitor, .0068uf, 20 wvdc
C2, C3	Capacitor, .1uf 20wvdc
C4	Capacitor, 150uf, 20wvdc
C5	Capacitor, 8.2uf, 20wvdc
D1, D2	Diode, type 1N914
R1	Resistor, variable 2K, wirewound
R2, R3	Resistor, fixed, 11K, 1% metal film
R4	Resistor, fixed, 200K, 1% metal film
R5	Resistor, fixed 4K, 1% metal film
R6, R7	Resistor, variable, 10K, wirewound
R8, R9, R10	Resistor, fixed, 10K, 1% metal film
R11	Resistor, fixed, 5.1K, 1%, metal film
R12	Resistor, fixed, 10K, 1%, metal film
R13	Resistor, variable, 5K, wirewound
R14, R15	Resistor, fixed, 1K, 1%, metal film

Figure 5-3. — Component placement on B1 card.

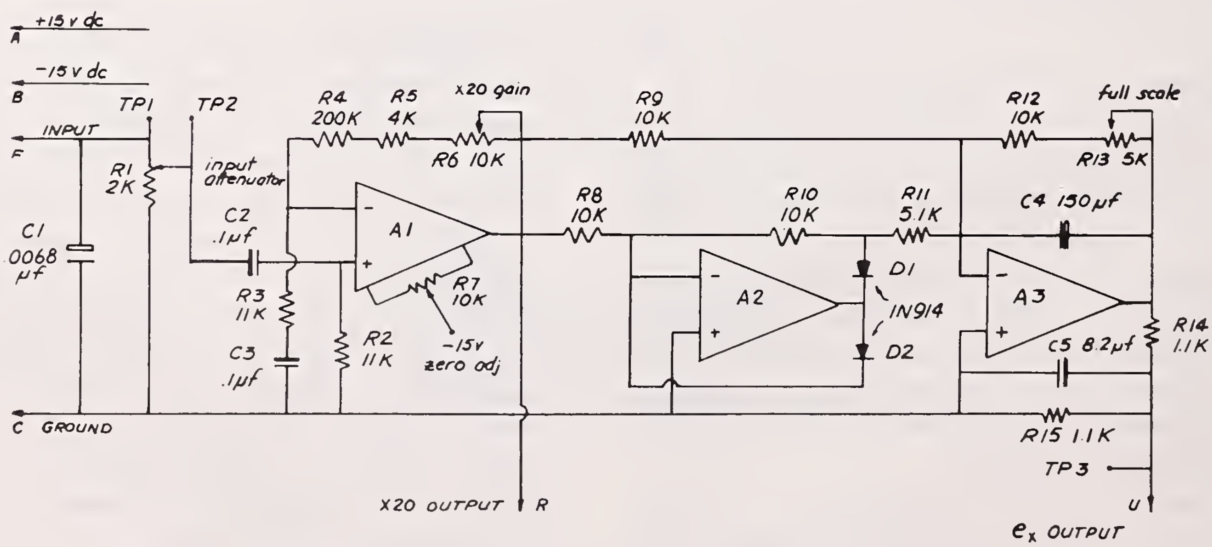

Figure 5-4. — Schematic diagram for B1 — input amplifier and AC-DC converter.

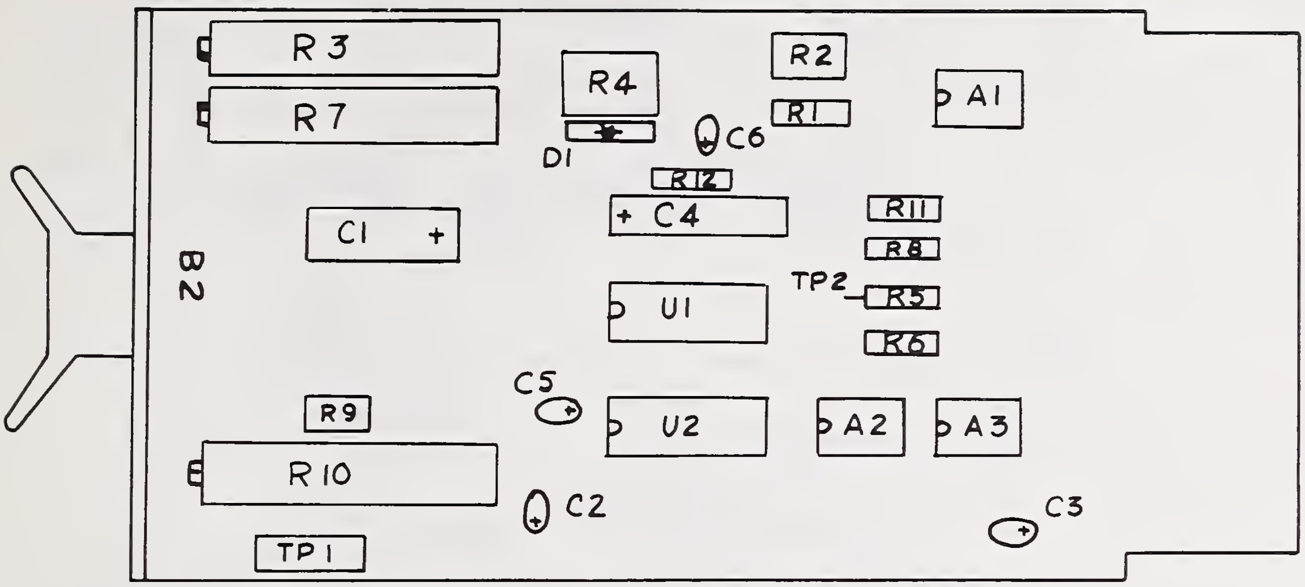

B2 Frequency DC Converter

List of Components

No.	
A1, A2, A3	Operational amplifier, type 741 commercial grade
C1	Capacitor, 8.2uf, 20wvdc
C2, C3	Capacitor, .1uf, 20wvdc
C4	Capacitor, .0068uf, 10%, 20wvdc
C5, C6	Capacitor, .1uf, 20wvdc
D1	Diode, zener, 4.7v ¼ watt
R1	Resistor, fixed, 10K, 1%, metal film
R2	Resistor, fixed, 30K, 1%, metal film
R3	Resistor, variable, 20K, wirewound
R4	Resistor, fixed, 130 ohms, 1%
R5, R8	Resistor, fixed, 10K, 1%, metal film
R6	Resistor, fixed, 100K, 1%, metal film
R7	Resistor, variable, 50K, wirewound
R9	Resistor, fixed, 51.1K, 1%, metal film
R10	Resistor, variable, 5K, wirewound
R11, R12	Resistor, Fixed, 10K, 1%, Metal film
U1	Integrated circuit, type 74121, monostable multivibrator
U2	Integrated circuit, type 7413, Schmitt trigger

Figure 5-5.—Component placement on B2 card.

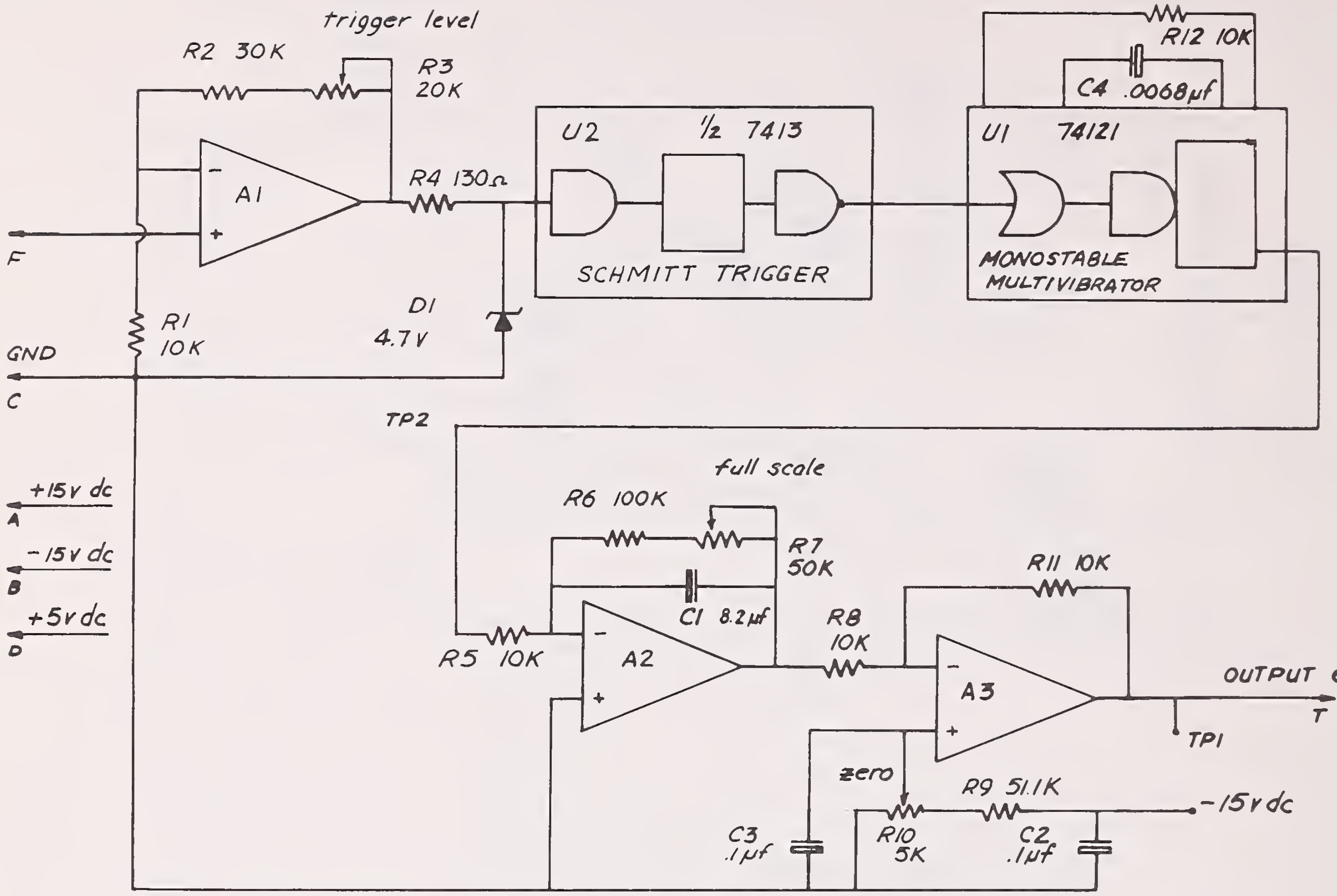

Figure 5-6.—Schematic diagram for B2 — frequency to DC converter.

V1 Analog Squaring Circuit

This printed circuit uses an encapsulated multiplier to obtain a voltage proportional to the square of average particle diameter. The output voltage e_x produced by the a.c.-d.c. converter on B1 is related to average particle diameter by the equation $e_x = (X-100)/100$ where X is the diameter in microns. A voltage proportional to the square of average diameter would result from $(e_x + 1)^2$.

Amplifier V1A1 is employed to sum the input voltage e_x and a constant 1-V d.c. signal obtained from the +15-V supply through adjustable voltage divider R1 and R3. Gain of this amplifier is adjusted by R6 to give an output of $-5(e_x + 1)$, and when the input e_x is zero, amplifier offset is adjusted by R7 to give -5.00 V output.

The multiplier M1 squares this signal to yield $2.5(e_x + 1)^2$. With zero input e_x, the multiplier output at TP2 is adjusted to 2.5 V by R9, and with $e_x = 1.00$ V, the full-scale output is set to 10 V by R8.

V2 Multiplier and Windspeed Amplifier

This circuit board performs two separate functions. The multiplier M1 computes a voltage proportional to the product of frequency and diameter squared, while limiting amplifier A1 generates an inverted windspeed signal.

Input e_f from B2 and $2.5(e_x + 1)^2$ from V1 are multiplied by M1. Output is internally scaled by a factor of 10 to give $.25e_f(e_x + 1)^2$. With $e_f = 0.0$ V and $2.5(e_x + 1)^2 = 2.5$ V, R11 is adjusted for +10 V at TP2.

The d.c. generator of the anemometer is calibrated for a total load of 429 ohms. When connected to the computer, the value of R1 is adjustable to provide this load. If no recorder is connected to the optional output at H, then R1 should be set for 429 ohms, since the amplifier load is negligible. Otherwise, R1 should be set so the total load of R1 in parallel with R2 and the recorder is 429 ohms.

Amplifier A1 inverts and amplifies the windspeed signal e_u by a factor of 2.5, adjusted by R6. Because this signal $(-2.5e_u)$ is the denomi-

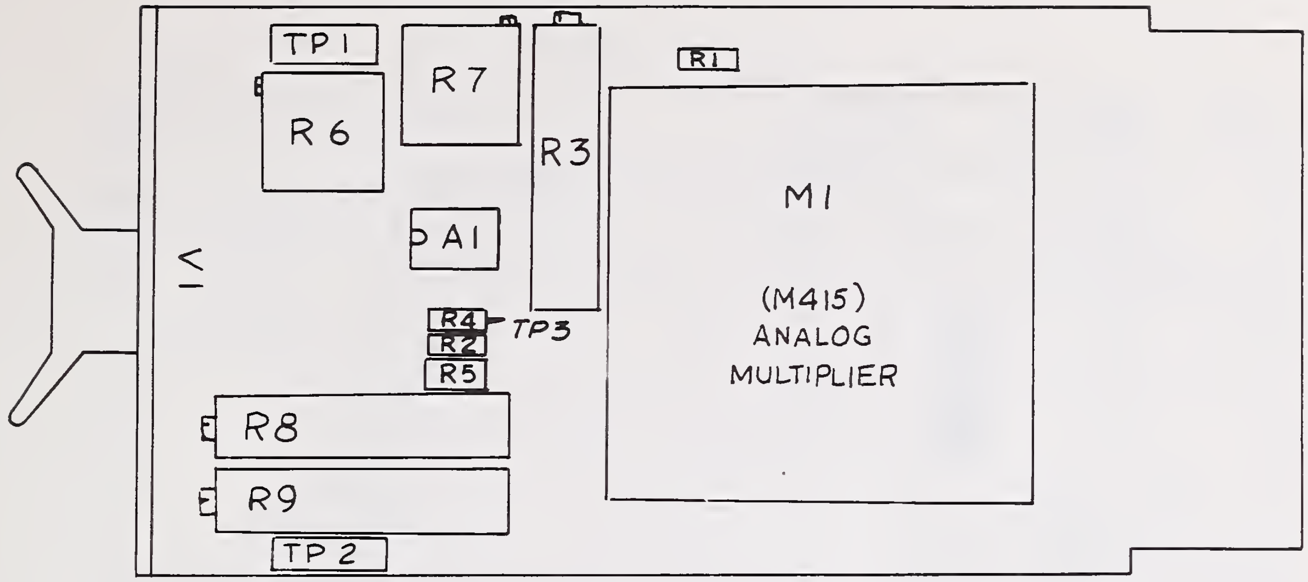

V1 Analog Squaring Circuit

List of Components

No.	
A1	Operational amplifier, type 741, commercial grade
M1	Analog multiplier, Intronics type M415
R1, R2, R4	Resistor, fixed, 11K, 1%, metal film
R3	Resistor, variable, 1K, wirewound
R5	Resistor, fixed, 51.1K,1%, metal film
R6, R7	Resistor, variable, 10K, wirewound
R8	Resistor, variable, 5K, wirewound
R9	Resistor, variable, 20K, wirewound

Figure 5-7. — Component placement on V1 card.

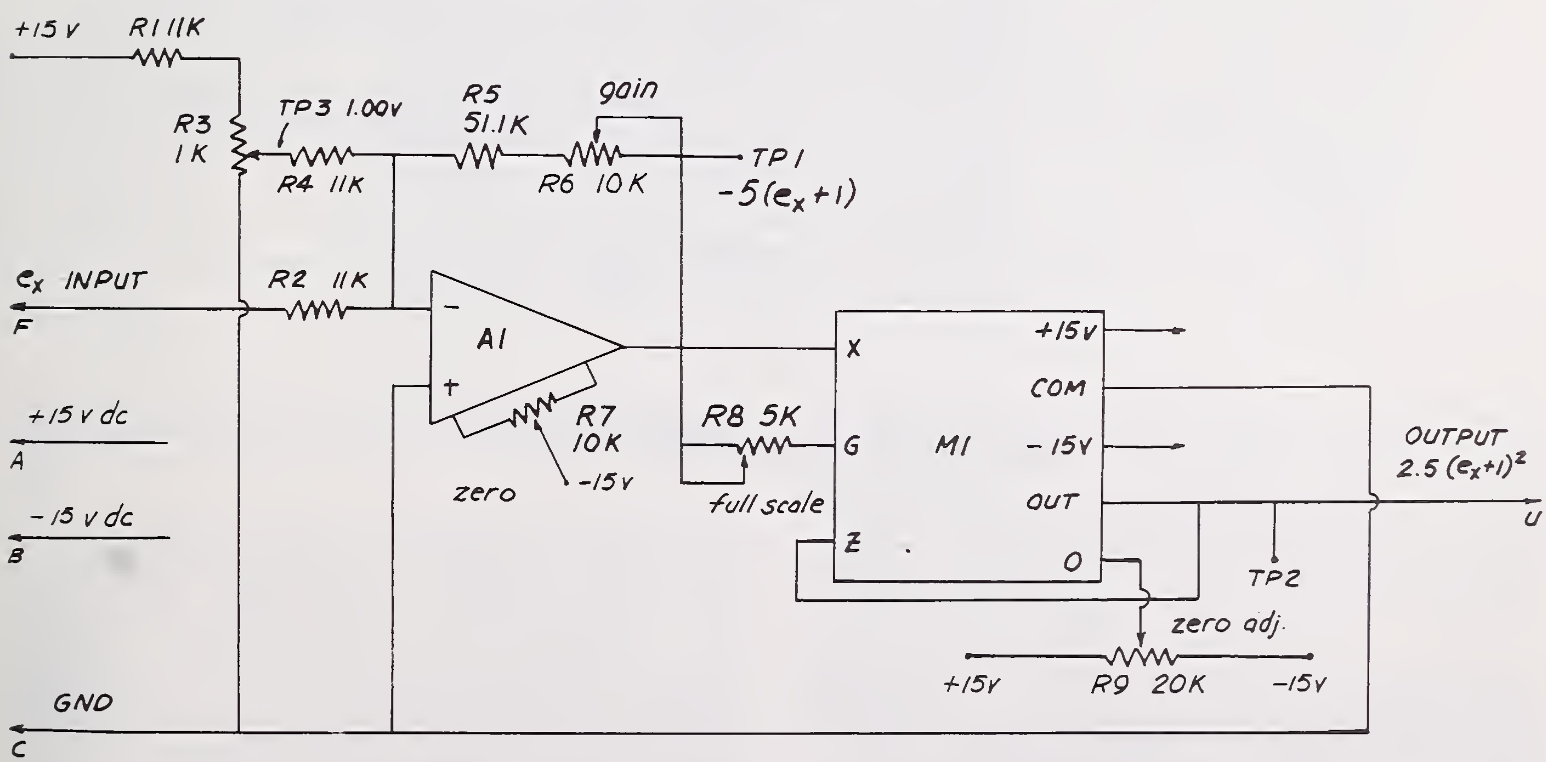

Figure 5-8. — Schematic diagram for V1 — analog squaring circuit.

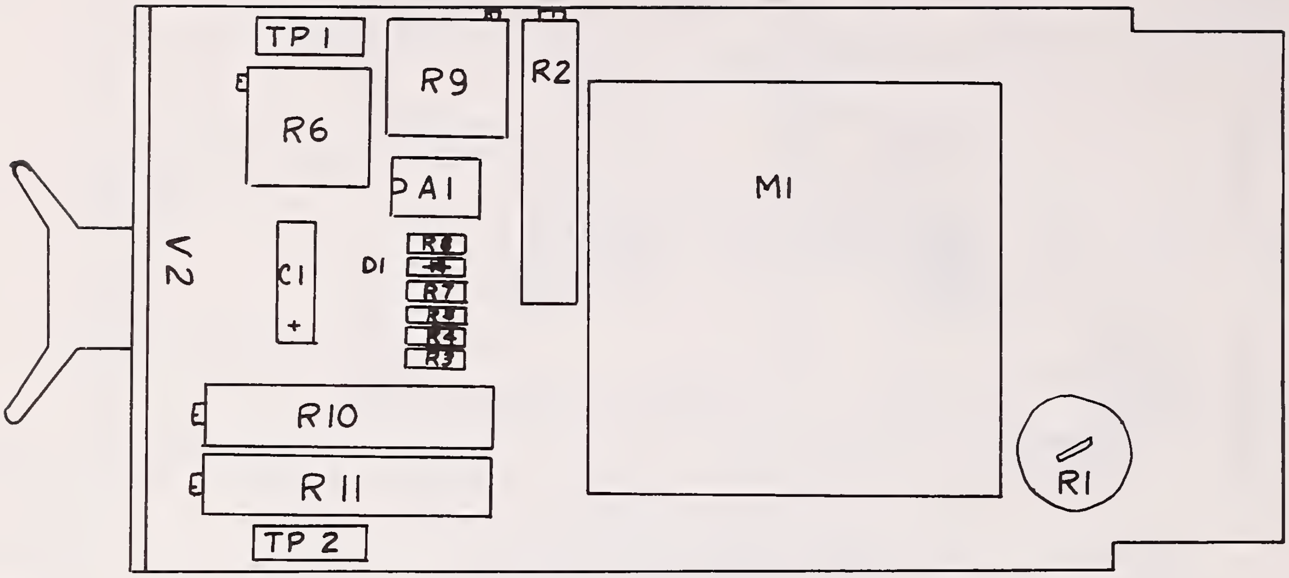

V2 MULTIPLIER and WIND SPEED AMPLIFIER

List of Components

No.	
A1	Operational amplifier, type 741, commercial grade
C1	Capacitor, 15uf, 20 wvdc
D1	Diode, type 1N914
M1	Analog multiplier, Intronics type M415
R1	Resistor, variable, 1K wirewound
R2	Resistor, variable, 5K, wirewound
R3, R4, R5	Resistor, fixed, 10K, 1%, metal film
R6, R9	Resistor, variable, 10K, wirewound
R7, R8	Resistor, fixed, 10K, 1%, metal film
R10	Resistor, variable, 5K, wirewound
R11	Resistor, variable, 20K, wirewound

Figure 5-9.—Component placement on V2 card.

nator input to the divider on V3, it is desirable to avoid letting the value go to zero. The limiting circuit R7, R8, and D1 accomplish this, as shown in figure 4-9. The break point is adjusted by R9, so, the output at TP1 is -1.00 V when input e_u is zero. Feedback capacitor C1 is employed to match the response time of this circuit to those of B1 and B2.

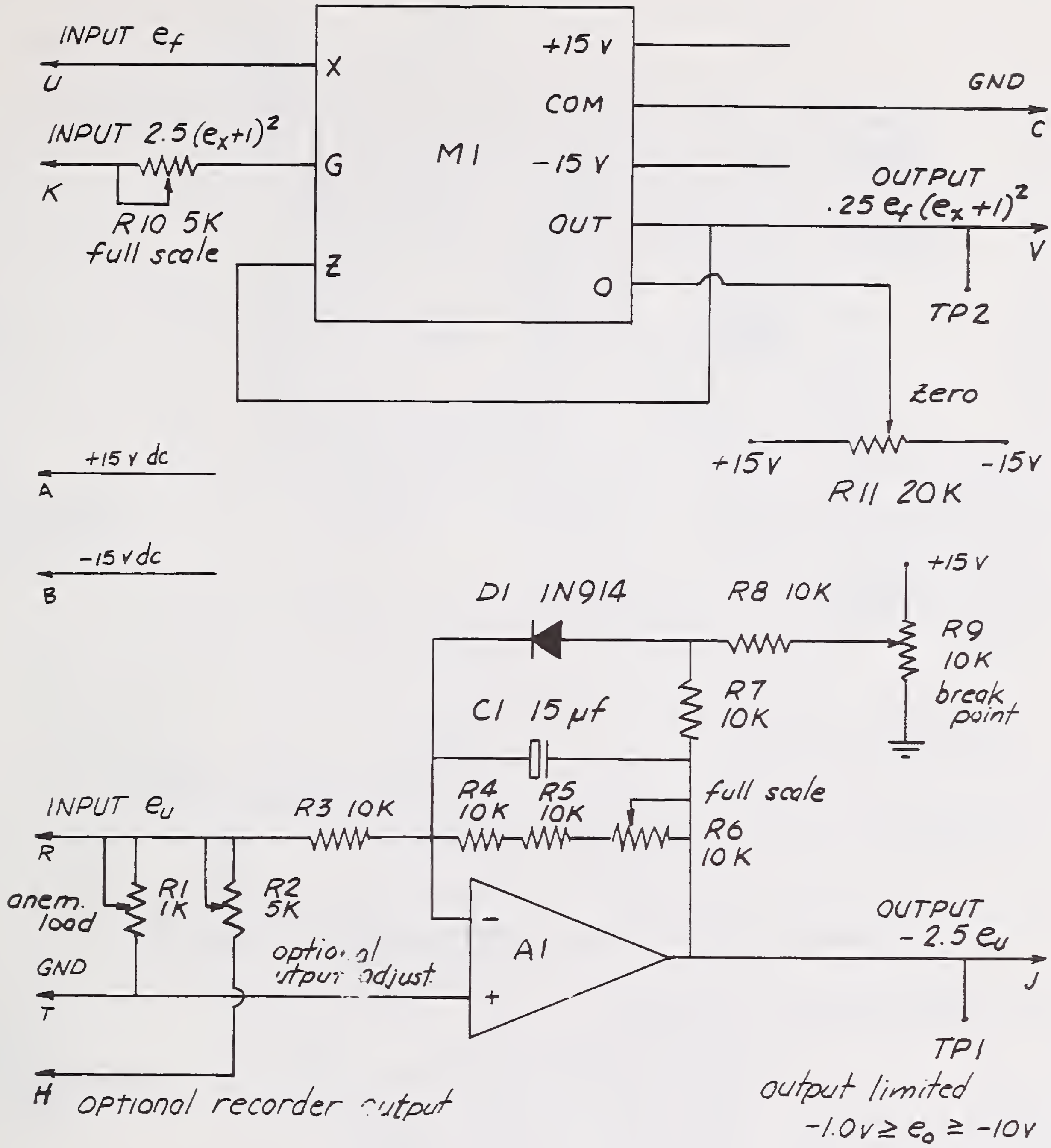

Figure 5-10.—Schematic diagram for V2 — multiplier and windspeed amplifier.

V3 Analog Divider and Output Scaling Amplifier

Final computation of a voltage inversely proportional to visual range is accomplished by this circuit. In addition to a non-inverted, undamped windspeed signal is provided for recording.

Divider M1 computes the ratio $-e_f(e_x + 1)^2/e_u$ from the outputs of V2. With no input, the product $.25e_f(e_x + 1)^2$ is zero and $-2.53e_u$ is -1.0 V. Output at TP3 is adjusted to zero by R1. Full-scale inputs of $+10$ V and -10 V are used to give full-scale output of -10 V adjusted by R2. This output is scaled and further damped by A1 with feedback capacitor C1. Gain of A1 is adjusted by R4 as discussed in the subsection on adjusting V3, final scaling amplifier.

The windspeed output $2.5e_u$ is obtained from A2. No zero adjustment is provided. The full-scale output is set by R7.

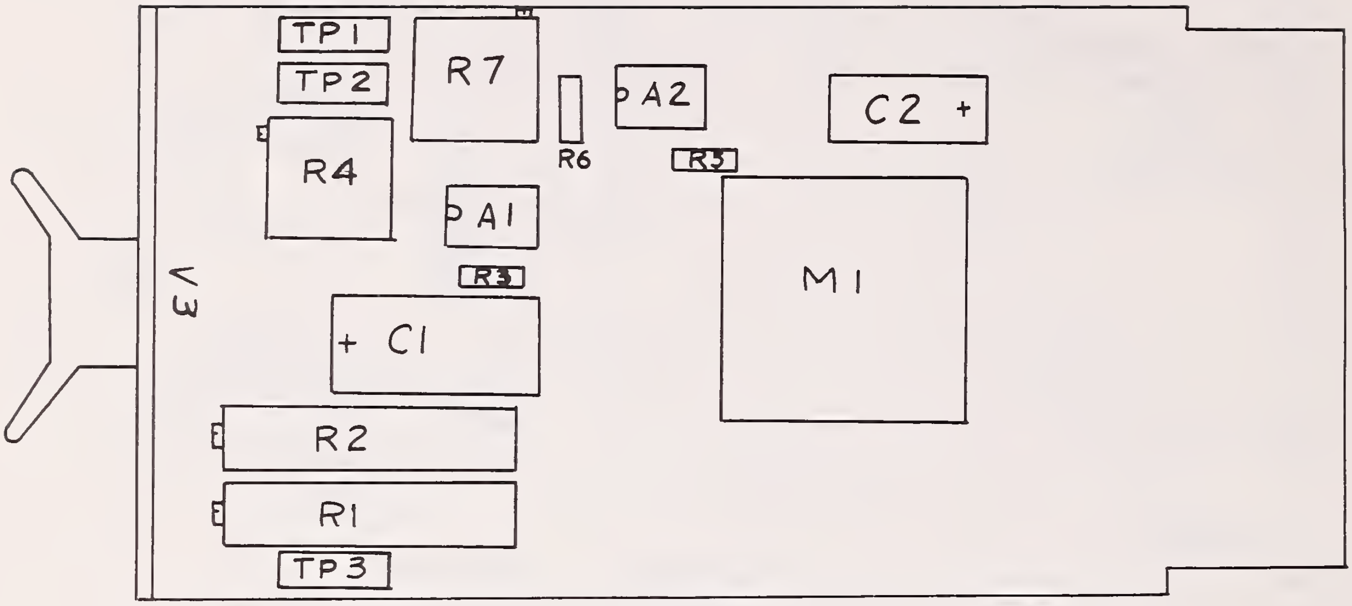

V3 ANALOG DIVIDER and OUTPUT SCALING AMPLIFIER

List of Components

No.	
A1, A2	Operational amplifier, type 741, commercial grade
C1	Capacitor, 150uf, 20wvdc
C2	Capacitor, 8.2uf, 20wvdc
M1	Analog multiplier, Intronics type M441
R1, R2	Resistor, variable, 20K, wirewound
R3	Resistor, fixed, 5.1K, 1%, metal film
R4, R7	Resistor, variable, 10K, wirewound
R5, R6	Resistor, fixed, 10K, 1%, metal film

Figure 5-11.—Component placement on V3 card.

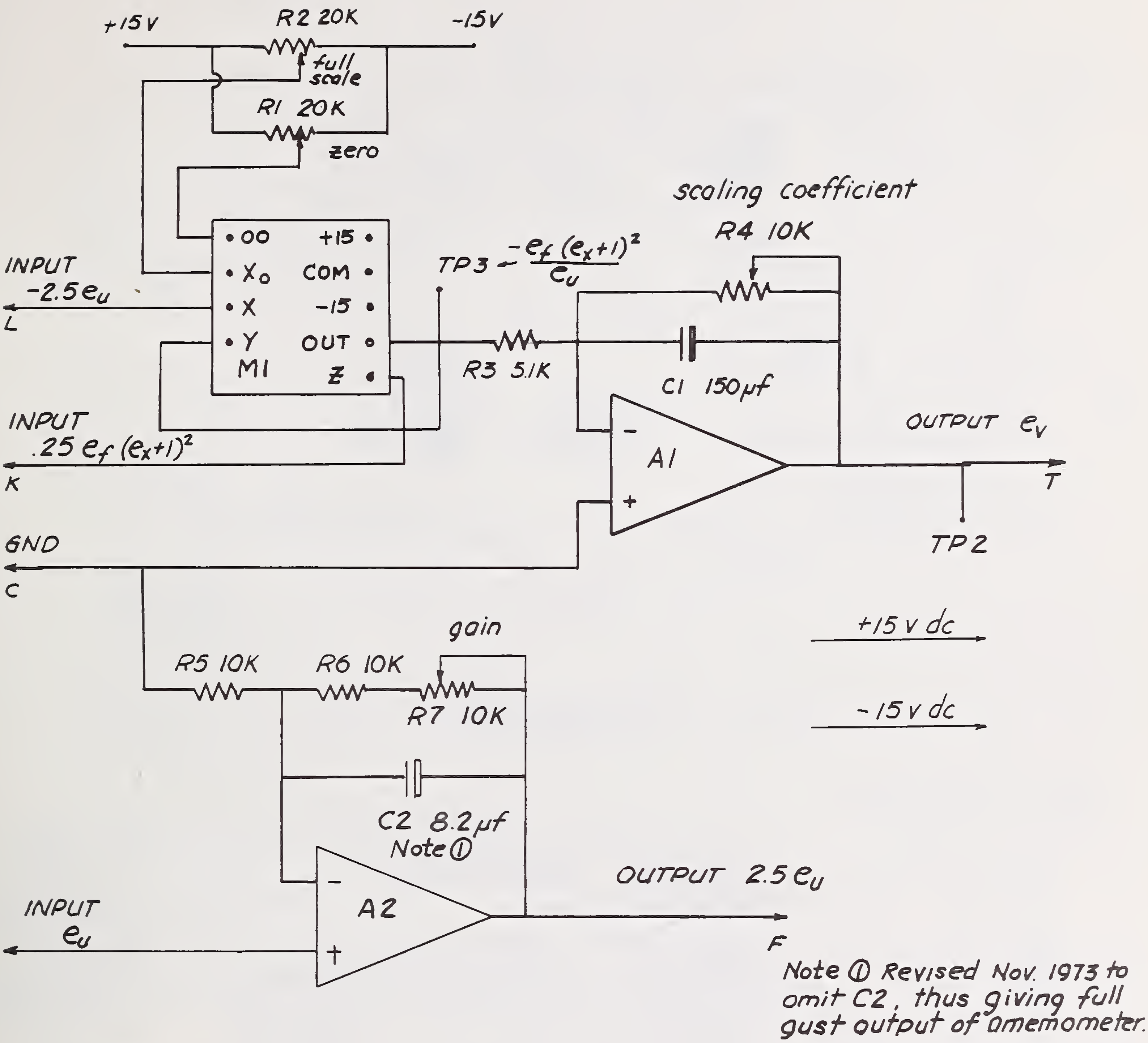

Figure 5-12.—Schematic diagram for V3 — analog divider and output scaling amplifier.

C1 Calibrator

A simple Wien bridge oscillator, and a zener regulated d.c. reference amplifier provide the full-scale input signals used to check operation of the VRM.

The oscillator frequency is determined by R1 + R2 and C1. Stability and distortion are set by R3. Amplitude is adjusted by R7 and A2 is a voltage follower that prevents loading from changing the oscillator output.

Amplifier A3 provides an adjustable output while maintaining constant load conditions on zener diode D3.

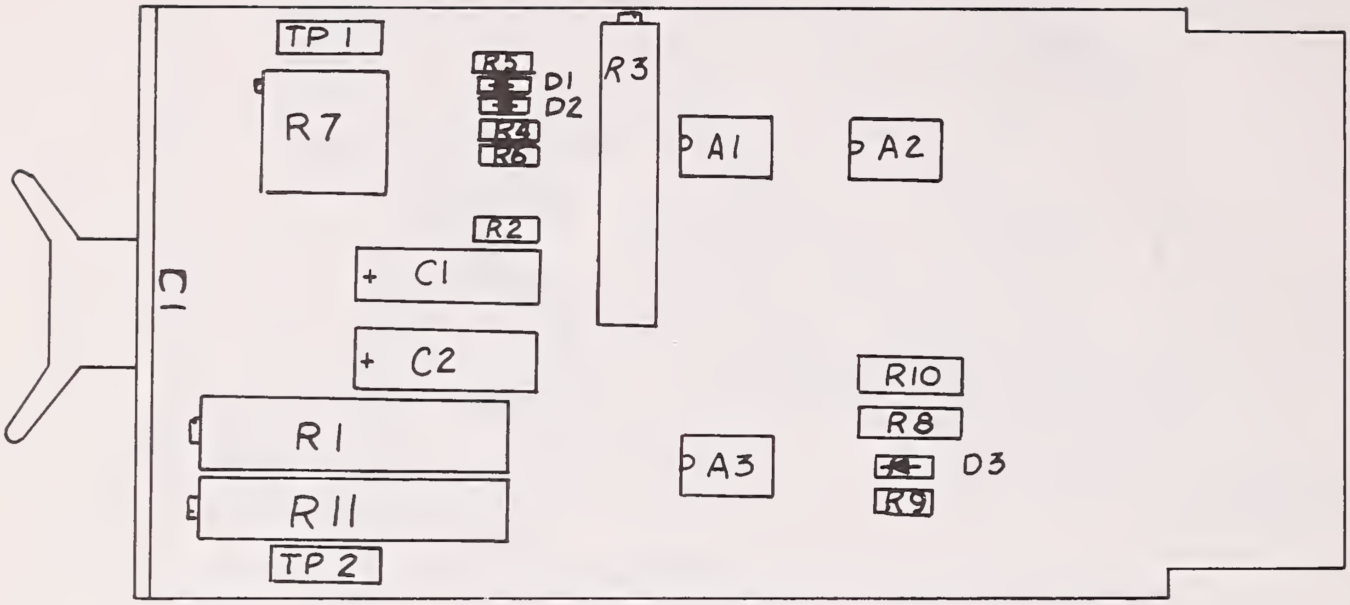

C1 CALIBRATOR

List of Components

No.	
A1, A2, A3	Operational amplifier, type 741, commercial grade
C1, C2	Capacitor, .0033uf 20wvdc
D1, D2	Diode, type 1N914
D3	Diode, zener, 4.7v, ¼ watt
R1	Resistor, variable, 1K, wirewound
R2, R5	Resistor, fixed, 10K, 1%, metal film
R3	Resistor, variable, 50K, wirewound
R4	Resistor, fixed, 11K, 1%, metal film
R6	Resistor, fixed, 200K, 1%, metal film
R7	Resistor, variable, 10K, wirewound
R8	Resistor, fixed, 576 ohms, 1%
R9	Resistor, fixed, 10K, 1%, metal film
R10	Resistor, fixed, 7.32K, 1%, metal film
R11	Resistor, variable, 1K, wirewound

Figure 5-13.—Component placement on C1 card.

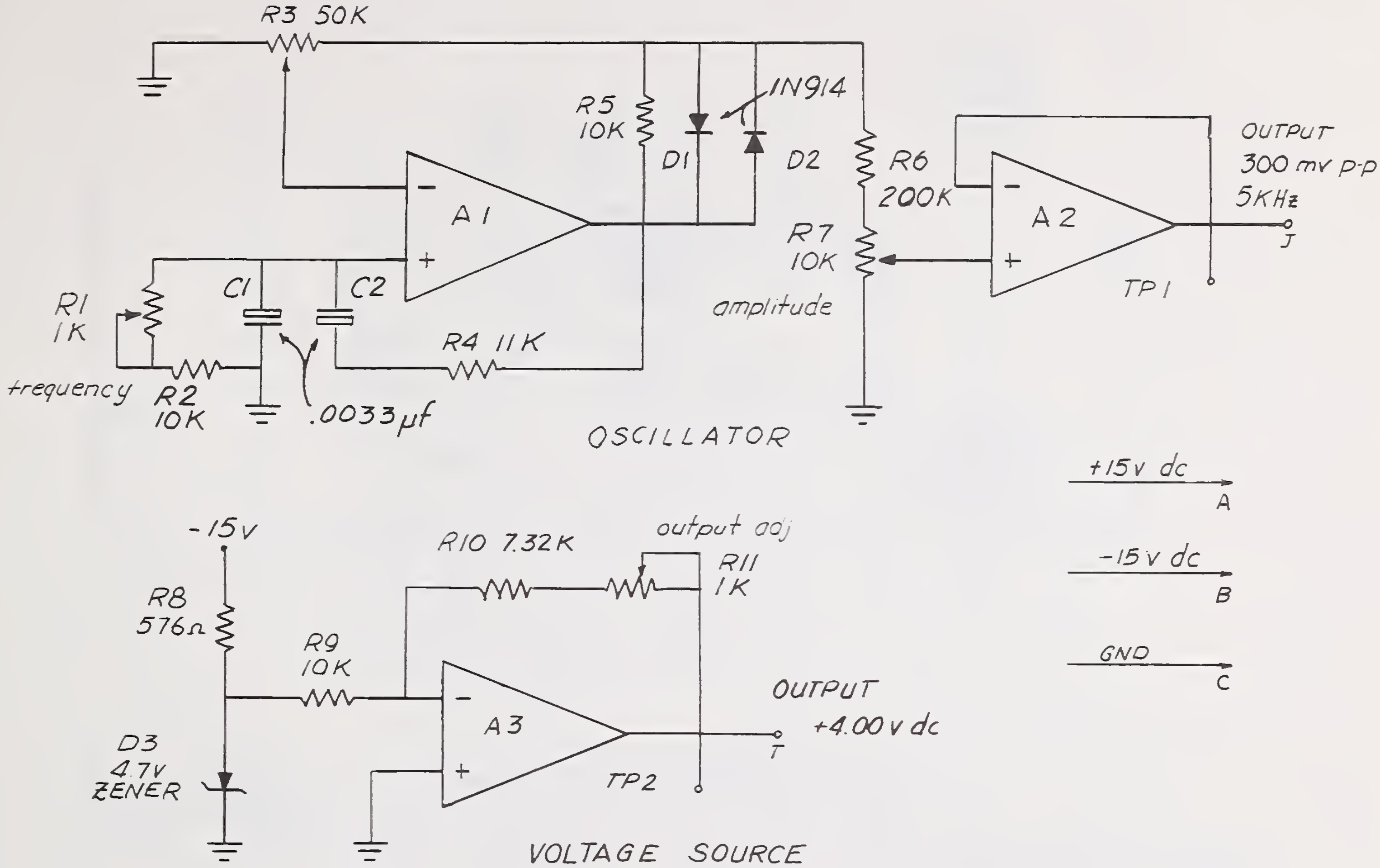

Figure 5-14. — Schematic diagram for C1 — calibrator.

M1 Computer Mode Control

This printed circuit provides test points for the system power supplies, and provides the TEST-RUN switching function.

A solid-state latch is formed by two NAND gates to hold the TEST-RUN switch commands generated by the momentary contact mode switches. This latch drives three transistors which turn on the TEST and RUN lamps and drive the relay K1.

In the RUN mode, 01 and 02 are off, K1 is not energized and Q3 is on, lighting the RUN lamp. When the TEST switch is pushed, Q1 and Q2 conduct, energizing K1 and the TEST lamp. The inputs to B1 and V2 are disconnected from the sensors and connected to the poles of the CHECK switch. Power is also applied to Calibrator C1.

D1 Galvanometer Drivers

Amplifiers A1 and A2 provide the same function of converting an input voltage into a current to deflect the recorder galvonometers. This current is scaled by resistors R1 and R3 so that +10 V d.c. input voltage produces a 1 mA current through the recorder, which is connected in the amplifier feedback loop. Thus the recorder must be "floating"; that is, neither galvonometer input may be grounded.

Computer Back Plane Wiring

The computer back plane is an eight-position connector block that makes all the interconnections between the circuit boards. The connector block is wired to hold the boards in the order shown in figure 4-1, as viewed from the front access opening of the VRM computer.

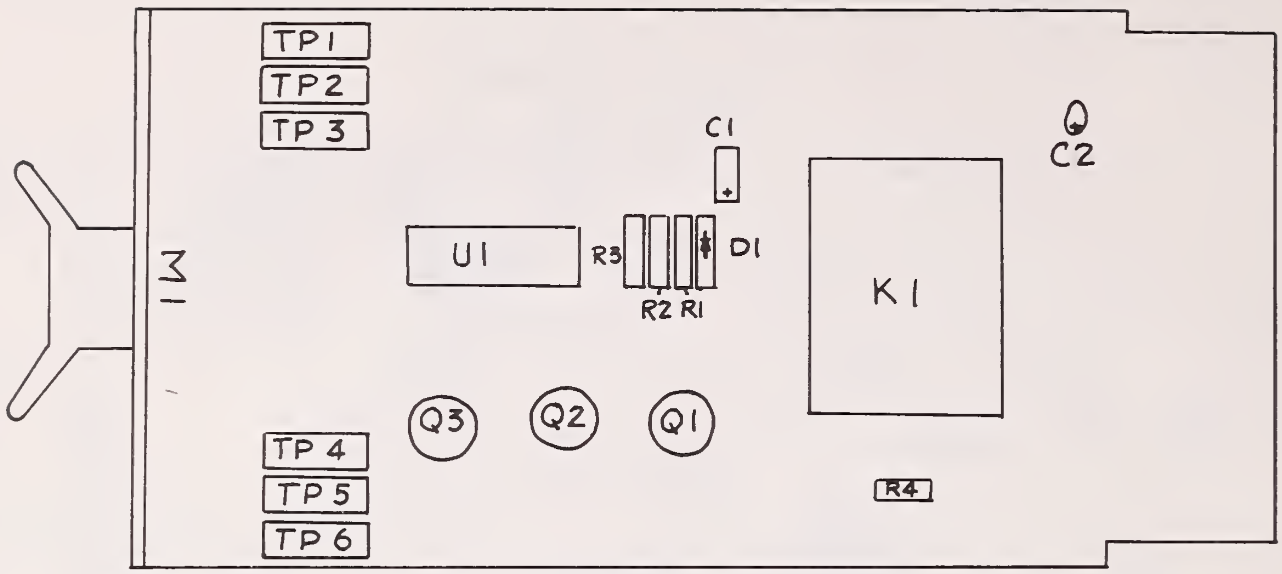

M1 COMPUTER MODE CONTROL

List of Components

No.	
C1	Capacitor, 15uf, 20wvdc
C2	Capacitor, .1uf, 20wvdc
D1	Diode, type 1N914
K1	Relay Clare type MRB 4PDT, 5v coil
Q1, Q2,Q3	Transistor, NPN, type 2N657
R1, R2, R3	Resistor, fixed, 2.8K, 1%
R4	Resistor fixed, 10K, 1%, metal film
U1	Integrated circuit, type 7400, quad nand gates

Figure 5-15.—Component placement on M1 card.

Power Supplies

The system uses modular power supplies throughout. The VRM computer uses three, mounted on the back panel. The recorder employs one which is mounted on a pc card. These supplies are not designed to be repaired, and should be replaced if troubleshooting proves them defective.

Connectors and Cables

Two cables connect the sensors to the VRM computer. The SPC cable terminates in a special connector at the sensor, allowing the cable and sensor to be clamped to a mast. This cable contains six individually shielded conductors. The anemometer cable is a two-conductor unshielded cable.

All other connections are terminated with BNC connectors except the power cords which have standard three-prong plugs.

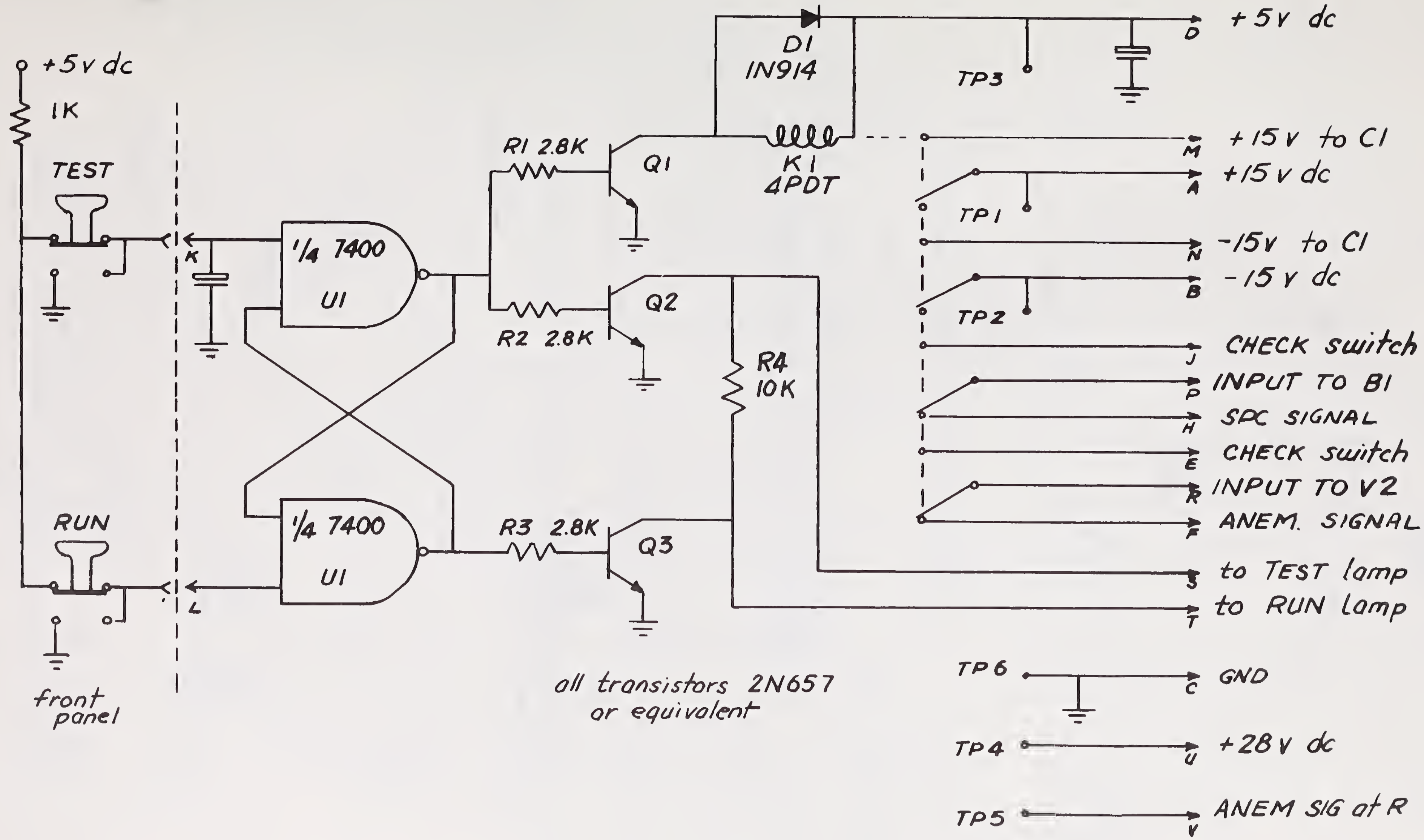
+5v dc
1K
TEST
RUN
front panel
K
L
1/4 7400
U1
1/4 7400
U1
R1 2.8K
R2 2.8K
R3 2.8K
Q1
Q2
Q3
D1
1N914
K1
4PDT
R4
10K
all transistors 2N657 or equivalent
TP3
TP1
TP2
TP6
TP4
TP5
D +5v dc
M +15v to C1
A +15v dc
N -15v to C1
B -15v dc
J CHECK switch
P INPUT TO B1
H SPC SIGNAL
E CHECK switch
R INPUT TO V2
F ANEM. SIGNAL
S to TEST lamp
T to RUN lamp
C GND
U +28v dc
V ANEM SIG at R

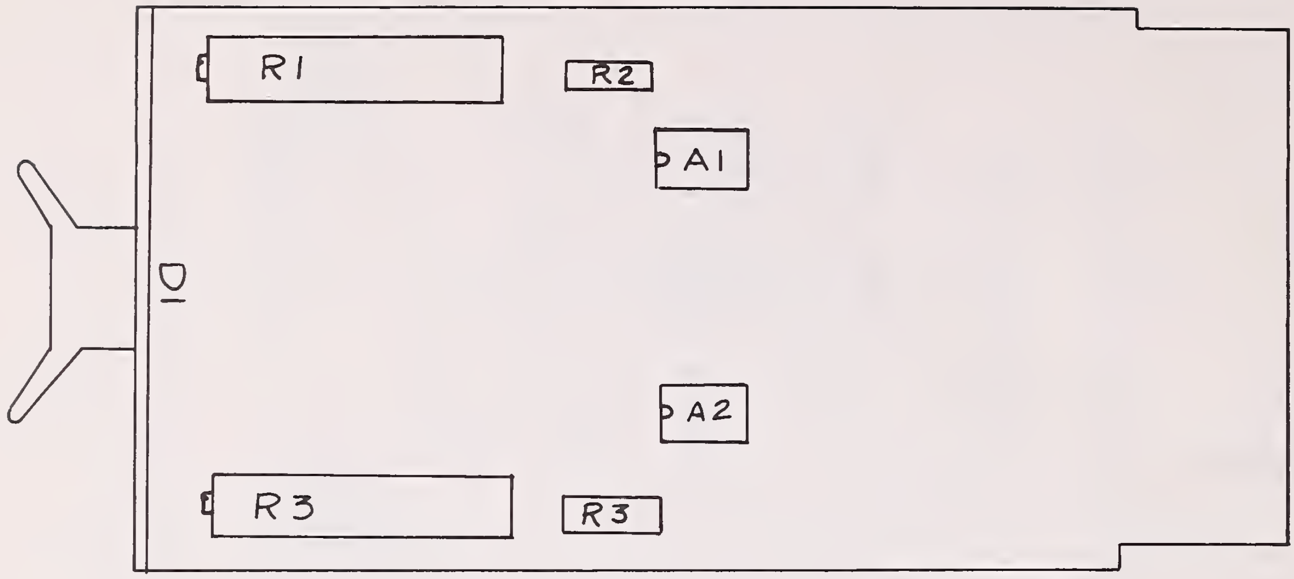

D1 GALVANOMETER DRIVERS

List of components

No.	
A1, A2	Operational amplifier, type 741, commercial grade
R1, R3	Resistor, variable, 5K, wirewound
R2, R4	Resistor, fixed, 7.3K, 1%, metal film

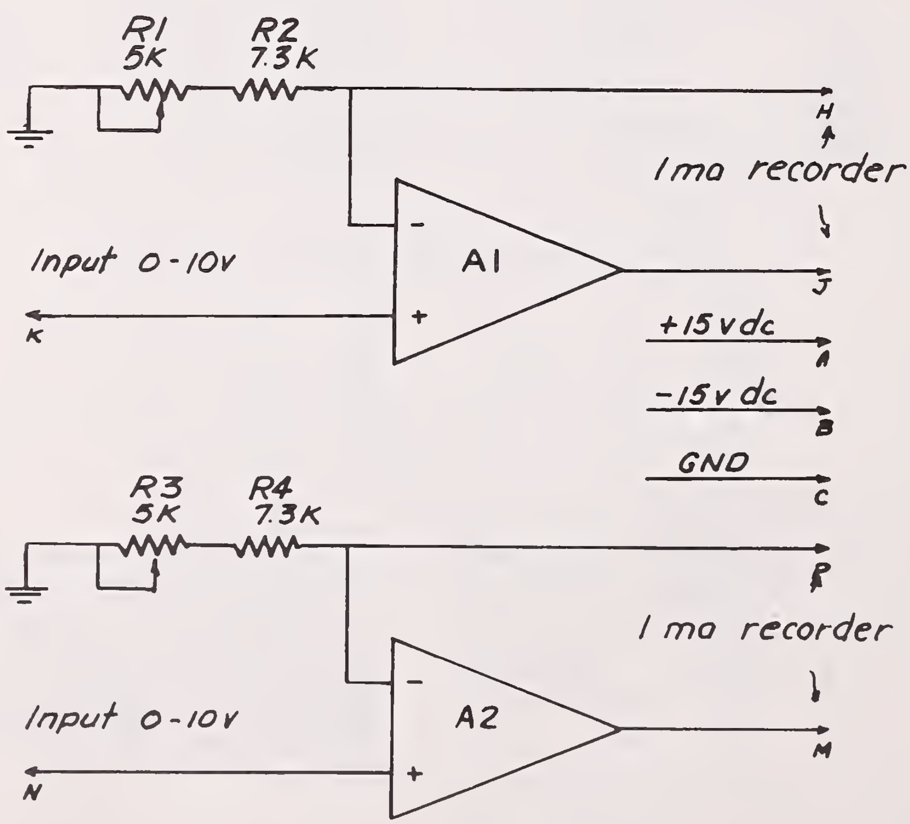

Figure 5-17.—Component placement and schematic diagram for D1 — galvanometer drivers.

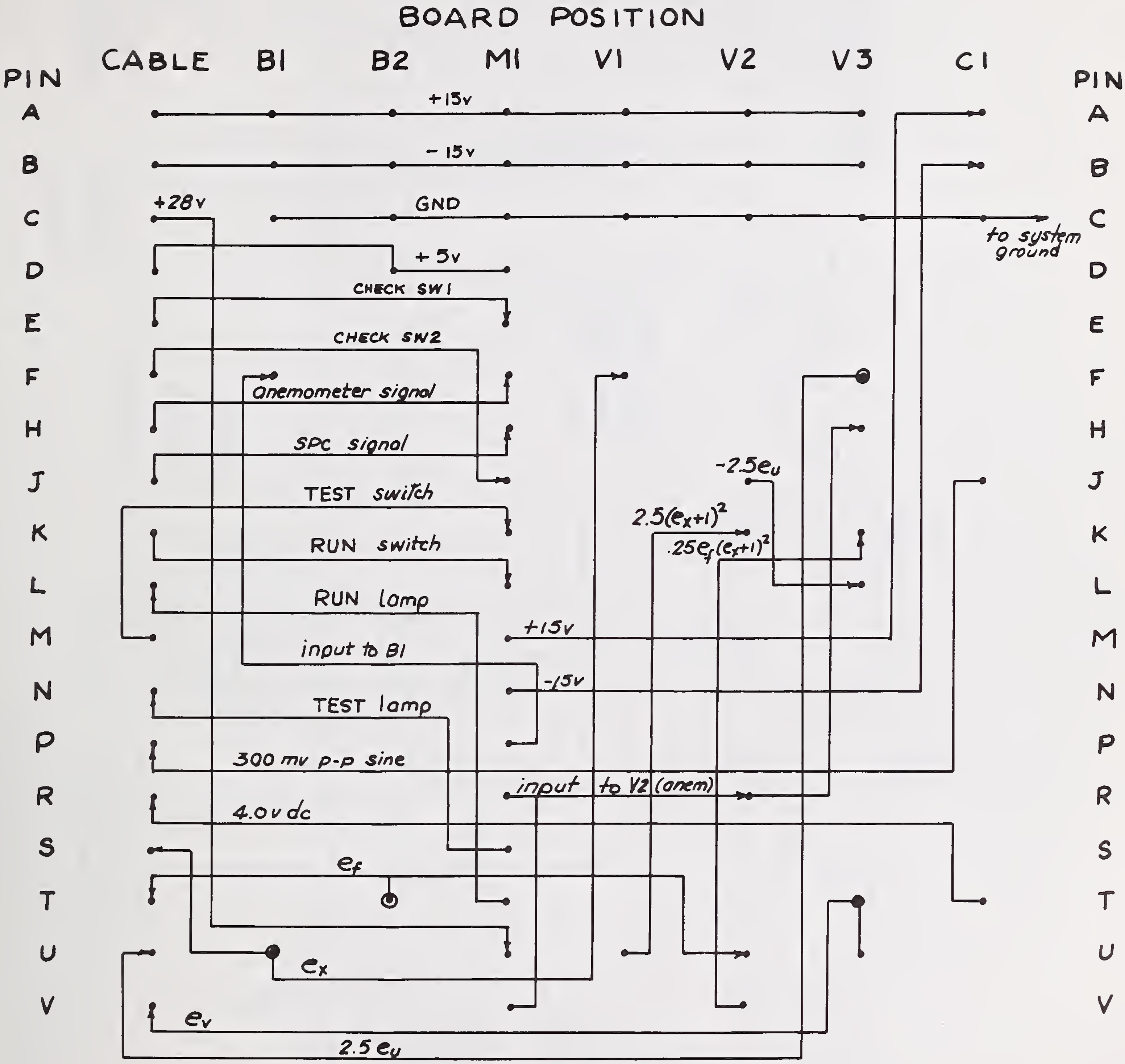

Figure 5-18.—Computer backplane wiring diagram.

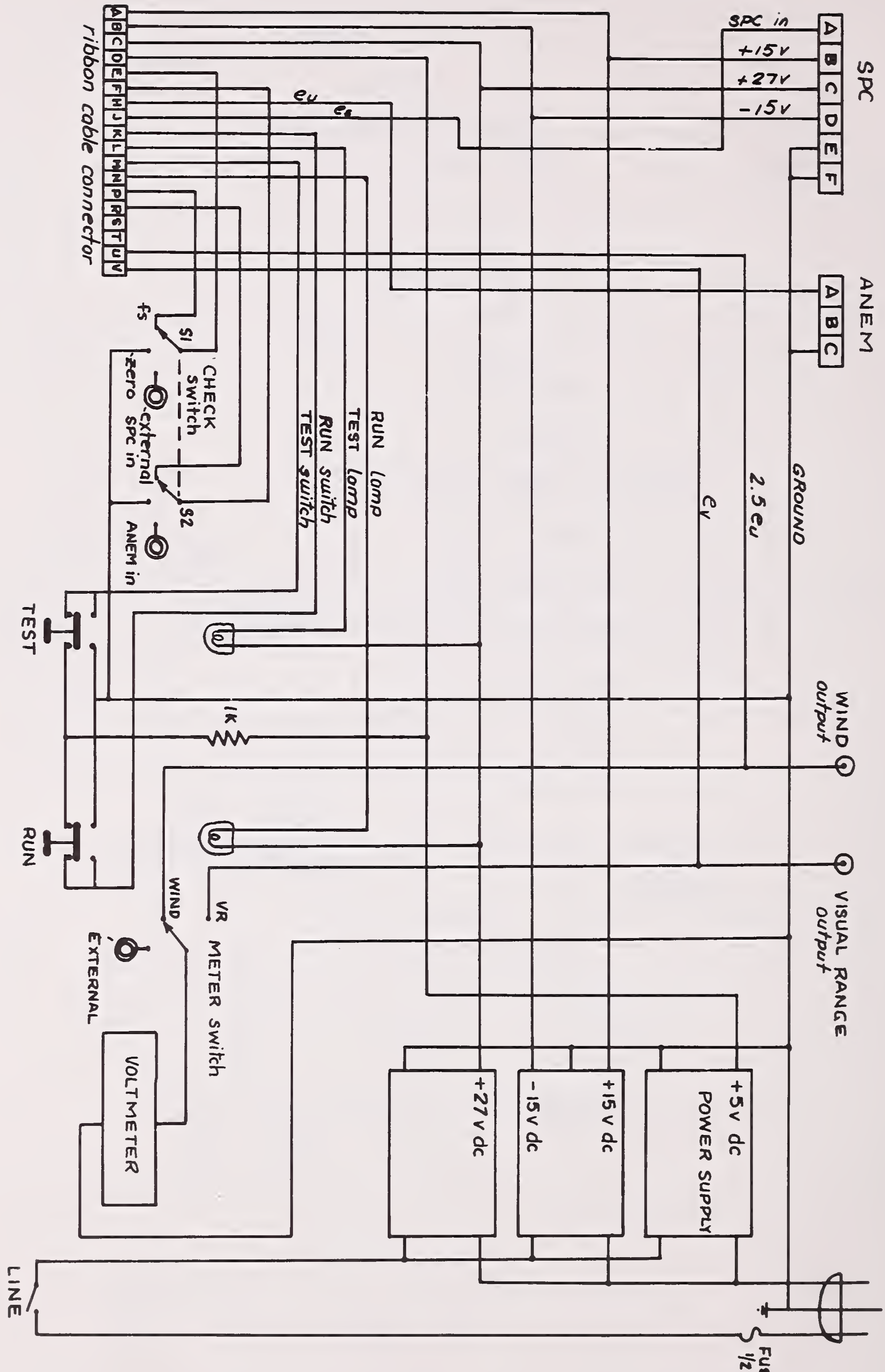
SPC
A B C D E F
SPC in
+15v
+27v
-15v
ANEM
A B C
GROUND
2.5 eu
ev
eu
es
ribbon cable connector
A B C D E F H J K L M N P R S T U V
RUN lamp
TEST lamp
RUN switch
TEST switch
CHECK switch
S1
S2
fs
external
zero SPC in
ANEM in
TEST
RUN
1K
WIND output
VISUAL RANGE output
VR
WIND
METER switch
EXTERNAL
VOLTMETER
+5v dc
POWER SUPPLY
+15v dc
-15v dc
+27v dc
LINE
FUSE
1/2

APPENDIX II

Snow Particle Counter
Shop Drawings

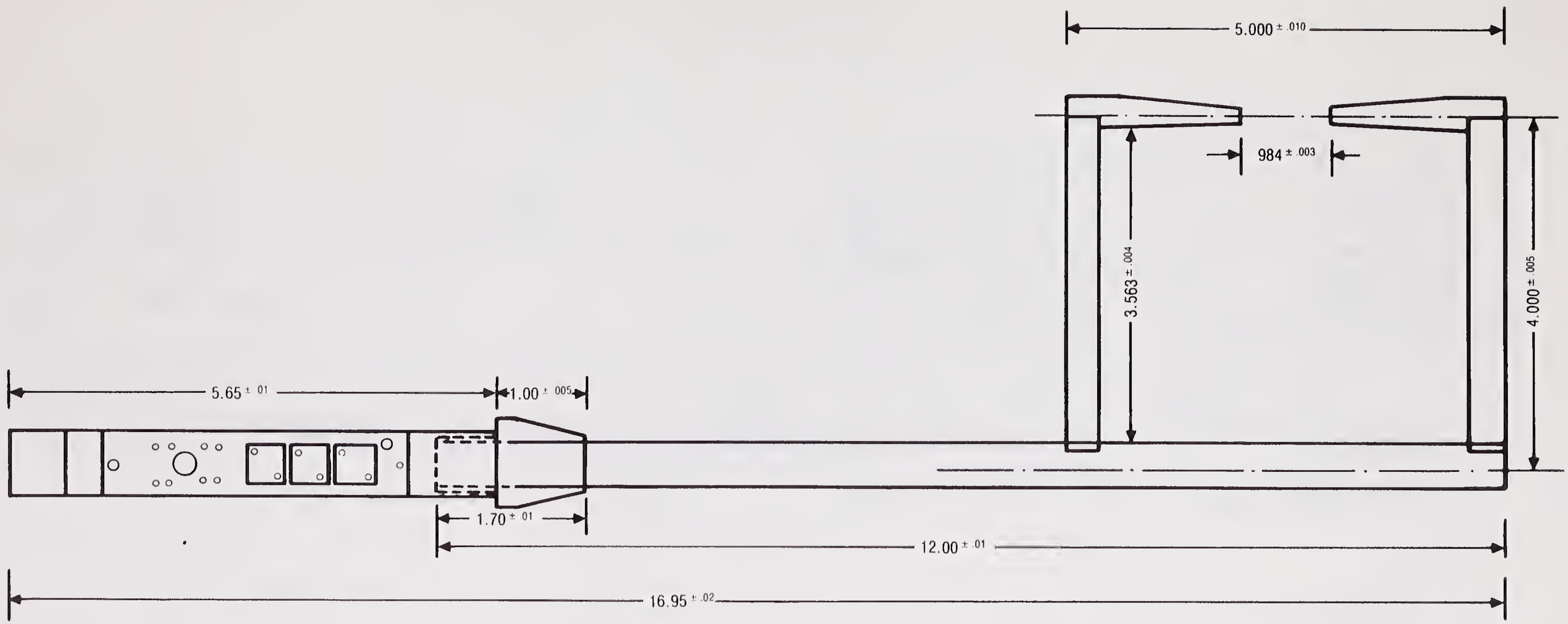

All dimensions in inches

Overall dimensions of SPC

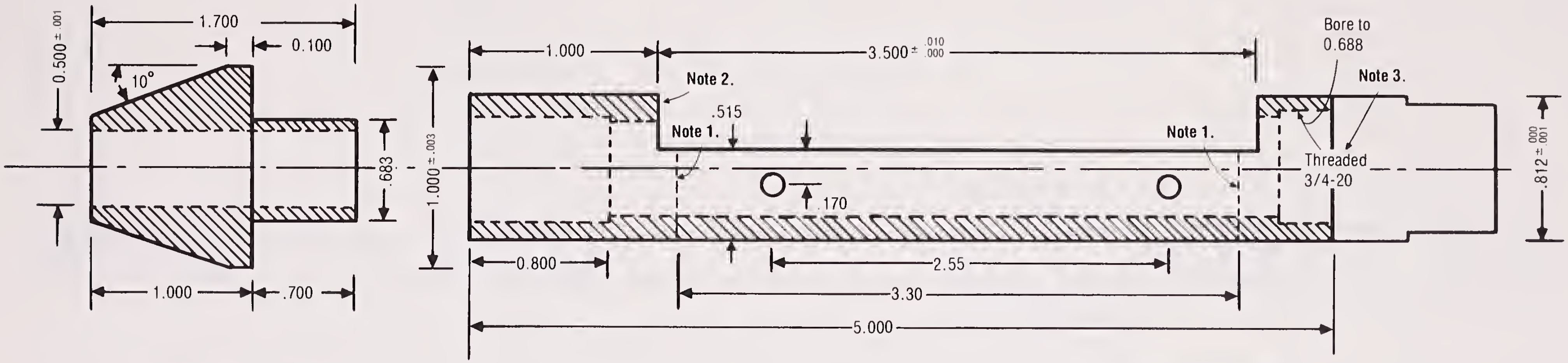

All dimensions in inches

Notes:

1. Threaded holes (2.56) on center
2. This piece is made from pipe (½ inch)
3. Aluminum connector housing Amphenol MS 3102 14S

Amplifier housing

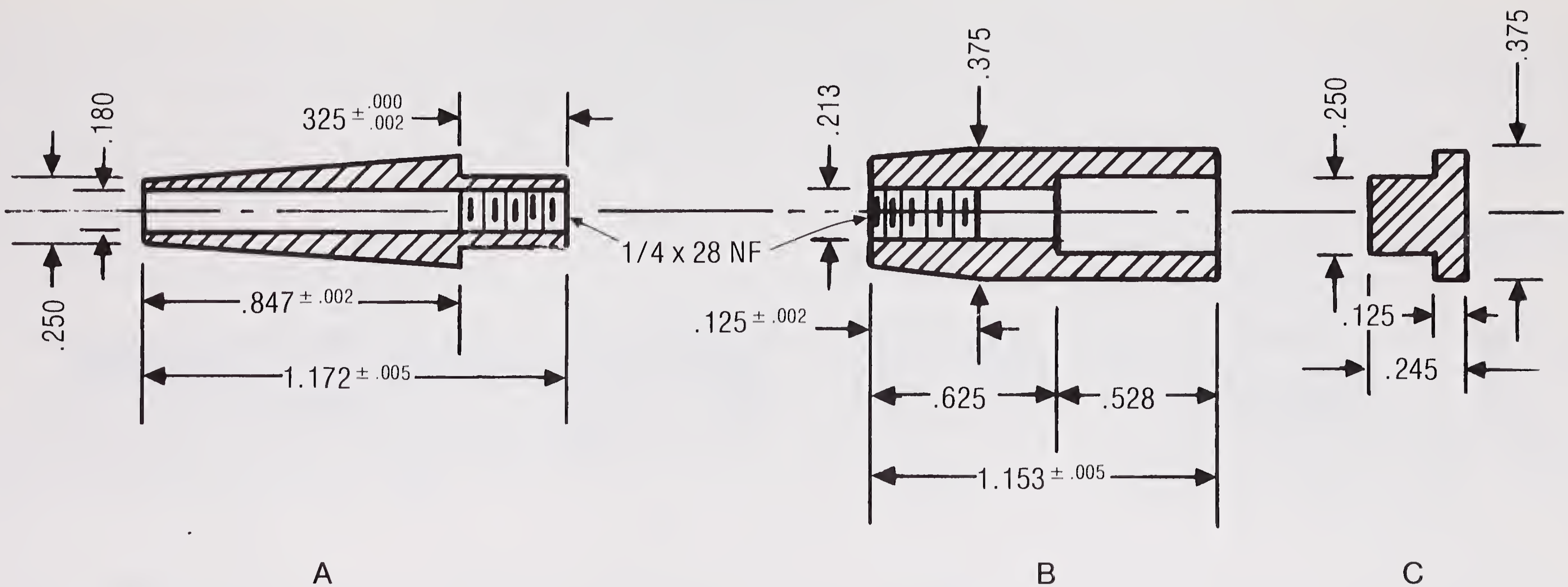

1. Parts A and B are of aluminum alloy. C is of acrylic.
2. Taper on parts A and B to be cut with parts tightly threaded.

Lamp housing

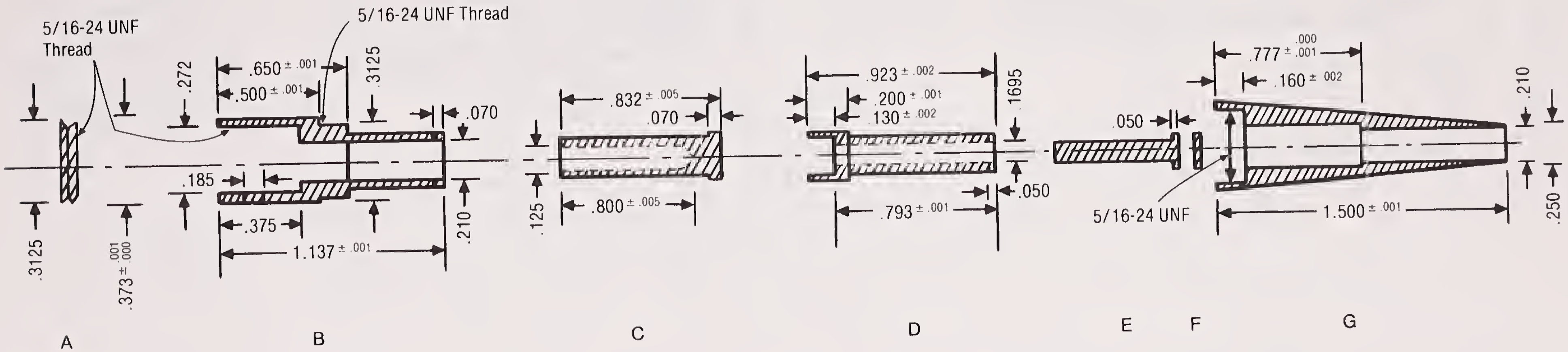

Notes:

1. Parts B, D, and G are of mild steel.
2. Parts A and C are acrylic.
3. Part E is of .004 brass shim stock.
4. Part F is thick base (.007) film.

Phototransistor housing

☆ U S GOVERNMENT PRINTING OFFICE · 1977·0 781-562-136

Schmidt, R. A. 1977. A system that measures blowing snow. USDA For. Serv. Res. Pap. RM-194, 80 p. Rocky Mt. For. and Range Exp. Stn., Fort Collins, Colo. 80521

A snow particle counter based on a prototype design that originated at the University of Washington, was developed and tested for research in the fundamentals of snow transport by wind. Further work created an electronic system that monitors visual range in blowing snow. The system has been applied to interstate highway traffic control.

All design and test data are included in this paper, together with shop drawings for fabrication of the sensor, and an operating and service manual for the visual range monitor.

Keywords: Snow, particle size, blowing snow, snow transport, drifting snow, instrumentation, visibility.

Schmidt, R. A. 1977. A system that measures blowing snow. USDA For. Serv. Res. Pap. RM-194, 80 p. Rocky Mt. For. and Range Exp. Stn., Fort Collins, Colo. 80521

A snow particle counter based on a prototype design that originated at the University of Washington, was developed and tested for research in the fundamentals of snow transport by wind. Further work created an electronic system that monitors visual range in blowing snow. The system has been applied to interstate highway traffic control.

All design and test data are included in this paper, together with shop drawings for fabrication of the sensor, and an operating and service manual for the visual range monitor.

Keywords: Snow, particle size, blowing snow, snow transport, drifting snow, instrumentation, visibility.

Schmidt, R. A. 1977. A system that measures blowing snow. USDA For. Serv. Res. Pap. RM-194, 80 p. Rocky Mt. For. and Range Exp. Stn., Fort Collins, Colo. 80521

A snow particle counter based on a prototype design that originated at the University of Washington, was developed and tested for research in the fundamentals of snow transport by wind. Further work created an electronic system that monitors visual range in blowing snow. The system has been applied to interstate highway traffic control.

All design and test data are included in this paper, together with shop drawings for fabrication of the sensor, and an operating and service manual for the visual range monitor.

Keywords: Snow, particle size, blowing snow, snow transport, drifting snow, instrumentation, visibility.

Schmidt, R. A. 1977. A system that measures blowing snow. USDA For. Serv. Res. Pap. RM-194, 80 p. Rocky Mt. For. and Range Exp. Stn., Fort Collins, Colo. 80521

A snow particle counter based on a prototype design that originated at the University of Washington, was developed and tested for research in the fundamentals of snow transport by wind. Further work created an electronic system that monitors visual range in blowing snow. The system has been applied to interstate highway traffic control.

All design and test data are included in this paper, together with shop drawings for fabrication of the sensor, and an operating and service manual for the visual range monitor.

Keywords: Snow, particle size, blowing snow, snow transport, drifting snow, instrumentation, visibility.

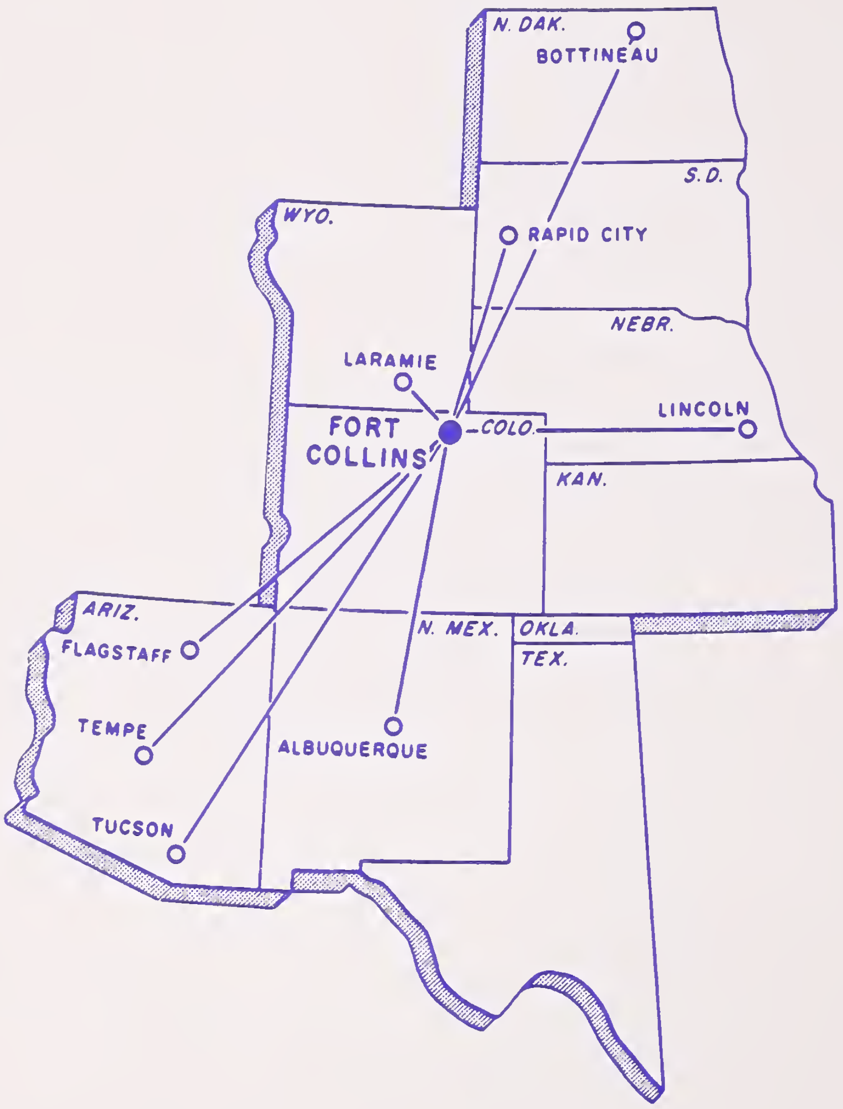
N. DAK.
BOTTINEAU
S.D.
WYO.
RAPID CITY
NEBR.
LARAMIE
LINCOLN
FORT COLLINS
COLO.
KAN.
ARIZ.
N. MEX.
OKLA.
TEX.
FLAGSTAFF
TEMPE
ALBUQUERQUE
TUCSON